DOTTORATO DI RICERCA IN BIOINGEGNERIA

UNIVERSITÀ DEGLI STUDI DI BOLOGNA

XXV CICLO

PHD THESIS:
MOVEMENT ANALYSIS BY MEANS OF INERTIAL SENSORS: FROM BENCH TO BEDSIDE

Mellone Sabato

Supervisore:	Prof. Lorenzo Chiari *Università degli Studi di Bologna*
Correlatore:	Prof. Angelo Cappello *Università degli Studi di Bologna*
Controrelatore:	Prof. Ugo Della Croce *Università degli Studi di Sassari*
Controrelatore Esterno:	Prof. Wiebren Zijlstra *German Sport University, Cologne*

MACROSETTORE: 09/G Ingegneria dei sistemi e bioingegneria
SETTORE CONCORSUALE: 09/G2 Bioingegneria
SETTORE SCIENTIFICO-DISCIPLINARE: ING-INF/06 Bioingegneria Elettronica e Informatica

ABSTRACT

Objective assessment implies quantitative measurement. Clinical assessments tools are usually quick, easy to use, and make use of inexpensive equipment. Nevertheless, the results can be biased by the rater, there can be ceiling effects, and can be not sensitive enough for detecting/monitoring small changes. On the other hand by instrumenting a functional test it is possible to provide automatic algorithms for an objective and comprehensive assessment which goes well beyond a simple temporal measure obtained with a stopwatch. Not only clinicians need reliable information leading to a real benefit to the patient but it is very important to provide this information with a minimal effort otherwise it will not be useful in the everyday clinical practice. Having this in mind, the choice of a simple setup would not be enough because, even if the setup is quick and simple, the instrumental assessment would still be in addition to the daily routine. The will to overcome this limit has led to the idea of instrumenting already existing and widely used functional tests. In this way the sensor based assessment becomes an integral part of the clinical assessment. Reliable and validated signal processing methods have been successfully implemented in Personal Health Systems based on smartphone technology. At the end of this research project there is evidence that such solution can really and easily used in clinical practice in both supervised and unsupervised settings. Smartphone based solution, together or in place of dedicated wearable sensing units, can truly become a pervasive and low-cost means for providing suitable testing solutions for quantitative movement analysis with a clear clinical value, ultimately providing enhanced balance and mobility support to an aging population.

ACKNOWLEDGEMENTS

Sapiens fingit fortunam sibi...

TABLE OF CONTENTS

ABSTRACT 2
ACKNOWLEDGEMENTS 3
TABLE OF CONTENTS 4
1 INTRODUCTION 5
1.1 TRADITIONAL CLINICAL ASSESSMENT 5
1.2 STEREOPHOTOGRAMMETRY SYSTEMS AND FORCE PLATES 6
1.3 RESEARCH PROJECT AND AIMS 8
2 INSTRUMENTING FUNCTIONAL TESTS 11
2.1 STATIC POSTUROGRAPHY: FROM FORCE PLATES TO THE INERTIAL SENSORS 11
2.1.1 LINEAR AND NON-LINEAR FILTERING 12
2.1.2 FEATURE EXTRACTION 14
2.1.3 HHT-BASED FILTERING: VALIDATION PROCEDURE AND RESULTS 16
2.1.4 DETECTING DYSKINESIA 23
2.2 GAIT ANALYSIS 25
2.2.1 HEEL STRIKE DETECTION 27
2.2.2 VALIDATION PROCEDURE AND RESULTS 30
2.2.3 FEATURE EXTRACTION 32
2.3 THE TIMED UP AND GO TEST 33
2.3.1 POSTURAL TRANSFERS 34
2.3.2 POSTURAL TRANSFERS: VALIDATION PROCEDURE AND RESULTS 38
2.3.3 TURNING 41
2.3.4 TURNING: VALIDATION PROCEDURE AND RESULTS 44
2.3.5 FEATURE EXTRACTION 48
2.4 CLINICAL APPLICATIONS 49
2.4.1 INSTRUMENTED ANALYSIS OF POSTURAL SWAY 49
2.4.2 INSTRUMENTED TIMED UP AND GO TEST 52
3 FROM BENCH TO BEDSIDE 55
3.1 PERSONAL HEALTH SYSTEMS 55
3.2 LONG-TERM MONITORING 55
3.2.1 IT IS ALL ABOUT RELIABILITY 56
3.3 SMARTPHONES 59
3.3.1 A SMARTPHONE FOR INSTRUMENTING THE TIMED UP AND GO TEST: UTUG 61
3.3.2 A SMARTPHONE AS A WEARABLE SENSING UNIT AND FALL DETECTOR: UFALL 66
3.4 CLINICAL APPLICATIONS 69
4 CONCLUSIONS 71

1 INTRODUCTION

…IT IS TRUE THAT

"Decision-making about health services for individuals and populations should be guided by evidence on the need, effectiveness, and ways to use resources optimally"[1]

…BUT

Clinical judgment is still central to clinical practice because even the most validated medical evidence has to deal with the uniqueness of the individual; after taking the initial clinical data and making observation, clinicians make judgments before taking clinical decision[2].

What prompts a clinician to seek new sources of information is not just the willingness to bring oneself up to date but is the need to solve a clinical problem[3]; basically a clinician wants to:

1) obtain information that is relevant in everyday practice
2) obtain reliable information
3) obtain information with minimal effort
4) obtain information leading to a real benefit to the patient

From the patient point of view the solution must be as much unobtrusive as possible, ideally transparent.

From the clinician point of view the solution must be easy to handle in the everyday clinical practice.

1.1 TRADITIONAL CLINICAL ASSESSMENT

The aim of the clinical assessment is to evaluate, diagnose, and treat individuals. In this chapter the focus is on the assessment of the functional status i.e. a person's ability to perform tasks required for living. Functional limitations are usually assessed by means of standardized functional tests. Assessment tools can be structured as a series of motor tasks like the Berg Balance Scale[4] or the Tinetti Mobility Scale[5], providing a full picture about the functional status of a specific domain with a cost in terms of time and resources, while other assessment tools focus on a specific task like the gait speed or the ability to raise from a chair. Other assessment tools are designed for the follow up of motor symptoms related with a specific pathology like the Unified Parkinson's Disease Rating Scale[6].
Tests of physical performance are routinely included in clinical practice for investigating functional limitations in mobility and balance. A variety of methods and tools have been proposed in literature, many of them suffer from ceiling or floor effect limitations meaning that a specific population reaches the top or the bottom of the score distribution and it may not be responsive enough to measure small progress or deterioration in a subject's ability Among the most popular there are:

- Berg Balance Scale[1]: designed to measure functional standing balance of older adults
- Balance Evaluation Systems Test[7]: designed for assessing postural control systems
- Tinetti Mobility Scale[2]: A performance-oriented assessment of mobility for older adults

The above mentioned assessment tools takes from few minutes to about half an hour to be administered. Among the tools targeting specific motor task there are:

- Functional Reach Test: Assesses a patient's stability by measuring the maximum distance an individual can reach forward while standing in a fixed position
- Five Times Sit to Stand Test[8]: A measure of functional lower limb muscle strength

[1] Muir Gray JA. Evidence-based Healthcare. How to make health policy and management decisions. London: Churchill Livingstone 1997.
[2] Kenny NP. Does good science make good medicine? Incorporating evidence into practice is complicated by fact that clinical practice is as much art as science. Can Med Assoc J 1997; 157: 336.
[3] Slawson DC, Shaughnessy AF. Obtaining useful information from expert based resources. BMJ 1997; 314: 947-9.
[4] Muir SW, Berg K, Chesworth B, Speechley M (2008). Use of the Berg Balance Scale for predicting multiple falls in community-dwelling elderly people: a prospective study. Phys Ther; 88(4): pp.449-59
[5] Tinetti ME (1986). Performance-oriented assessment of mobility problems in elderly patients. J Am Geriatr Soc; 34: pp.119-26
[6] Fahn S, Elton RL, UPDRS program members. Unified Parkinsons Disease Rating Scale. In: Fahn S, Marsden CD, Goldstein M, Calne DB, editors. Recent developments in Parkinsons disease, vol 2. Florham Park, NJ: Macmillan Healthcare Information; 1987. p 153–163.
[7] Horak FB, Wrisley DM, Frank J (2009). The Balance Evaluation Systems Test (BESTest) to differentiate balance deficits. Phys Ther; 89(5): pp.484-98
[8] Guralnik JM., Ferrucci L, et al. (2000). "Lower extremity function and subsequent disability: consistency across studies, predictive models, and value of gait speed alone compared with the short physical performance battery." J Gerontol A Biol Sci Med Sci 55(4): M221-31.

There are simple clinical tools like the Standing Balance[1] test for assessing postural control. The Standing Balance for example consists of three tasks performed in a predefined order:
Participant should stand for 10 seconds with one foot behind the other so that the big toe of one foot is touching the side of the heel of the other (Semi-tandem stand). Participant who fails semi-tandem stand is asked to stand for 10 seconds feet side-by-side (Side-by-side stand) while participant whose semi-tandem stand is successful is asked to stand for 10 seconds with one foot behind the other so that the big toe of one foot is touching the heel of the other foot (Full-tandem stand). Although such a tool is very fast and easy to administer it also provide poor sensitivity.

Gait analysis is also very important in clinical practice and there are many tools proposed in literature, some of the outcome measures are listed below:

- 10 or 20 Meter Walk Test: assesses walking speed in meters per second over a short duration[2]
- Two- or six-minute walk test: measures the number of meters a person can walk in two or six minutes[11]
- Cadence: measures the number of steps taken in a given period of time[3]
- Stride length: measures the average distance between two successive placements of the same foot[4]
- Step length: measures the average distance between successive foot to floor contact with opposite feet[12]

There are also more structured tools like the Dynamic Gait Index[5] for investigating individual's ability to modify balance while walking.

Among the clinical functional test the Timed Up and Go test (TUG) is indeed one of the most popular and widely used [6] to assess balance, mobility and fall risk in the elderly[7] [8] [9] and in Parkinson's disease (PD)[10] [11]. It consists of rising from a chair, walking 3 meters at preferred speed, turning around, returning and sitting. It is simple and easy to perform in the clinic. The traditional clinical outcome of this test is its total duration[8], which is usually measured by a stop-watch.

1.2 STEREOPHOTOGRAMMETRY SYSTEMS AND FORCE PLATES

Human movement analysis requires optical motion analysis systems based on infrared video cameras and markers on the body or, more recently, markerless techniques, and standard video cameras[12] [13]

In the last decade, quantitative assessment of postural sway during quiet stance has become available as clinical tools for assessing postural control. The conventional method of analysis requires the use of force plates measuring the center of pressure (COP)[14] or, less frequently, a stereophotogrammetric system to estimate the center of mass (COM) displacement[15]. COP time series represents the evolution of the application point of the ground reaction force vector on the horizontal plane, along its antero-posterior (AP) and medio-lateral (ML) axes[16]. The human postural control system

[1] Guralnik JM. Simonsick EM. Ferrucci L. Glynn RJ. Berkman LF. Blazer DG. Scherr PA. Wallace RB. A short physical performance battery assessing lower extremity function: association with self-reported disability and prediction of mortality and nursing home admission. Journal of Gerontology. 1994;49(2):M85-94.

[2] Kersten P. Principles of physiotherapy assessment and outcome measures. In: Stokes M editor(s). Physical management in neurological rehabilitation. 2nd Edition. London: Elsevier Mosby, 2004:29–46.

[3] Trew M, Everett T. Human movement: an introductory text. 5th Edition. Edinburgh: Churchill Livingstone, 2005.

[4] Whittle M. Gait analysis: an introduction. 2nd Edition. Oxford: Butterworth-Heinemann, 1996.

[5] Whitney SL, Hudak MT, Marchetti GF. The dynamic gait index relates to self-reported fall history in individuals with vestibular dysfunction. J Vestib Res. 2000;10:99–105.

[6] D. Podsiadlo and S. Richardson, "The timed 'Up & Go': a test of basic functional mobility for frail elderly persons," Journal of the American Geriatrics Society, vol. 39, no. 2, pp. 142–8, Feb. 1991.

[7] A. Shumway-Cook, S. Brauer, and M. Woollacott, "Predicting the probability for falls in community-dwelling older adults using the Timed Up & Go Test," Physical Therapy, vol. 80, no. 9, pp. 896–903, Sep. 2000.

[8] L. K. Boulgarides, S. M. Mcginty, J. A. Willett, and C. W. Barnes, "Research report use of clinical and impairment-based tests to predict falls by community-dwelling older adults," Physical Therapy, pp. 328–39, 2003.

[9] T. Herman, N. Giladi, and J. M. Hausdorff, "Properties of the 'timed up and go' test: more than meets the eye," Gerontology, vol. 57, no. 3, pp. 203–10, Jan. 2011.

[10] S. Morris, M. E. Morris, and R. Iansek, "Reliability of measurements obtained with the Timed 'Up & Go' test in people with Parkinson's disease," Physical Therapy, vol. 81, no. 2, pp. 810–8, Feb. 2001.

[11] Y. Balash, C. Peretz, G. Leibovich, T. Herman, J. M. Hausdorff, and N. Giladi, "Falls in outpatients with Parkinson's disease: frequency, impact and identifying factors," Journal of Neurology, vol. 252, no. 11, pp. 1310–5, Nov. 2005.

[12] S. Corazza, E. Gambaretto, L. Mundermann, and T. Andriacchi, "Automatic generation of a subject specific model for accurate markerless motion capture and biomechanical applications," IEEE Trans. Biomed. Eng., vol. 57, no. 4, pp. 806–812, Apr. 2010.

[13] A. Cappozzo, U. Della Croce, A. Leardini, and L. Chiari, "Human movement analysis using stereophotogrammetry: Part 1. Theoretical background," Gait Posture, vol. 21, no. 2, pp. 186–196, Feb. 2005.

[14] T. S. Kapteyn, W. Bles, C. J. Njiokiktjien, L. Kodde, C. H. Massen, and J. M. Mol, "Standardization in platform stabilometry being a part of posturography", Agressologie, vol. 24, no. 7, pp. 321-326, June1983.

[15] J. W. Streepey, R. V. Kenyon, and E. A. Keshner, "Field of view and base of support width influence postural responses to visual stimuli during quiet stance", Gait Posture, vol. 25, no. 1, pp. 49-55, Jan.2007.

[16] D. A.Winter, A. E. Patla, and J. S. Frank, "Assessment of balance control in humans," Med. Prog. Technol., vol. 16, no. 1–2, pp. 31–51, May 1990.

has been the object of many investigations in the last few decades in various fields, including orthopedics, neurology, and rehabilitation[1] [2] [3] [4]. Quantitative analysis of COP displacement may disclose differences in age and disease, including the effects of therapies and treatments, and it is also found predictive of future risk of falling[5] [6] [7] [8].

Camera-based systems and force plates in laboratory settings has also been used for quantifying postural transition like sit-to-stand (STS) movements in order to better understand their biomechanical dynamics[9] [10].

Research on gait analysis has been extensively conducted over the years and it became popular in biomedical engineering with the availability of motion capture systems[11] [12] [13] [14]. The traditional method of analysis makes us of a stereophotogrammetric system and force plates for measuring ground-reaction forces[15] [16].

Although these movement analysis techniques have provided essential and accurate information for at least two decades[17], their use in clinical practice has been partly limited by cost and the need for qualified personnel.

[1] J. Massion, "Postural control system," Curr. Opin. Neurobiol., vol. 4, no. 6, pp. 877–887, Dec. 1994.

[2] F. B. Horak, "Postural orientation and equilibrium: What do we need to know about neural control of balance to prevent falls?" Age Ageing, vol. 35, no. Suppl. 2, pp. ii7–ii11, Sep. 2006.

[3] A. Nardone and M. Schieppati, "Balance in Parkinson's disease under static and dynamic conditions," Mov. Disord., vol. 21, no. 9, pp. 1515–1520, Sep. 2006.

[4] B.Missaoui, P. Portero, S. Bendaya, O. Hanktie, and P. Thoumie, "Posture and equilibrium in orthopedic and rheumatologic diseases," Neurophysiol. Clin., vol. 38, no. 6, pp. 447–457, Dec. 2008.

[5] T. E. Prieto, J. B. Myklebust, R. G. Hoffmann, E. G. Lovett, and B. M. Myklebust, "Measures of postural steadiness: differences between healthy young and elderly adults", IEEE Trans. Biomed. Eng, vol. 43, no. 9, pp. 956-966, Sept.1996.

[6] L. Rocchi, L. Chiari, and F. B. Horak, "Effects of deep brain stimulation and levodopa on postural sway in Parkinson's disease", J. Neurol. Neurosurg. Psychiatry, vol. 73, no. 3, pp. 267-274, Sept.2002.

[7] M. Mancini, L. Rocchi, F. B. Horak, and L. Chiari, "Effects of Parkinson's disease and levodopa on functional limits of stability", Clin. Biomech. (Bristol. , Avon.), vol. 23, no. 4, pp. 450-458, May2008.

[8] Melzer I, Benjuya N, Kaplanski J. Postural stability in the elderly: a comparison between fallers and non-fallers. Age Ageing. 33(6):602-7.

[9] Riley PO, Schenkman ML, Mann RW, Hodge WA. Mechanics of a constrained chair-rise. Journal of Biomechanics 1991;24(1):77–85.

[10] Lindemann U, Claus H, Stuber M, et al. Measuring power during the sit-tostand transfer. European Journal of Applied Physiology 2003;89(5):466–70.

[11] Karaulovaa I.A., Hallb P.M., Marshall A.D. Tracking people in three dimensions using a hierarchical model of dynamics. Image Vis. Comput. 2002;20:691–700.

[12] Furnée H. Real-time motion capture systems. In: Allard P., Cappozzo A., Lundberg A., Vaughan C.L., editors. Three-Dimensional Analysis of Human Locomotion. John Wiley & Sons; Chichester, UK: 1997. pp. 85–108.

[13] Chiari L., Della Croce U., Leardini A., Cappozzo A. Human movement analysis using stereophotogrammetry. Part 2: Instrumental errors. Gait Posture. 2005;21:197–211.

[14] Cappozzo A., Della Croce U., Leardini A., Chiari L. Human movement analysis using stereophotogrammetry. Part 1: Theoretical background. Gait Posture. 2005;21:186–196.

[15] Kim C.M., Eng J.J. Magnitude and pattern of 3D kinematic and kinetic gait profiles in persons with stroke: Relationship to walking speed. Gait Posture. 2004;20:140–146.

[16] Casadio M., Morasso P.G., Sanguineti V. Direct measurement of ankle stiffness during quiet standing: Implications for control modelling and clinical application. Gait Posture. 2005;21:410–424.

[17] TP Andriacchi, EJ Alexander, "Studies of human locomotion: Past, present and future," J. Biomech., vol. 33, no. 10, pp. 1217–1224, Oct. 2000.

1.3 RESEARCH PROJECT AND AIMS

Figure 1 summarizes my research approach. Starting from the practical needs of clinicians and patients, a series of experimental assessment protocols has been defined in order to obtain an instrumental assessment tool which was not only the solution to the problem but also easily and directly usable in clinical practice. All the collected data has been used for developing robust algorithms for movement analysis from which a series of clinically valuable metrics have been defined. The aim was to provide clinically relevant outcomes by means of a easy to handle technological solution which was also as transparent as possible for the patient.
Although the use of a body area network of wearable sensing unit enables to investigate the dynamics of all the different body segments, this solution is not really unobtrusive for the user and even if it is feasible to implement such a solution in a supervised environment like a movement lab, it would not be feasible to implement the same solution in unsupervised settings. For this reason I focused my research project on methods relying upon a single wearable sensing unit (Figure 2).

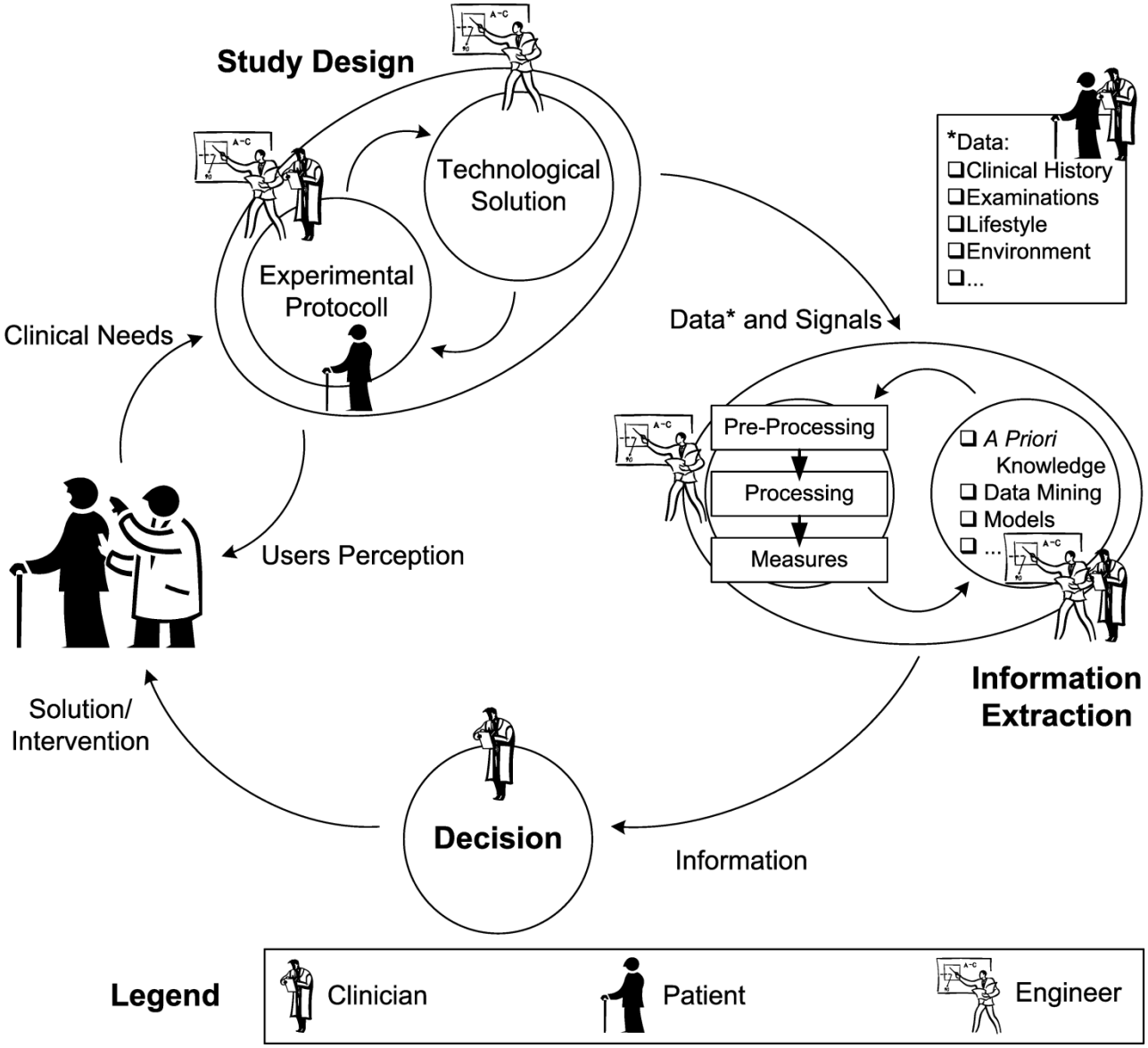

Figure 1 – The virtuous circle, clinical needs and user-centered design.

The use of wearable motion sensors requires intelligent signal processing and appropriate methods for monitoring of mobility-related postures and activities in both supervised and unsupervised settings. The aims of the present worlk are the design and the development of novel methods for wearable sensor-based functional assessment in supervised and unsupervised settings (Chapter 2). The ultimate goal of my research is to design Personal Health Systems as digital companions able to deliver personalized services anywhere and anytime (Chapter 3).

Figure 2 - A single sensor-approach is an easy to handle solution for both the clinician and the patient. In the figure a small waist mounted inertial sensor is controlled by a smartphone application.

2 INSTRUMENTING FUNCTIONAL TESTS

Objective assessment implies quantitative measurement. Clinical assessments tools, as those presented in Section 1, are usually quick, easy to use, and make use of inexpensive equipment. Nevertheless, the results can be biased by the rater, there can be ceiling effects, and can be not sensitive enough for detecting/monitoring small changes[1]. On the other hand by instrumenting a functional test it is possible to provide automatic algorithms for an objective and comprehensive assessment which goes well beyond a simple temporal measure obtained with a stopwatch.
As pointed out in Section 1, not only clinicians need reliable information leading to a real benefit to the patient but it is very important to provide this information with a minimal effort otherwise it will not be useful in the everyday clinical practice. Having this in mind, the choice of a single sensor alone would not be enough because, even if the setup is quick and simple, the instrumental assessment would still be in addition to the daily routine. The will to overcome this limit has led to the idea of instrumenting already existing and widely used functional tests. In this way the sensor based assessment becomes an integral part of the clinical assessment.
In this chapter are presented all the developed methods for signal processing and feature extraction which are used for assessing balance (Section 2.1), gait (Section 2.2), postural transfers and turns during the Timed Up and Go test (Section 2.3) but not limited to the Timed Up and Go test. Section 2.4 reports results obtained in clinical applications.

2.1 STATIC POSTUROGRAPHY: FROM FORCE PLATES TO THE INERTIAL SENSORS

Recent studies have shown that inertial sensors, e.g. accelerometers and gyroscopes, can be a valid and reliable alternative to force plate-based COP measures[2] [3] [4]. Accelerometers, in particular, due to their low power consumption, low cost, high sensitivity and resistance to drift effect in comparison to gyroscopes, provide a novel opportunity to measure postural sway by means of a wearable, miniaturized and ubiquitous platform[5]. As an example, accelerometers can be used to measure COM linear acceleration when worn on the subject's trunk, typically on the lower back between L3 and L5[6] as shown in Figure 3. Accelerometer-based measures of postural sway are already proven to be sensitive to the pathology and its progression[7].

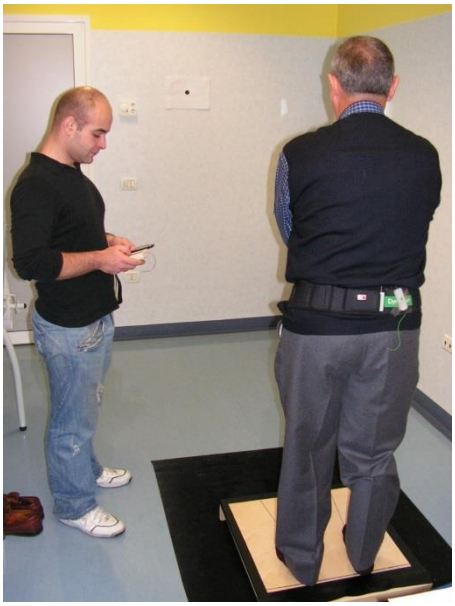

Figure 3 – Patient performing a quiet standing trial wearing an inertial sensing unit by means of an elastic belt. The wearable unit substitutes the traditional force plate.

[1] Blum L, Korner-Bitensky N. Usefulness of the Berg Balance Scale in stroke rehabilitation: a systematic review. Phys.Ther 2008;88:559–566.
[2] Chiari L, Dozza M, Cappello A, Horak FB, Macellari V, Giansanti D. Audio-biofeedback for balance improvement: an accelerometry-based system. IEEE Trans.Biomed.Eng 2005;52:2108–2111
[3] M. Mancini, P. Carlson-Kuhta, C. Zampieri, J.G. Nutt, L. Chiari, F.B. Horak, "Postural sway as a marker of progression in Parkinson's disease: A pilot longitudinal study," Gait Posture. 2012 Jun 29
[4] Mancini M, Horak FB. The relevance of clinical balance assessment tools to differentiate balance deficits. Eur J Phys Rehabil Med. 2010 Jun;46(2):239-48.
[5] R. E. Mayagoitia, J. C. Lotters, P. H. Veltink, and H. Hermens, "Standing balance evaluation using a triaxial accelerometer", Gait Posture, vol. 16, no. 1, pp. 55-59, Aug.2002.
[6] R. Moe-Nilssen and J. L. Helbostad, "Trunk accelerometry as a measure of balance control during quiet standing", Gait Posture, vol. 16, no. 1, pp. 60-68, Aug.2002.
[7] M Mancini,F.B. Horak, C. Zampieri, P. Carlson-Kuhta, J.G. Nutt, L. Chiari, "Trunk accelerometry reveals postural instability in untreated Parkinson's disease," Parkinsonism Relat Disord. 2011 Aug;17(7): 557-62

2.1.1 LINEAR AND NON-LINEAR FILTERING

Linear Filtering

Low-pass Butterworth filter is the most popular filter in this type of applications because its frequency response is maximally flat in the pass band. The frequency bandwidth of the stabilization process in quiet standing is mainly below 3Hz[1] so a cut-off frequency above 3Hz is recommended. It must be noted that choosing the right cut-off frequency becomes critical when dealing with subjects who exhibit tremor at rest like PD patients. Since tremor peak in PD is typically located between 4Hz and 7Hz[2], a maximum cut-off value of 3.5Hz must be selected or even lower depending on the tremor amplitude. It is recommended at least a fourth order filter to obtain a good attenuation in the stop band. Forward and backward filtering, which also doubles the filter order, must be applied in order to avoid phase distortion.

Linear VS Non-Linear Filtering

All the measurement techniques for measuring postural sway in quiet standing (force plates, stereophotogrammetry, and inertial sensors) are sensitive to tremor. It is worth noting that pathological tremor and body sway signals may have partially overlapping bandwidths. Hence, without a proper preprocessing method, tremor could affect measures related to other aspects of postural control, and thus cause misleading results or interpretations (e.g. finding a significant difference in a postural parameter between tremorous and non tremorous trials which is just a reflection of tremor). For this reason it is important to remove the tremor contribution from postural signals, which are characterized by a low signal-to-noise ratio, to get descriptive measures of postural function beyond the pure tremorous behavior.

Linear filters are commonly employed for this purpose. They are based on Fourier transformation that requires the fulfillment of two basic assumptions: the system must be linear and signals must be stationary. When dealing with real physiological data it is hard to meet these assumptions rigorously, and in most cases we have to work under approximation hypotheses. Not only is the system generally non-linear and non-stationary, but the available sample has a finite length. Furthermore, filters themselves can introduce amplitude and phase distortions.

Another way to obtain a noise-free estimation of a signal is through optimal filters like Kalman's and Wiener's[3]. The application of such state-space filters requires a proper and detailed model of the system, which has a strong impact on the filtering results. Kalman filter uses a physical model of the system while Wiener filter uses a statistical model which is based on the knowledge of signal and noise power spectra. The basic assumption of both filters is that the system is linear and, for Wiener filter, that the signal is stationary, at least within a certain time-window. Various extensions of the Kalman and Wiener filters have been developed to deal with non-stationary and non-linear signals; anyway they still rely on models to describe how the signal and the noise behave. In most cases, noise is defined as additive, white, and Gaussian. When the system under analysis is complex, like a biological system, it is difficult to characterize the relationship between noise and the desired signal, even when the noise sources are known. This is partly due to the lack of information about how noise is mixed into the signal.

Non-Linear Filtering based on Hilbert-Huang Transform

To overcome the above-mentioned limitations of digital filters, an alternative method is proposed to limit the effect of noise and tremor on postural signals. This method is based on Hilbert-Huang Transformation (HHT)[4]. The filtering method has been tailored to the specifications of acceleration signals.

Hilbert-Huang Transform

Developed by Huang (1998) for the study of non-linear and non-stationary processes, HHT is made up of two steps: *i*) a preprocessing step, the Empirical Mode Decomposition (EMD), which acting as a dyadic filter-bank[5] decomposes the original signal; *ii*) a second step where the Hilbert transform is applied to the decomposition to obtain an amplitude-frequency-time distribution. EMD is an iterative method that is also totally adaptive. This can be thought of as having several filters of overlapping frequency content which correspond to signal-dependent, time-variant filters[4]. The decomposition leads to a finite set of empirical modes directly derived from the data and a residue that can be the average trend of the time series or a constant value. This residue and the empirical modes allow the reconstruction of the original data.

These empirical modes are named Intrinsic Mode Functions (IMFs). An IMF is a function that meets two conditions: (I) in the whole data set, the number of extrema and the number of zero crossings must be equal or differ at most by one; (II) at any point, the mean value of the envelope defined by the local maxima and the envelope defined by the local

---

[1] I. D. Loram, C. N Maganaris and M. Lakie, " Human postural sway results from frequent, ballistic bias impulses by soleus and gastrocnemius", J. Physiol., vol. 564(Pt 1), pp. 295-311, Apr.2005.

[2] B. Hellwig, P. Mund, B. Schelter, B. Guschlbauer, J. Timmer, and C. H. Lucking, "A longitudinal study of tremor frequencies in Parkinson's disease and essential tremor", J. Clin. Neurophysiol., vol. 120, no. 2, pp. 431-435, Feb.2009.

[3] B Yang Zhan, Shuixia Guo, Keith M. Kendrick, Jianfeng Feng, " Filtering noise for synchronised activity in multi-trial electrophysiology data using Wiener and Kalman filters", Biosystems, vol. 96, no. 1, pp. 1-13, Apr.2009.

[4] N. E. Huang, Z. Shen, S. R. Long, M. L. C. Wu, H. H. Shih, Q. N. Zheng, N. C. Yen, C. C. Tung, and H. H. Liu, "The empirical mode decomposition and the Hilbert spectrum for nonlinear and non-stationary time series analysis", Proc. Roy. Soc. London Ser. A, vol. 454, no. 1971, pp. 903-995, Mar.1998.

[5] P. Flandrin, G. Rilling, and P. Goncalves, "Empirical mode decomposition as a filter bank", IEEE Signal Process. Lett., vol. 11, no. 2, pp. 112-114, Feb.2004.

minima is zero. Under conditions (I) and (II), an IMF is not limited to a narrow band signal and can be both amplitude- and frequency-modulated, so an IMF can be non-stationary. The time lapse between two extrema is then considered the time scale of the IMF; this means that time scales are directly derived from the data and that the oscillatory modes are considered at a very local level.

IMFs are extracted from the signal with an iterative "sifting process". IMFs extraction has been performed by means of the algorithm proposed in[1] with a single modification to account for the peculiar properties of postural signals. If $X(t)$ is our trunk acceleration time series then the algorithm can be described as follows:

1) Identify all extrema of $h_i(t)$, starting with $h_0(t)=X(t)$;
2) All the local maxima are interpolated using a cubic spline forming the upper envelope, $e_{max}(t)$; in the same way, the lower envelope, $e_{min}(t)$, is defined as the cubic spline of the local minima;
3) Compute the mean envelope as $m_{i1}(t)=(e_{max}(t)+e_{min}(t))/2$ and the mode amplitude as $A_i(t)=(e_{max}(t)-e_{min}(t))/2$;
4) Compute the difference between the data and $m_i(t)$, $h_{i1}(t)=h_i(t)-m_{i1}(t)$;
5) If conditions (I) and (II) are satisfied then $h_{i1}(t)$ is the i-th IMF, $IMF_i(t)=h_{i1}(t)$, and the residue $r_{i1}(t)=h_i(t)-IMF_i(t)$ is treated as a new signal and iteratively enters the steps from 1) to 5). If $h_{i1}(t)$ is not an IMF then it is treated as the new signal entering the steps from 1) to 5); the process is iterated until $h_{ik}(t)=h_i(t)-m_{ik}(t)$ satisfies conditions (I) and (II) and $h_{ik}(t)=IMF_i(t)$.

Condition (II) has been considered satisfied if $|m(t)/A(t)|<0.05$. This differs from the usage of two thresholds that was proposed in by Rilling et al.[1] to guarantee globally small fluctuations in the mean envelope and take into account locally large excursions. Indeed there is no reason here to hypothesize abrupt variations in trunk acceleration during unperturbed stance and hence the use for two different thresholds in different parts of the signal is not needed. Extrema have been added by mirror symmetry to take into account the issue related to the spline interpolation and the boundary condition. Once the algorithm ends, one obtains n IMFs and a residue, $r_n(t)$, hence the original data will be decomposed as:

$$X(t) = \sum_{i=1}^{n} IMF_i(t) + r_n(t)$$

Once this representation of the signal as a superposition of zero-mean oscillatory modes is obtained, the Hilbert transform can be applied to each mode. The residue, $r_n(t)$, should be left out of the Hilbert spectral analysis since it is a monotonic function or a constant. Naming the Hilbert Transform of $IMF_i(t)$ as $Y_i(t)$, we can define the analytic signal $Z_i(t)$:

$$Z_i(t) = IMF_i(t) + jY_i(t) = a_i(t)e^{j\varphi_i(t)}$$

The instantaneous frequency associated with the mode can be calculated through the derivative of the phase $\varphi_i(t)$. For each $IMF_i(t)$ we then have the amplitude, a_i, and the instantaneous frequency as functions of time. The resulting time-frequency distribution of the amplitudes is the Hilbert spectrum of the signal.

Mode selection criterion in absence of Dyskinesia

The frequency bandwidth of the stabilization process in quiet standing is mainly below 3Hz[2]. Based on this a priori knowledge, an IMF is descriptive of the stabilization process (and hence can be assigned to the "signal" component) if its frequency content is essentially at low frequencies and becomes negligible above 3Hz. On the contrary, an IMF which does not meet the aforementioned characteristics is considered artifactual and will be then assigned to the "noise/tremor" component. By construction, after an IMF is extracted from the data, the number of extrema in the residue decreases, which means that the next IMF will have a larger time scale. For this reason, we only have to identify the first IMF that satisfies our hypothesis about power distribution since the following IMFs will satisfy it as well. Details and the validation procedure are reported in section 2.1.3. The mode selection algorithm can be summarized as follows: where Median value of its Instantaneous Frequency (MIF) and the Median value of its Amplitude (MA)

1) Apply the HHT to each signal (EMD and Hilbert spectral analysis);
2) for each IMF of the decomposition calculate the Median value of Instantaneous Frequency (MIF) and the Median value of Amplitude (MA);
3) If MIF < 2.4Hz and MA < 30mm/s2 the corresponding IMF is used for signal reconstruction, otherwise the IMF is summed to the noise/tremor component of the signal.

Since time scales of the IMFs are in increasing order, applying this algorithm means selecting the first k IMFs which reconstruct the noise/tremor component, and the last n-k IMFs which reconstruct the signal.

Mode selection criterion in presence of Dyskinesia

Since Levodopa-induced Dyskinesia can significantly alter the normal body sway, the criterion based on the Median value of the Amplitude can't be applied and the selection criterion becomes simply:

1) Apply the HHT to each signal (EMD and Hilbert spectral analysis);
2) for each IMF of the decomposition calculate the Median value of Instantaneous Frequency

[1] G. Rilling, P. Flandrin, and P. Gonçalvès, "On empirical mode decomposition and its algorithms", Proc. 6th IEEE/EURASIP Workshop on Non Linear Signal and Image Processing (NSIP '03), Grado, Italy, 2003.

[2] I. D. Loram, C. N Maganaris and M. Lakie, " Human postural sway results from frequent, ballistic bias impulses by soleus and gastrocnemius", J. Physiol., vol. 564(Pt 1), pp. 295-311, Apr.2005.

3) If MIF < 2.4Hz the corresponding IMF is used for signal reconstruction, otherwise the IMF is summed to the noise/tremor component of the signal.

2.1.2 FEATURE EXTRACTION

Postural sway in quiet standing can be quantified by means of several parameters computed from the acceleration and gyroscope signals in both time and frequency domains[1] [2] [3] [4]. In this section is reported a non-exhaustive set of measures among the many that can be found in literature (Table XYZ). In addition to the measures which can be directly extracted from raw signals, it is possible to have measure related to the Center of Mass (CoM) displacement in analogy to those computed from the Center of Pressure. In order to get measures related to displacement of CoM on the horizontal plane, acceleration signals can be low-pass filtered, with a cutoff frequency of 0.5Hz and a static gain of $-1/g$, where g is the gravitational acceleration. This transfer function is obtained from a simple biomechanical model, in the sagittal plane, based on inverted pendulum modeling of the human body during QS[5]. This assumption leads to the following equation, which relates acceleration to sway angle and CoM height

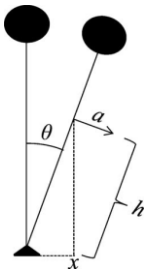

$$a(t) = h\ddot{\theta}(t) - g\sin\theta(t) \approx h\ddot{\theta}(t) - g\theta(t) \qquad (1)$$

where a is the accelerometer output in the AP direction, θ is the sway angle with respect to vertical, and h is the height of the inertial sensor (which is assumed to be the same height as the CoM). The corresponding transfer function is

$$H(s) = \frac{\theta(s)}{a(s)} = -\frac{1}{g - hs^2} \qquad (2)$$

Equation (2) in the frequency domain can be written as

$$H(j\omega) = -\frac{1}{g + h\omega^2} = -\frac{1}{g}\frac{1}{1 + (\omega/\omega_n)^2}, \qquad \omega_n = \sqrt{\frac{g}{h}} \qquad (3)$$

With the reasonable assumption of h being, on average 1 m, the displacement of the CoM projection on the ground, $x = h\ sin(\theta)$, can be approximated as $x = sin\ \theta \approx \theta$ for small θ. Thus, (3) represents the relation between the acceleration and the AP projection of CoM in the frequency domain. The same processing can be performed on ML signals. It must be noted that the aim of the reported procedure was not a precise estimation of the COM displacement, but rather the achievement of a signal reasonably approximating the characteristics of a displacement.

[1] B. E. Maki, P. J. Holliday, and A. K. Topper, "A Prospective Study of Postural Balance and Risk of Falling in an Ambulatory and Independent Elderly Population", J. Gerontol., vol. 49, no. 2, pp. M72-M84, Mar.1994.

[2] L. Chiari, L. Rocchi, and A. Cappello, "Stabilometric parameters are affected by anthropometry and foot placement", Clin. Biomech. (Bristol, Avon), vol. 17, no. 9-10, pp. 666-677, Nov.2002.

[3] T. Flash, N. Hogan, "The coordination of arm movements: an experimentally confirmed mathematical model", J. Neurosci., vol. 5, no. 7, pp. 1688-1703, Jul. 1985.

[4] T. E. Prieto, J. B. Myklebust, R. G. Hoffmann, E. G. Lovett, and B. M. Myklebust, "Measures of postural steadiness: differences between healthy young and elderly adults", IEEE Trans. Biomed. Eng, vol. 43, no. 9, pp. 956-966, Sept.1996.

[5] D. A.Winter, A. E. Patla, and J. S. Frank, “Assessment of balance control in humans,” Med. Prog. Technol., vol. 16, no. 1–2, pp. 31–51, May 1990.

TABLE XYZ_ POSTURAL PARAMETERS: ACRONYMS AND DESCRIPTIONS

MEASURE	DESCRIPTION	SIGNAL TYPE	M.U.	DIRECTIONS
Range	Range of the signal during the considered component	Displacement; Acceleration; Angular Velocity	[mm]; [m/s^2]; [°/s]	AP, ML, V
RMS	Root mean square of the signal, *s*, during the considered component: $$RMS = \sqrt{\frac{1}{N}\sum_{i=1}^{N}(s(i) - mean(s))^2}$$	Displacement; Acceleration; Angular Velocity	[m/s^2]; [°/s]	AP, ML, V
SP	Sway Path, the total length of the sway trajectory, computed as the sum of the distances between consecutive points in the time series. When considering a single direction of the sway: $$SP = \sum_{i=1}^{N-1}\left(s(i+1) - s(i)\right)$$ When considering the sway path on the horizontal plane: $$SP = \sum_{i=1}^{N-1}\sqrt{\left(s_{AP}(i+1) - s_{AP}(i)\right)^2 + \left(s_{ML}(i+1) - s_{ML}(i)\right)^2}$$ Where *s* is a generic signal, s_{AP} and s_{ML} are the two sway components on the horizontal plane. N is the total number of points of the signal time series. The accelerometer-based postural parameter can be defined by analogy with the parameter based on the displacement.	Displacement; Acceleration	[mm]; [m/s^2]	AP, ML, V, PLANAR
MV	Mean Velocity of the postural sway computed as the median of the absolute value of the time series obtained integrating the acceleration: $$VAB = \left|\int_{Tstart}^{Tend} a(t)dt\right| \text{ and } MV = median(VAB)$$ Where *a* is the acceleration component m/s^2, *Tend*/*Tstart* are the end and the beginning of the observation time respectively, and VAB is the acronym of Velocity Absolute Value. An alternative definition can be based upon the SP of the displacement: $$MV = \frac{SP}{T_{end} - T_{start}}$$	Displacement; Acceleration	[mm/s] or [m/s]	AP, ML, V, PLANAR
MAV	Mean Angular Velocity of the postural sway computed as the median of the absolute value of the angular velocity: $$MAV = median\left(|\omega|\right)$$	Angular Velocity	[°/s]	AP, ML, V
SA	Sway area estimated as the sum of the triangles formed by two consecutive points on the sway trajectory on the horizontal plane and the mean point on the plane: $$SA = \frac{1}{2}\sum_{i=1}^{N-1}\left|\left(s_{AP}(i+1) - m_{AP}\right)\left(s_{ML}(i) - m_{ML}\right) - \left(s_{AP}(i) - m_{AP}\right)\left(s_{ML}(i+1) - m_{ML}\right)\right|$$ The accelerometer-based postural parameter can be defined by analogy with the parameter based on the displacement.	Displacement; Acceleration	[mm^2]; [m/s^2]^2	PLANAR
95%EA	The 95% confidence ellipse area is the area of the confidence ellipse enclosing 95% of the points on the sway trajectory. The complete procedure for estimating this parameter is reported by Prieto et al.[1] The accelerometer-based postural parameter can be defined by analogy with the parameter based on the displacement.	Displacement; Acceleration	[mm^2]; [m/s^2]^2	PLANAR
F50%	Median frequency; frequency below which 50% of total signal power (TP) is present. Starting from the Power Spectral Density (PSD) of the signal: $$g(n) = \sum_{i=1}^{n} PSD(i);\ F50\% = f(n), \min(n) : g(n) \geq 50\%TP$$ Where the second formula mean that F50% is the frequency, *f*, corresponding to the nth index which is the smallest index such that *g(n)* is ≥ 50% of the total power. The total power is equal to *g(N)* where *N* is the total number of points of the PSD. Frequencies below 0.15Hz are usually ignored.	Displacement; Acceleration; Angular Velocity	[Hz]	AP, ML, V
F95%	Frequency below which 95% of total signal power (TP) is present. Starting from the Power Spectral Density (*PSD*) of the signal: $$g(n) = \sum_{i=1}^{n} PSD(i);\ F95\% = f(n), \min(n) : g(n) \geq 95\%TP$$ Where the second formula mean that F95% is the frequency, *f*, corresponding to the nth index which is the smallest index such that *g(n)* is ≥ 95% of the total power. The total power is equal to *g(N)* where *N* is the total number of points of the *PSD*. Frequencies below 0.15Hz are usually ignored.	Displacement; Acceleration; Angular Velocity	[Hz]	AP, ML, V

[1] T. E. Prieto, J. B. Myklebust, R. G. Hoffmann, E. G. Lovett, and B. M. Myklebust, "Measures of postural steadiness: differences between healthy young and elderly adults", IEEE Trans. Biomed. Eng, vol. 43, no. 9, pp. 956-966, Sept.1996.

CF	Centroidal frequency; frequency at which spectral mass is concentrated. Spectral moments are needed for the estimate: $\mu_0 = \sum_{i=1}^{N} PSD(i) = TP\,;\ \mu_2 = \sum_{i=1}^{N} f^2(i)PSD(i)$ Where *PSD* is the Power Spectral Density of the signal, *f* is the frequency vector, and *N* is the total number of points of the *PSD*. Frequencies below 0.15Hz are usually ignored. $CF = \sqrt{\frac{\mu_2}{\mu_0}}$	Displacement; Acceleration; Angular Velocity	[Hz]	AP, ML, V
FD	Frequency dispersion; unitless measure of the variability of the power spectral density frequency content (zero for pure sinusoid; increases with spectral bandwidth to one). Spectral moments are needed for the estimate: $\mu_0 = \sum_{i=1}^{N} PSD(i) = TP\,;\ \mu_1 = \sum_{i=1}^{N} f(i)PSD(i)\,;\ \mu_2 = \sum_{i=1}^{N} f^2(i)PSD(i)$ Where *PSD* is the Power Spectral Density of the signal, *f* is the frequency vector, and *N* is the total number of points of the *PSD*. Frequencies below 0.15Hz are usually ignored. $FD = \sqrt{\frac{1-\mu_1^2}{\mu_0\mu_2}}$	Displacement; Acceleration; Angular Velocity	[-]	AP, ML, V
JI	Jerk Index of the acceleration: $JI = \frac{1}{2}\int_{Tstart}^{Tend} (\dot{a})^2\,dt$ where *T* is the duration (*Tend-Tstart*) of the considered component and *a* is the acceleration measured in m/s^2.	Acceleration	[m^2/s^5]	AP, ML, V
tNJS	Time-normalized jerk score of the acceleration: $NJS = \sqrt{\frac{T^5}{2}\int_{Tstart}^{Tend} (\dot{a})^2\,dt}$ where *T* is the duration (*Tend-Tstart*) of the considered component and *a* is the acceleration measured in m/s^2.	Acceleration	[m]	AP, ML, V
NJS	Normalized jerk score of the acceleration: $NJS = \sqrt{\frac{T^5}{2SP^2}\int_{Tstart}^{Tend} (\dot{a})^2\,dt}$ where *T* is the duration (*Tend-Tstart*) of the considered component and *a* is the acceleration measured in m/s^2. SP is the sway path of the displacement.	Acceleration	[-]	AP, ML, V
NAJS	Normalized Angular jerk score: $NJS = \sqrt{\frac{T^5}{2TA^2}\int_{Tstart}^{Tend} (\ddot{\omega})^2\,dt}\,;\ TA = \int_{Tstart}^{Tend} \omega dt$ where *T* is the turn duration (*Tend-Tstart*) of the considered component, ω is the angular velocity °/s, and TA is the Total Angle in °	Angular Velocity	[-]	AP, ML, V

AP = ANTERO-POSTERIOR; ML = MEDIO-LATERAL; PLANAR = PLANE (AP,ML) V = VERTICAL, [-] = UNITLESS; M.U. = MEASUREMENT UNIT

2.1.3 HHT-BASED FILTERING: VALIDATION PROCEDURE AND RESULTS

METHODS

20 early-mild PD subjects OFF medication (Hoehn&Yahr ≤ 3, 62±7 years old, 8 women) and 20 control (CTRL) age-matched subjects (64±6 years old, 14 women) were recruited. Disease severity of the PD group was assessed by qualified medical staff at the Department of Neuroscience, University of Modena and Reggio Emilia, by means of the UPDRS scale. Medical Item 20 of the UPDRS section III, "tremor at rest", was 3.35±2.5 out of 20. The OFF condition was obtained by a levodopa washout of at least 18 hours and a dopamine-agonists washout of at least 36 hours.

Subjects were asked to stand quietly, barefoot, arms crossed on the chest, 2.5 meters from a visual marker placed on a wall (a black circle, diameter 5cm). Foot placement was standardized using an averaged preferred position traced on the floor[1]. To instrument the test we used a tri-axial accelerometer, McRoberts© Dynaport Micromod, with a sample rate of 100Hz and a range of ±2g. The accelerometer was worn on the lower back, by means of a waist belt, at the level of the fifth lumbar vertebra. Two quiet standing conditions were analyzed: single-task (ST) and dual-task (DT). During DT a cognitive subtraction task, from 100 by 3's, was performed. The measurement session included six trials, each lasting T = 30 s, organized in three sequential blocks of the two conditions.

[1] W. E. McIlroy and B. E. Maki, "Preferred placement of the feet during quiet stance: Development of a standardized foot placement for balance testing," Clin. Biomech. (Bristol, Avon), vol. 12, no. 1, pp. 66–70, Jan. 1997.

The aim of the study was to compare the effectiveness of linear low-pass filters (LPF) and HHT-based filtering for tremor removal to estimate a set of postural parameters extracted from acceleration signals. Only a part of the PD group exhibited tremor in some trials; consequently it is possible to evaluate how these preprocessing techniques work with normal subjects, and with both tremorous and non tremorous PD subjects.
The implementation of the HHT is reported in Section 2.1.1. As discussed in Section 2.1.1, the analysis has been limited to the ML direction and the implemented LPF is a Zero-lag 4^{th} order low-pass Butterworth filter with a cut-off frequency of 3.5Hz. We quantified postural sway in quiet standing by means of a subset of parameters computed from the acceleration signal in the time and frequency domains as reported in Section 2.1.2.

Trials classification

The presence of tremor in each trial was detected by visual inspection of the Power Spectral Density (PSD) of the raw signal. Welch's modified periodogram has been used for PSD estimation with Hanning windows of 5s and 50% overlap. A trial was classified as tremorous if all of the following conditions were verified:

- At least one peak was observable in the PSD between 4 and 7Hz;
- The peak was clearly recognizable, even with varying length and % overlapping of the Hanning windows in the PSD estimation;
- The peak was present at approximately the same frequency in both AP and ML direction;

The length of the Hanning window was varied from 3 to 10s, while the overlap was varied from 10 to 60%.

Materials and statistical analysis

MATLAB R2008a was used for signal processing and statistical analysis. Jarque-Bera and Levene tests were used to assess normality and homogeneity of the data, respectively. A Kruskal-Wallis one-way ANOVA and multiple comparisons z-value test with Bonferroni correction have been used to identify differences between three groups of trials: CTRL, PD without tremor (PD-NT), and PD with tremor (PD-T).

Mode Selection Criteria

In order to define a fully automated algorithm for mode inclusion, the selection criterion has been tuned on the IMFs extracted from the Medio-Lateral (ML) acceleration of the CTRL group. HHT has been applied to the signals to obtain the Hilbert spectrum. Considering the time-amplitude-frequency distribution of each IMF, the Median value of its Instantaneous Frequency (MIF) and the Median value of its Amplitude (MA) have been computed. The frequency radius, centered on MIF, containing 95% of the Instantaneous Frequency values (IF95) has also been computed. Because tremor is a non-stationary phenomenon, a threshold of 5% the IMF instantaneous amplitude range has been decided in order to avoid MIF and IF95 overestimation due to noise when the phenomena have very low amplitude.
In most cases, the number of the IMFs obtained through the decomposition is ten. The same characteristic pattern has been observed for all signals consisting of a clear time scale separation (see standard deviations in Table I). For those trials whose decomposition leads to a higher (eleven) or lower (nine) number of IMFs, MIF values and the corresponding MA and IF95 are assigned to the distribution of the time scale with the most consistent statistics. In Table I the distributions of MIF, MA, and IF95 are shown for the first seven time scales.

TABLE I
DISTRIBUTIONS OF MIF, IF95AND MA, MEAN VALUE (STANDARD DEVIATION), OF THE CTRL AND PD GROUP FOR FIRST SEVEN TIME SCALES OF THE EMD.

GROUP	*CONDITION*	*PARAMETER*	*Time Scale 1*	*Time Scale 2*	*Time Scale 3*	*Time Scale 4*	*Time Scale 5*	*Time Scale 6*	*Time Scale 7*
CTRL	*Single Task*	*MIF (Hz)*	32.2(2.3)	11.6(1.1)	6.3(0.6)	3.9(0.3)	2(0.3)	1.1(0.2)	0.5(0.1)
		IF95 (Hz)	22.8(1.9)	12.6(2)	5.2(0.8)	2.6(0.4)	1.6(0.3)	0.9(0.3)	0.5(0.2)
		MA (mm/s²)	5.3(1.4)	11.8(4.2)	13.6(4.4)	10.3(3.1)	9(3.7)	7.9(3.6)	8.8(3.7)
	Dual Task	*MIF (Hz)*	30.5(3.4)	11.4(0.8)	6.3(0.5)	3.7(0.3)	1.8(0.2)	1(0.2)	0.5(0.1)
		IF95 (Hz)	22.3(1.7)	12.5(1.9)	5.1(0.6)	2.7(0.3)	1.6(0.2)	0.8(0.1)	0.5(0.1)
		MA (mm/s²)	7.2(3.2)	16.4(7.3)	19.2(6.3)	15.8(6.1)	17(9.6)	14.6(9.2)	15.7(18.6)
PD	*Single Task*	*MIF (Hz)*	32.2(2.4)	11.3(1)	6.5(0.7)	4.1(0.4)	2.2(0.3)	1.2(0.2)	0.6(0.1)
		IF95 (Hz)	22.8(2.2)	12.6(1.8)	5(0.8)	2.6(0.4)	1.7(0.2)	0.9(0.1)	0.6(0.1)
		MA (mm/s²)	6.5(2.9)	25.5(46.3)	33.3(55.8)	21.3(29)	9.4(6.9)	7.4(3.8)	8.8(5.4)
	Dual Task	*MIF (Hz)*	30.3(3.7)	10.7(1)	6(0.5)	3.7(0.4)	1.9(0.2)	1.1(0.2)	0.5(0.1)
		IF95 (Hz)	22.4(1.7)	11.9(1.6)	4.7(0.5)	2.5(0.3)	1.6(0.3)	0.9(0.1)	0.5(0.1)
		MA (mm/s²)	13.1(22.5)	107.7(228.3)	117.1(229.2)	33.6(54.8)	14.7(10.2)	10.8(6.8)	10.1(6)

As can be seen in Table I, the first four time scales are clearly attributable to noise/tremor since their frequency content cannot be associated with the postural stabilization process. Time scales 6, 7, and higher can be included in the signal reconstruction, because their characteristics are compatible with the bandwidth of postural sway. As for time scale 5, if we consider its MIF and IF95, the associated bandwidth partially overlaps the bandwidth of the tremor at rest in most cases. For all time scales, MA values of the CTRL group are quite homogeneous.
In Table I the values obtained for the PD group are also reported. It can be noted that MIF and IF95 values are quite similar between groups for all time scales. In contrast, MA values show different behaviors across scales: at time scales 2, 3, and 4 they are higher and more variable in the PD than in the CTRL group, particularly in DT condition, while at

time scale 5 they are comparable between groups. Notably, at time scale 1 mode properties are consistent with those of white noise in both groups. On the basis of these findings we decided to include in the signal reconstruction only those modes (IMFs) that exhibit an MIF below 2.4Hz and an MA below 30mm/s^2. Considering values computed in all conditions, the chosen MIF and MA thresholds are about halfway between the minimum value of time scale 4 and the maximum value of time scale 5. An example of the mode selection algorithm is presented Figure 4, the signal reported in the figure refers to the decomposition of the ML acceleration of a healthy subject.

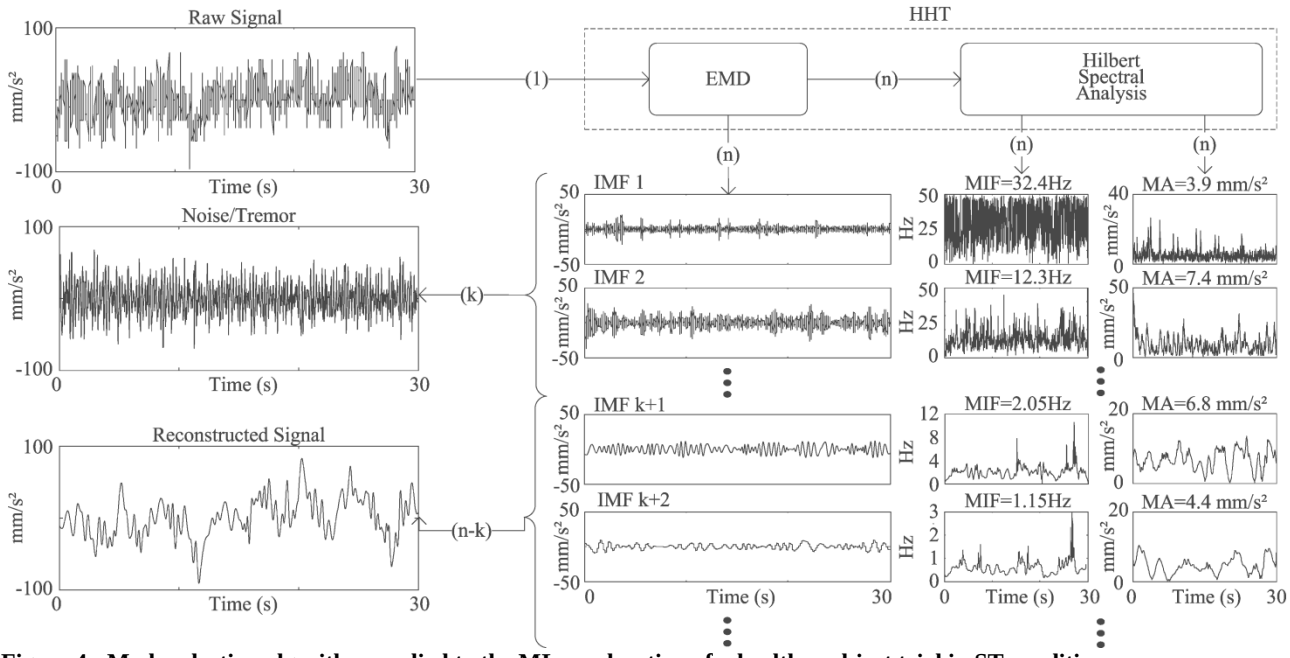

Figure 4 - Mode selection algorithm applied to the ML acceleration of a healthy subject trial in ST condition.

RESULTS

Trials classification

Out of 60 PD trials, 28 and 36 trials were classified as tremorous in ST and DT conditions, respectively. Seven subjects had all 3 trials classified as tremorous in ST, eleven subjects in DT. Some subjects exhibited both tremorous and non tremorous behavior (5 in ST, 2 in DT).

LPF and HHT comparison

Table II summarizes the results of the two preprocessing methods, LPF and HHT. Postural parameters are reported for the three groups of trials (CTRL, PD-NT, and PD-T) in the ST and DT conditions. In most cases, normality is not verified for either HHT or LPF; that is the reason for the adoption of the Kruskal-Wallis non-parametric test. Values are reported with a grey background when variance homogeneity is not verified.

TABLE II
DISTRIBUTION MEAN VALUE (STANDARD DEVIATION) OF THE POSTURAL PARAMETERS FOR CTRL, PD-NT AND PD-T TRIALS

METHOD & CONDITION	GROUP	RMS [mm/s^2]	RANGE [mm/s^2]	MV [mm/s]	F95 [Hz]	CF [Hz]	JI [m^2/s^5]
HHT-ST	CTRL	21.3(9.8)	119.8(55.2)	4.51(2.23)	2.24(0.4)	1.05(0.23)	0.16(0.19)
	PD-NT	21.7(12.3)	104.1(44.4)	3.83(1.86)	2.25(0.48)	1.02(0.29)	0.1(0.06)
	PD-T	25.7(15.3)	136.1(78.7)	4.67(2.71)	2.14(0.59)	0.98(0.29)	0.25(0.47)
HHT-DT	CTRL	29.8(15.3)	177.2(128.1)	5.88(3.21)	2.15(0.56)	1.06(0.31)	0.39(0.42)
	PD-NT	20(9.6)	110.7(40.3)	4.56(3.3)	2.54(0.39)	1.22(0.26)	0.18(0.12)
	PD-T	28(10.3)	163.7(77.7)	6.86(5.52)	2.2(0.47)	1.07(0.28)	0.35(0.45)
LPF-ST	CTRL	21.8(9.7)	130.2(56.6)	7.15(4.87)	2.87(0.56)	1.32(0.29)	0.27(0.27)
	PD-NT	21.9(12.3)	109.9(46.8)	6.42(5.02)	2.62(0.54)	1.19(0.35)	0.17(0,16)
	PD-T	26.6(15.5)	158.8(89.4)	11.09(12.3)	3.55(1.01)	1.7(0.68)	1.1(2.07)
LPF-DT	CTRL	35.3(23.3)	233.3(192.1)	13.63(12.76)	2.96(0.48)	1.4(0.27)	1.08(1.26)
	PD-NT	21(10.4)	126.3(64.9)	9.22(7.29)	3.12(0.45)	1.52(0.36)	0.51(0.98)
	PD-T	31.3(14.3)	266.6(222.6)	39.69(67.17)	3.89(1.02)	1.96(0.79)	3.46(6.43)

CTRL: control group trials. PD-NT: PD group trials with no tremor. PD-T: PD group trials with tremor. Grey background means that variance homogeneity is not verified. Brackets refer to the Kruskal-Wallis multiple comparison test with Bonferroni correction.
(*:$P < 0.05$,**:$P<0.01$;***:$P<0.001$)

None of the parameters computed using HHT in ST condition shows significant statistical differences among the groups of trials. In DT condition, statistical differences can only be noted between PD-NT and the other two groups, with the exception that MV that is significantly different only between PD-NT and PD-T ($p<0.05$). Statistical comparison of RMS leads to a significant difference between PD-NT and both CTRL ($p<0.001$) and PD-T ($p<0.01$); for RANGE,

significant differences are $p<0.01$ and $p<0.05$ respectively; for F95, they are $p<0.01$ and $p<0.01$ respectively; and for JI they are $p<0.01$ and $p<0.05$ respectively. There are no significant differences for CF in any case.
For LPF in ST condition: F95 of PD-T group is statistically significantly different from both CTRL ($p<0.01$) and PD-NT ($p<0.001$); RANGE and CF of PD-T group are statistically significantly different from CTRL ($p<0.05$ and $p<0.01$, respectively) JI distribution of PD-NT group is statistically significantly different from both CTRL ($p<0.01$) and PD-T ($p<0.001$). In DT condition: for RMS, RANGE and JI,, differences are found between PD-NT and both CTRL ($p<0.001$ for RMS and JI, $p<0.01$ for RANGE) and PD-T ($p<0.01$ for RMS and RANGE, $p<0.001$ for JI). Regarding MV, the PD-T distribution is statistically significantly different from that of PD-NT group ($p<0.001$). Considering the frequency parameters F95 and CF, PD-T group is statistically significantly different from both CTRL ($p<0.001$ for F95 and CF) and PD-NT ($p<0.001$ for F95 and $p<0.05$ for CF).

DISCUSSION

A novel non-linear method, based on Hilbert-Huang transformation, has been introduced for filtering the tremor component and high-frequency noise from accelerometer recordings of trunk sway during quiet stance. Tremor suppression is important because accelerometer signals recorded during quiet standing are usually very sensitive to the presence of a pronounced rhythmic behavior. Approximately half of the trials of our PD patients exhibited tremor, whose amplitude may vary between and within subjects/trials. Most of our PD group is composed of subjects at an early stage of the disease, when tremor at rest is often at higher frequency and lower amplitude. During the disease progression the frequency of tremor tends to decrease and, at the same time, the amplitude tends to increase[1]. This means that the use of a reliable tremor suppression method becomes far more critical as the disease severity increases.

Pre-processing effects

As can be observed in Table II, summary statistics measures associated with properties of the signals in the time domain, like RMS and RANGE, are almost insensitive to the preprocessing method. What can be noted, when LPF is used, is that for each parameter the variability and mean value are always higher in any condition, particularly for the PD-T group. For RMS the difference between LPF and HHT-based filtering is really small; however, the difference in RANGE values increases as the signal-to-noise ratio worsens. As far as MV is concerned, it shows a high sensitivity to noise/tremor if LPF is used, which is greatly magnified by the presence of the DT. This sensitivity can be ascribed to an inefficient tremor suppression which affects the integration involved in the parameter computation. The proper estimation of MV (or similar velocity-related parameters) is particularly important since this parameter has been proven of clinical value in several contexts where subjects suffer from tremor, including studies about age-related postural changes[2], the prediction of future falls, and identification of recurrent fallers[3].
Not surprisingly, frequency domain parameters were also very sensitive to the filtering method; values obtained using LPF are up to two times higher than those using HHT (F95 reaches 5Hz and CF can be higher than 3Hz). The higher values obtained for F95 and CF using LPF, for some trials well beyond the typical postural frequency bandwidth, are the effect of higher frequency components due to tremor and noise which are not adequately suppressed. The effect of tremor was particularly high in DT.
It has to be noted that, as described in Section 2.1.2, postural parameters in the frequency domain were calculated using a PSD estimation which is based on Fourier transformation. As pointed out in Section 2.1.1, it is not easy to characterize how, in a biological system like posture control, unwanted components (e.g. tremor) and noise are mixed with the desired signal. So, with an uncertainty about the linear and stationary properties of the signal, the computation of parameters like CF and F95 may violate the validity assumptions of the Fourier Transformation. Still, the parameters have been computed using FFT-based PSD estimation in accordance with what is done in literature [2 4 5]. JI is commonly employed in motor control studies as an index of smoothness[6]. In one of the first applications of this parameter to the assessment of postural sway in early PD[7], it was found to be very sensitive to the disease and its progression. Table II shows that the mean and variance of the JI distribution computed using LPF are higher than those computed using HHT. This difference can be ascribed to the time-derivative of the acceleration, which acts as a noise amplifier: the higher the noise/tremor remaining in the signal, the larger the JI.

---

[1] B. Hellwig, P. Mund, B. Schelter, B. Guschlbauer, J. Timmer, and C. H. Lucking, "A longitudinal study of tremor frequencies in Parkinson's disease and essential tremor", J. Clin. Neurophysiol., vol. 120, no. 2, pp. 431-435, Feb.2009.

[2] T. E. Prieto, J. B. Myklebust, R. G. Hoffmann, E. G. Lovett, and B. M. Myklebust, "Measures of postural steadiness: differences between healthy young and elderly adults", IEEE Trans. Biomed. Eng, vol. 43, no. 9, pp. 956-966, Sept.1996.

[3] M. Piirtola, P. Era, "Force platform measurements as predictors of falls among older people - a review", Gerontology, vol. 52, no. 1, pp. 1-16, Jan.2006.

[4] L. Rocchi, L. Chiari, and F. B. Horak, "Effects of deep brain stimulation and levodopa on postural sway in Parkinson's disease," J. Neurol. Neurosurg. Psychiatry, vol. 73, no. 3, pp. 267–274, Sep. 2002.

[5] R. E. Mayagoitia, J. C. Lotters, P. H. Veltink, and H. Hermens, "Standing balance evaluation using a triaxial accelerometer," Gait Posture, vol. 16, no. 1, pp. 55–59, Aug. 2002.

[6] T. Flash, N. Hogan, "The coordination of arm movements: an experimentally confirmed mathematical model", J. Neurosci., vol. 5, no. 7, pp. 1688-1703, Jul. 1985.

[7] M. Mancini, C. Zampieri, F.B. Horak and L. Chiari, "Accelerometry-based longitudinal biomarkers of stance posture in early Parkinson's disease", Gait Posture, vol. 29, suppl. 1, pp. e25, Jan.2009.

As far as statistical testing is concerned, it is worth noting that variance homogeneity is always verified using HHT but not LPF (see Table II). For this reason, the statistical comparisons involving LPF-based parameters should be interpreted with care.

To make a clarifying example, a trial has been selected which is always quite noisy but tremor is clearly present only in its last part. In Figure 5(a), the first and second halves of the trial have been treated as two independent signals. As can be seen in the PSD estimation, the second half of the signal (PSD dotted line in Figure 5(a)) shows a tremor peak near 5Hz. Parameters computed using HHT (black bars in Figure 5(b)) are quite homogeneous between the first and second halves of the signal. In contrast, parameters computed using LPF in the second half (grey bars in Figure 5(b)) are always higher than the ones computed in the first half, MV and JI in particular, which are the most sensitive. F95 and CF are also very sensitive to the filtering method reaching 5Hz and 2.3Hz respectively in the second half. RMS, as can be seen in Table II, is quite insensitive to the filtering method. Signal-to-noise ratio is low and the values obtained are systematically lower using HHT compared to LPF.

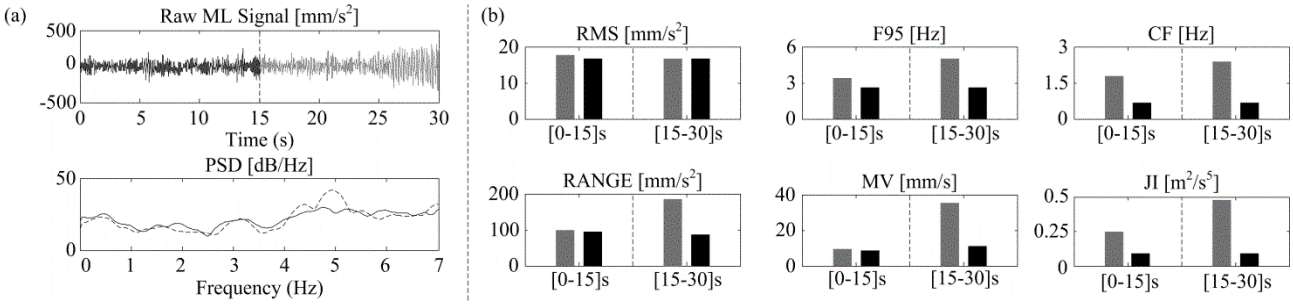

Figure 5 - (a) Raw ML acceleration divided in two independent signals of the same length (top), (bottom) PSD of the first half is reported with a solid line while PSD of the second half is reported with a dotted line. It can be noted that in the PSD estimation of the second half of the signal (dotted line) a peak due to tremor is present near 5 Hz. (b) Postural parameters: values relative to the first half are shown on the left; values relative to the second half are shown on the right. Grey bars refers to the values computed using LPF while black bars refers to the values computed using HHT.

The empirical nature of HHT and its ability to handle non-stationary and non-linear time series allow the adaptive identification of faster/slower dynamics, which may take place in the signal within the same time scale. These features of HHT are particularly evident when the tremor amplitude is high. The capability of HHT to selectively track and preserve local structures of the original time series, which Fourier-based LPF does not have, is highlighted in the representative example of Figure 3. The two signals represent a non tremorous trial (Figure 6(a)) and a tremorous trial (Figure 6(b)) for the same PD subject, who exhibits tremor with very high amplitude in stressful conditions such as DT. When there is no tremor, no significant differences are observed between HHT and LPF within the pass-band. However, in DT condition a pronounced tremor peak is present near 5Hz; the PSD of the noise/tremor component obtained from HHT shows large values within the pass-band that capture the low frequency sub-harmonics of tremor (not captured by LPF). Instantaneous frequencies of time scales 4, 5, 6, and 7, obtained through the decomposition of the signal in Figure 6(b), are reported in Figure 6(c).

The adaptivity of HHT is disclosed by the time-frequency features of time scale 5 (represented by the instantaneous frequency of the corresponding IMF), assigned by the mode selection criterion to the signal component, which shows how dynamics both faster and slower than 3.5Hz are preserved in the reconstructed signal. It is worth noting that time scale 4 in Figure 6(c) contains the tremor dynamics centered on the same frequency of the peak in the PSD reported in the central-right panel in Figure 6(b). On the other hand, LPF is only able to block or smooth the overall dynamic of the signal that exceeds its cut-off frequency (see central-right panels in Figure 6). The residual peak of tremor, clearly present in the PSD of the difference between HHT and LPF (Figure 6(b) right panel), can be eliminated by lowering the cut-off frequency and increasing the filter order, but nothing can be done to the frequency content within the pass band.

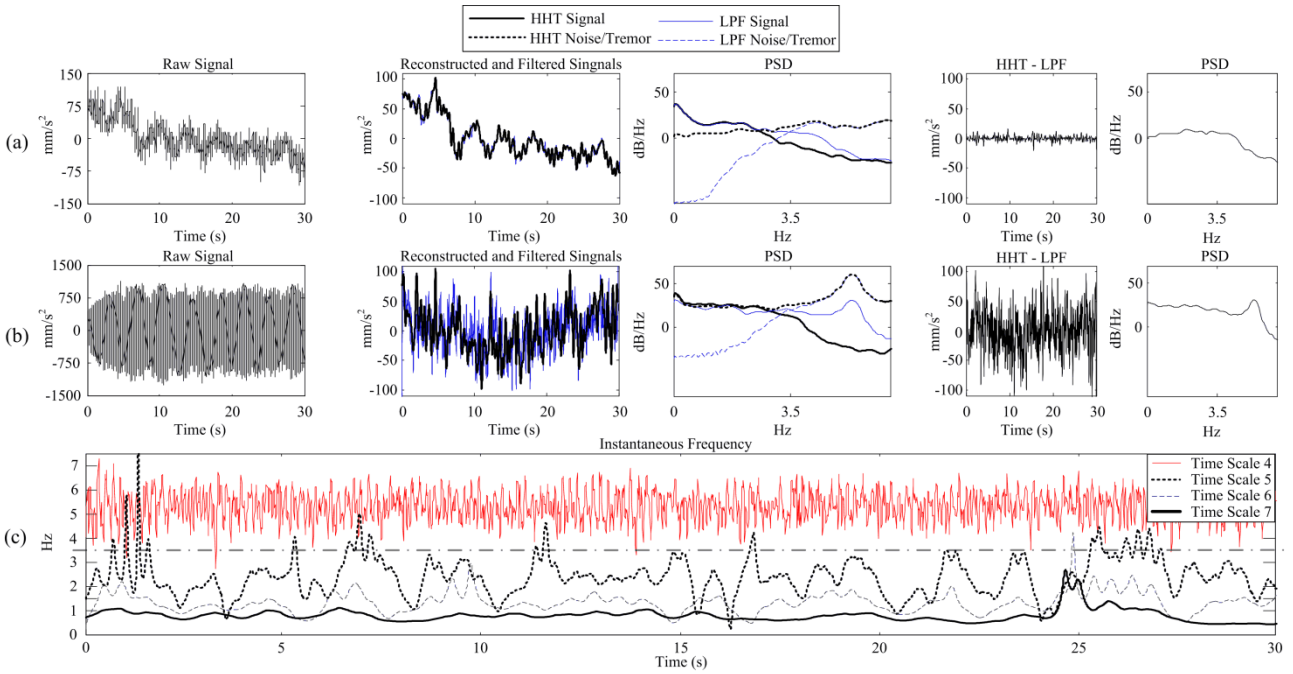

Figure 6 - Pre-processed ML acceleration relative to (a) a non tremorous trial in ST condition and (b) a tremorous trial in DT condition relative to the same PD subject. In the left panels the raw signals are shown. In the central-left panels, the reconstructed signal, using HHT (thick line), and the filtered signal, using LPF (thin line), are shown. In the central-right panels the PSD of the reconstructed signal (thick line), the filtered signal (thin line), the HHT noise/tremor component (dotted thick line), and the LPF noise/tremor component (dashed thin line) are shown. In the two smaller right panels the difference between the reconstructed and the filtered signal is displayed together with the corresponding PSD. (c) Instantaneous frequency of the time scales 4, 5, 6, and 7 obtained from the decomposition of the tremorous trial shown in (b).

HHT design issues

HHT, or more often the EMD algorithm alone, has been applied in many research fields; when a reference solution was available, performance comparisons have been made with other analysis techniques such as wavelet, autoregressive methods, traditional filters, and Independent Component Analysis[1] [2] [3]. These comparisons show that HHT/EMD can work better than traditional methods. Dealing with biological processes, typically characterized by some degree of non-linearity and non-stationarity, HHT/EMD has been successfully used for denoising, detrending, identification of modes with physical meaning, artifact removal and other applications[4] [5].

As a consequence of the empirical nature of HHT, it is important to control options during the decomposition and mode selection phases. One can choose these options from observation and *a priori* knowledge of the studied phenomena, but there are also methodological issues that have to be considered. (i) The estimation of the upper and lower envelopes is usually done, as in this study, by a cubic spline interpolation, but other types of interpolation may work equally well or even better (e. g. applications involving irregular waves[6]). (ii) Close attention must be paid to the borders of the time series in order to avoid large swings in the envelope, since uncontrolled swings could be very critical in a low frequency signal. The solution of adding extrema by mirror symmetry[7] gave good results for the presented data, but other methods have been proposed[8] [9] to control this border effect. (iii) Oversampling is needed to correctly identify extrema and to prevent mode-mixing. To this aim, sampling at 100Hz proved adequate for postural signals which have a bandwidth (even in the eventuality of tremor) well below 10Hz. The following are other ways to control mode-mixing. In a later

[1] S. Liu, Q. He, R. X. Gao, and P. Freedson, "Empirical mode decomposition applied to tissue artifact removal from respiratory signal", Conf. Proc. IEEE Eng Med. Biol. Soc., vol. 2008, pp. 3624-3627, 2008.

[2] B. N. Krupa, M. A. M. Ali, and E. Zahedi, "The application of empirical mode decomposition for the enhancement of cardiotocograph signals", Physiol. Meas., vol. 30, no. 8, pp. 729-743, Aug.2009.

[3] Y. Ye-Lin, J. Garcia-Casado, G. Prats-Boluda, J. L. Ponce, and J. L. Martinez-de-Juan, "Enhancement of the non-invasive electroenterogram to identify intestinal pacemaker activity", Physiol. Meas., vol. 30, no. 9, pp. 885-902, Sept.2009.

[4] H. L. Liang, S. L. Bressler, E. A. Buffalo, R. Desimone, and P. Fries, "Empirical mode decomposition of field potentials from macaque V4 in visual spatial attention", Biol. Cybern., vol. 92, no. 6, pp. 380-392, June2005.

[5] M. Costa, A. A. Priplata, L. A. Lipsitz, Z. Wu, N. E. Huang, A. L. Goldberger, and C. K. Peng, "Noise and poise: Enhancement of postural complexity in the elderly with a stochastic-resonance-based therapy", Europhys. Lett., vol. 77, no. 6, 68008, Mar.2007.

[6] M. Datig and T. Schlurmann, "Performance and limitations of the Hilbert-Huang transformation (HHT) with an application to irregular water waves", Ocean Eng., vol. 31, no. 14-15, pp. 1783-1834, Oct.2004.

[7] G. Rilling, P. Flandrin, and P. Gonçalvès, "On empirical mode decomposition and its algorithms", Proc. 6th IEEE/EURASIP Workshop on Non Linear Signal and Image Processing (NSIP '03), Grado, Italy, 2003.

[8] J. Wang, Y. Peng, and X. Peng, "Similarity searching based boundary effect processing method for empirical mode decomposition", Electron. Lett., vol. 43, no. 1, pp. 58-59, Jan.2007.

[9] Z. Zhao and Y. Wang, "A New Method for Processing End Effect In Empirical Mode Decomposition", Proc. Int. Conf. Communications, Circuits and Systems (ICCCAS '07), Kokura, Fukuoka, Japan, pp. 841-845, 2007.

interpretation of EMD as a filter bank[1], it was shown that the use of a masking signal[2] could improve mode separation during the sifting process. Another way to effectively overcome mode-mixing is to use a uniform reference time scale with different white noises; this method is called Ensemble EMD (EEMD) and has been developed by Wu and Huang[3]. EEMD introduces two new parameters for the decomposition: the number of ensembles and the noise amplitude that must be properly selected. Notably, modes obtained with EEMD are not necessarily IMFs; in this case the Hilbert spectral analysis may not be feasible since such components can have significant alias. For these reasons, in the absence of a proper reference solution, the original EMD method has been applied, but potential refinement of the filtering method may be discussed in future studies. (iv) Over-decomposition should be avoided, so the stopping criterion of the sifting process is also important [36]. At any point, has been assumed that the mean value of the envelope defined by the local maxima and the envelope defined by the local minima is zero if $|m(t)/A(t)| < 0.05$. This differs from the usage of two thresholds in different parts of the signal that was proposed in [21]; there is no reason here to hypothesize abrupt variations in trunk acceleration during unperturbed stance. (v) A proper mode selection criterion should be applied after the decomposition, in order to correctly separate the signal from noise/tremor components. Based on *a priori* knowledge about the stabilization process in quiet standing, it has been hypothesized that an IMF is descriptive of this process if its frequency content becomes negligible above 3Hz and its amplitude does not exceed the values obtained in the absence of tremor. Hence a novel mode selection criterion has been developed without using Fourier transformation of the signal, although it is the procedure most commonly used in the literature.

The time-frequency distribution has been estimated through Hilbert spectral analysis. Computing MIF and MA for each IMF, a clear time scale separation and the same characteristic pattern for each signal have been verified. On the basis of the MIF values obtained in the CTRL group, in the signal reconstruction are included only those modes which exhibit an MIF below 2.4Hz and an MA below 30mm/s^2.

There are two recent advancements by Huang and colleagues: the first concerns a refinement of the EEMD method, called Complementary EEMD[4], which seems to effectively eliminate the residual noise in the signal reconstruction; the second concerns the correlation analysis between non-linear and non-stationary time series[5]. The impact of these advancements on the current issue may be evaluated in a future study.

LPF design issues

As discussed in Section 2.1.1, linear filtering is the most common technique to remove tremor contribution from postural signals. The filter design process can be described as an optimization problem where several factors, including filter type, order, and cut-off frequency, need to be properly set to maximize filter performance and avoid non-ideal behaviors. Figure 7 shows the effects of different choices for LPF order (from 2 to 12) and cut-off frequency (from 1.5 to 4.25Hz) on two postural parameters which proved to be sensitive to tremor, using a Butterworth filter. As expected, the choice is less critical when trials do not exhibit pathological tremor (CTRL and PD-NT). In this case as the cut-off frequency increases we observe only a slight increase of the parameter value, which is essentially due to the amount of high frequency noise that increases with bandwidth. In contrast, in the PD-T trials, filter order and cut-off frequency are both critical. The cut-off frequency (3.5Hz) and filter order (4) used so far in this paper are within the range of typical values found in the literature for force plate-based postural investigations. The use of accelerometers in posture analysis is in fact relatively new, but it must be considered that force plate and accelerometer measures have similar frequency content[6] and sensitivity to tremor[7]. It is true that most of the postural signal power is at lower frequencies, but postural control mechanisms also act at higher frequencies[8]; a bandwidth too narrow may not be able to collect the whole signal dynamics. Keeping a wider bandwidth is important, particularly when investigating pathological subjects.

[1] P. Flandrin, G. Rilling, and P. Goncalves, "Empirical mode decomposition as a filter bank", IEEE Signal Process. Lett., vol. 11, no. 2, pp. 112-114, Feb.2004.

[2] R. Deering and J. F. Kaiser, "The use of a masking signal to improve empirical mode decomposition", Proc. IEEE Int. Conf. Acoustic, Speech, and Signal Processing (ICASSP '05), vol.4 , pp. iv/485-iv/488, 2005.

[3] Z. Wu and N. E. Huang, "Ensemble Empirical Mode Decomposition: A Noise-Assisted Data Analysis", Adv. Adapt. Data Anal., vol. 1, no. 1, pp. 1-41, Jan.2009.

[4] J. R. Yeh, J. S. Shieh, N. E. Huang, "Complementary Ensemble Empirical Mode Decomposition: a Novel Noise Enhanced Data Analysis Method", Adv. Adapt. Data Anal., vol. 2, no. 2, pp. 135-156, Apr.2010.

[5] X. Chen, Z. Wu, N. E. Huang, "The Time-Dependent Intrinsic Correlation Based on the Empirical Mode Decomposition", Adv. Adapt. Data Anal., vol. 2, no. 2, pp. 233-265, Apr.2010.

[6] L. Chiari, M. Dozza, A. Cappello, F.B. Horak, V. Macellari and D. Giansanti, "Audio-biofeedback for balance improvement: an accelerometry-based system", IEEE Trans. Biomed. Eng., vol. 52, no. 12, pp. 2108-2111, Dec.2005.

[7] K. Yarrow, P. Brown, M. A. Gresty, and A. M. Bronstein, "Force platform recordings in the diagnosis of primary orthostatic tremor", Gait Posture, vol. 13, no. 1, pp. 27-34, Feb.2001.

[8] I. D. Loram, C. N Maganaris and M. Lakie, " Human postural sway results from frequent, ballistic bias impulses by soleus and gastrocnemius", J. Physiol., vol. 564(Pt 1), pp. 295-311, Apr.2005.

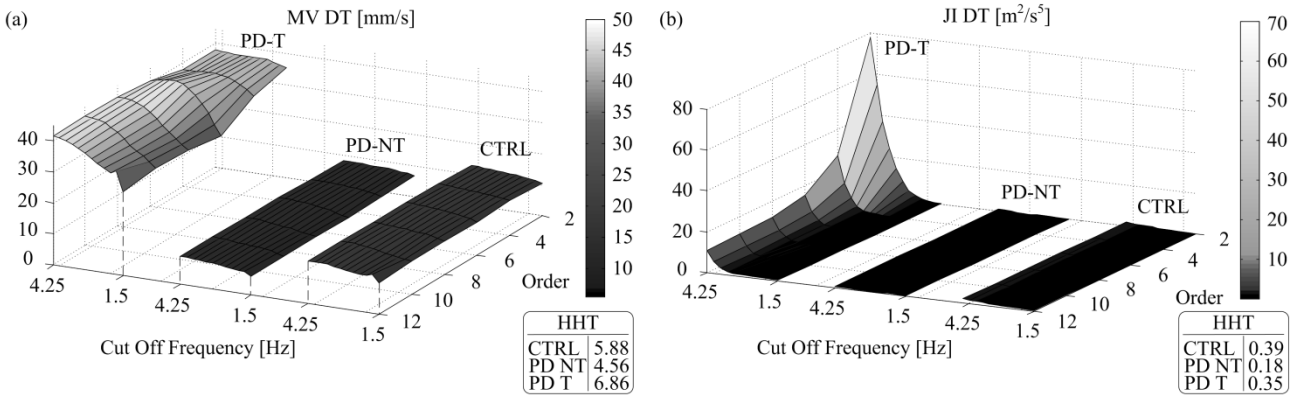

Figure 7 - (a) Mean Value of MV distribution in DT condition calculated using LPF, as a function of filter order and cut-off frequency. (b) Mean Value of JI distribution in DT condition calculated using LPF, as a function of filter order and cut-off frequency. The mean values of the same parameters computed after HHT are reported in the boxes.

CONCLUSIONS

HHT can be used to effectively remove tremor artifacts from postural parameters in those trials of Parkinson's subjects which are most affected by this non-stationary symptom of the disease. This work shows that LPF and HHT-based filtering leads to similar results when subjects do not have tremor. However, some postural parameters (mean velocity, frequency-domain parameters, and jerk) are strongly affected by high-frequency tremor components; thus inefficient tremor suppression may mask the underlying postural performance. Using LPF, cut-off frequency and the order of the filter must be accurately set to avoid misleading results and interpretations. On the other hand, HHT is a very powerful tool for signal analysis, capable of handling non-linear and non-stationary signals. On the basis of the results presented and discussed so far, HHT-based filtering is recommended as an efficient and robust tool for tremor removal that allows the preservation of local dynamics without sacrificing frequency bandwidth. Findings in this study, which are valuable for a clinical application, are reported in Section 2.4.

2.1.4 DETECTING DYSKINESIA

Levodopa remains the most-effective treatment for Parkinson's disease (PD) despite the risk of Levodopa-Induced Dyskinesia (LID). Assessment of LID is based on clinical scales administered by physicians. Movement disorders in PD not only can rapidly change over time, but their characteristics and intensity can fluctuate in relation to Levodopa treatment during the day[1]. The possibility to obtain reliable and clinically relevant information about LID, by means of a wearable inertial sensor, would allow an objective assessment in both supervised and unsupervised settings. It has been verified if inertial sensor-based static posturography can reliably detect LID during kinetic-dynamic Levodopa monitoring in a group of PD patients.

Methods

46 PD patients (28 males; 63±9 yrs; Hoehn-Yahr 1-3) underwent kinetic-dynamic Levodopa monitoring with the intake of the usual morning dose followed by serial measurements of plasma Levodopa concentration, motor tests, and dyskinesia rating. The assessment was performed every 15 minutes for the first 90 minutes, then every 30 minutes, for a maximum of 4 hours. 18 de novo PD patients (13 males; 59±9 yrs; Hoehn-Yahr 1-2) and 18 healthy controls (CTRL; 9 males; 60±11 yrs) performed the same motor tests. Dyskinesia were rated and scored by means of the Clinical Dyskinesia Rating Scale (CDRS, range 0-4). Motor tests included Quiet Standing (QS) trials.

Subjects were asked to stand upright, barefoot, with arms crossed on the chest, looking at a visual marker (a black circle, 5 cm in diameter) placed on a wall 2m in front of them. Foot placement was kept consistent over trials using an averaged preferred position traced on the floor[2]. The subjects were tested with Eyes Open (EO), Eyes Closed (EC), and Eyes Open Dual Task (EODT). Each trial lasted 30s. A serial 3 subtraction task, randomly starting from 80 to 100, was performed during Dual Task. To instrument the test, we used an inertial sensing unit embedding a tri-axial accelerometer, and gyroscope (McRoberts Dynaport Hybrid, sample rate 100 Hz, accelerometer range ±2 g, gyroscope range ±200 °/s). The device was worn on the lower back (L5) by means of an elastic belt.

Raw signals were transformed to a horizontal-vertical coordinate system[3] in order to compensate the tilt of the device. The nonlinear filtering procedure based on Hilbert–Huang Transform described in Section 2.1.3 was applied to the raw signals for tremor removal. Postural sway in QS has been quantified by means of a set of parameters as described in

[1] Jankovic J, Poewe W. Therapies in Parkinson's disease. Curr Opin Neurol. 2012 Aug;25(4):433-47

[2] L. Chiari, L. Rocchi, and A. Cappello, "Stabilometric parameters are affected by anthropometry and foot placement," Clin. Biomech. (Bristol, Avon), vol. 17, no. 9–10, pp. 666–677, Nov. 2002.

[3] R. Moe-Nilssen. A new method for evaluating motor control in gait under real-life environmental conditions. Part 1: The instrument. Clinical Biomechanics1 3(1998)3 20-327

Section 2.1.2. CTRL and de novo PD performed 5 repetitions with a 10 to 15 minutes resting period in between during which the belt was often removed. A reliability analysis was performed (Intraclass Correlation Coefficients, ICC(3,1)) on CTRL and de novo PD measures over 4 repetitions not including the first one because subjects tended to move or talk during the first assessment. PD group was not included in the reliability analysis because of the Levodopa-induced motor changes during the monitoring.

The values obtained in the healthy age-matched control group have been used as a reference in order to define the distribution of "normal" values. The ninetieth percentiles (90p) and the range of the normal distributions have been used to define the dyskinesia identification criteria. Tremor at rest, measured by means of the ML acceleration, has been used for discriminating between Dyskinesia-induced sway modifications and Tremor-induced sway modifications. A threshold defined as 90p of the tremor parameter plus one fourth of the CTRL measured range has been used for discriminating between Dyskinesia-induced sway modifications and Tremor-induced sway modifications. Three thresholds were defined for assigning a score to each parameter: A score of 0 was assigned to the measure if below 90p (no dyskinesia), a score of 1 was assigned to the measure if above 90p but below 90p plus half of the normal range, a score of 2 was assigned to the measure if above 90p plus half the normal range but below 90p plus the normal range, a score of 3 was assigned to the measure if above 90p plus the normal range. LID was considered present if two or more consecutive repetitions had a score ≥ 1, at least one of the repetitions had a score = 3, and the tremor was sub-threshold. The time of the onset of a dyskinesia episode was then defined as the time when the first repetition included in the episode was performed and the end was defined as the time when the last repetition included was performed.

Results

A subset of 5 parameters has been selected as suitable for clinical applications which were reliable in every condition (ICC $\geq$ 0.7 in EO, EC, and EODT condition). The subset included measures from both accelerometer and gyroscope and they were mostly related with the linear/angular sway velocity in Medio-Lateral (ML) direction and with tremor at rest (Table XYZ). 13 patients were classified as dyskinetic according with CDRS

TABLE XYZ
RELIABILITY ANALYSIS: POSTURAL PARAMETERS FROM CONTROL GROUP AND DE NOVO PARKINSON'S DISEASE PATIENTS. ANALYSIS PERFORMED OVER 4 REPETITIONS

PARAMETER	ICC(3,1) EYES OPEN	ICC(3,1) EYES CLOSED	ICC(3,1) DUAL TASK
ML Mean Velocity (displacement)	0,90	0,81	0,77
ML Mean Angular Velocity	0,92	0,88	0,83
ML %Tremor (acceleration)	0,84	0,84	0,78
AP %Tremor (acceleration)	0,79	0,74	0,81
V %Tremor (acceleration)	0,84	0,80	0,76

ACRONYMS: ML = MEDIO-LATERAL; AP = ANTERO-POSTERIOR; V = VERTICAL; %TREMOR = POWER PERCENTAGE IN THE TREMOR FREQUENCY BAND; ICC = INTRACLASS CORRELATION COEFFICIENTS

Best results in detecting dyskinesia during QS trials were obtained considering mean angular velocity in medio-lateral direction in EODT condition (Figure 8 A, 97.5% of overall accuracy). Time to onset and offset of dyskinesia as assessed by CDRS *vs* single inertial sensor is reported for each patient in QS (Figure 8 A). Intra-patient dyskinesia patterns overlapped in most cases. Instrumental dyskinesia detection was lacking when low-severity involuntary movements affected distal body segments (face, feet).

The same method developed for QS sway quantification was applied while patients were sitting and free to perform any activity. The aim was to simulate a hypothetical monitoring protocol to be performed at home when the person is safely seated. Subjects were not only monitored while performing functional tests but their activities were continuously recorded during the whole time spent in the clinic. It was possible to manually select a series of time intervals when the subject was seated for the 13 patients who were classified as diskinetic by means of the clinical assessment. Patients did not receive any instruction and they were free to perform any activity. Results in detecting dyskinesia in sitting position are reported in Figure 8 B.

Conclusions

Although the proposed approach is not effective when dyskinesia is only distal with a low to moderate intensity, this preliminary results support the hypothesis that a safe, reliable, and relatively easy monitoring of dyskinesia is possible and it could be performed even in unsupervised settings like the home environment.

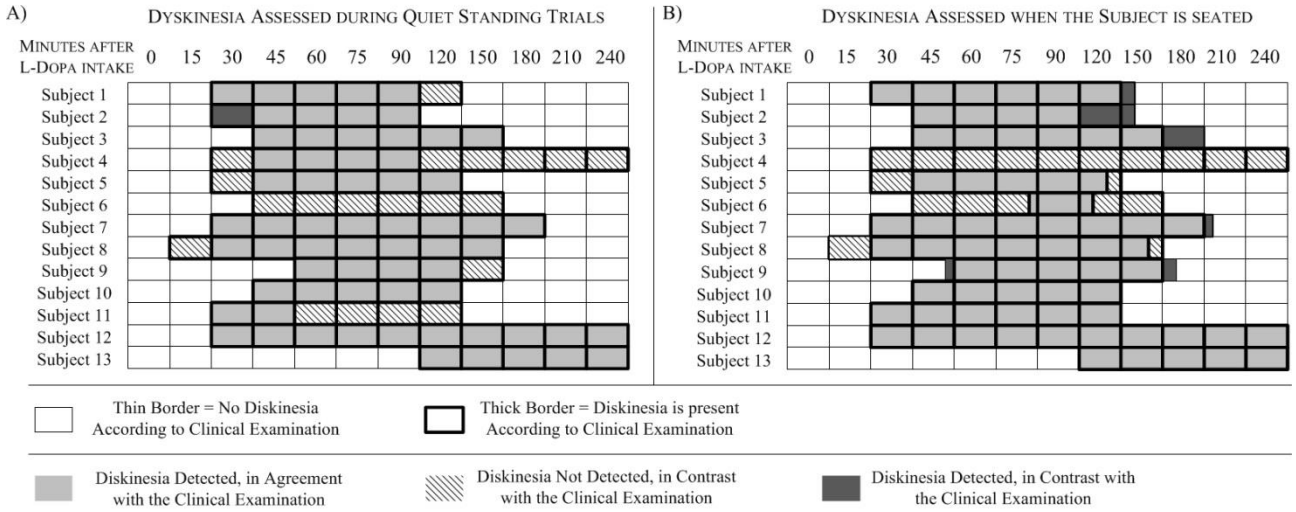

Figure 8 – A) Results in detecting Dyskinesia during quiet standing trials including onset and offset estimate. A) Results in detecting Dyskinesia when subjects were seated including onset and offset estimate. Acronyms: L-Dopa = Levodopa.

2.2 GAIT ANALYSIS

As reported in Section 1, the evaluation of motor control during walking is very important in clinical practice. Deviations from the normal gait pattern can be caused by many factors like trauma, neurological diseases, or simply age and weight. Recent developments of feasible body worn accelerometer- and gyroscope-based sensor systems have made it possible to develop algorithms for calculation of gait characteristics over longer distances in natural settings instead of being limited to be inside a movement analysis lab but the next step is to develop reliable methods for long-term monitoring in real life during the daily routine.

Several methods have been proposed in literature for estimating spatio-temporal gait parameters but most of them make use of multiple wearable sensing units[1] while the present work focuses on a minimal setup. The possibility to make use of trunk accelerometry for gait analysis has already been investigated in literature[2] and few methods relying upon a single inertial sensor have been developed: the assessment of gait characteristics has been performed by detecting gait events like heel strike and toe-off[3] [4] or even without a direct identification of these events[5]. Even though the validity of such approaches has been proven in laboratory settings, there is evidence that most of the gait data obtained during daily life differs from the data obtained during standardized conditions[6].

The aim of the present work is to develop and validate methods for movement analysis which must be robust and reliable in both supervised settings (like a functional test performed in a clinic or a laboratory) and unsupervised settings. As shown in Figure 9, it happens often that the expected ideal gait pattern shown in literature (Figure 9 A) becomes very altered even in healthy subjects (Figure 9 B). It is also evident in Figure that the expected pattern can be very different between straight-path walking and curved-path walking and the latter condition is the most frequent in real life[6]. For these reason it has been chosen to develop a robust method for detecting heel strikes along with a method which is used for segmenting walking intervals into straight-path walking and curved-path walking in order to apply the heel strike detection algorithm only when the subject is walking on a straight path; different metrics are used for turns and curved-path walking. The method for segmenting walking intervals is based on the turning detection algorithm described in Section 2.3.3 and it has been applied in Section 3.2.1.

The heel strike detection algorithm is described and divided in three flowchart in Section 2.2.1, Figure 10, Figure 11, and Figure 12 which also show representative examples. Validation procedure and results are instead reported in Section 2.2.3.

[1] J Rueterboriesa, EG Spaicha, B Larsenb, OK. Andersena. Methods for gait event detection and analysis in ambulatory systems. Medical Engineering & Physics 32 (2010) 545–552

[2] M Henriksen, H. Lund, R. Moe-Nilssen, H. Bliddal, B. Danneskiod-Samsøe, Test–retest reliability of trunk accelerometric gait analysis, Gait & Posture, vol. 19, no. 3, June 2004, pp 288-97

[3] W Zijlstra. Assessment of spatio-temporal parameters during unconstrained walking. Eur J Appl Physiol (2004) 92: 39–44

[4] A Kose, A Cereatti, U Della Croce. Bilateral step length estimation using a single inertial measurement unit attached to the pelvis. J Neuroeng Rehabil. 2012; 9: 9.

[5] R Moe-Nilssen, JL. Helbostad. Estimation of gait cycle characteristics by trunk accelerometry. Journal of Biomechanics 37 (2004) 121–126

[6] A Zijlstra, W Zijlstra. Sensor based assessment of standardized and daily-life gait in independent-living older adults. Proceedings of the 1st Joint World Conference of ISPGR and Gait & Mental Function, Trondheim, Norway, pp. 329-330, June 2012.

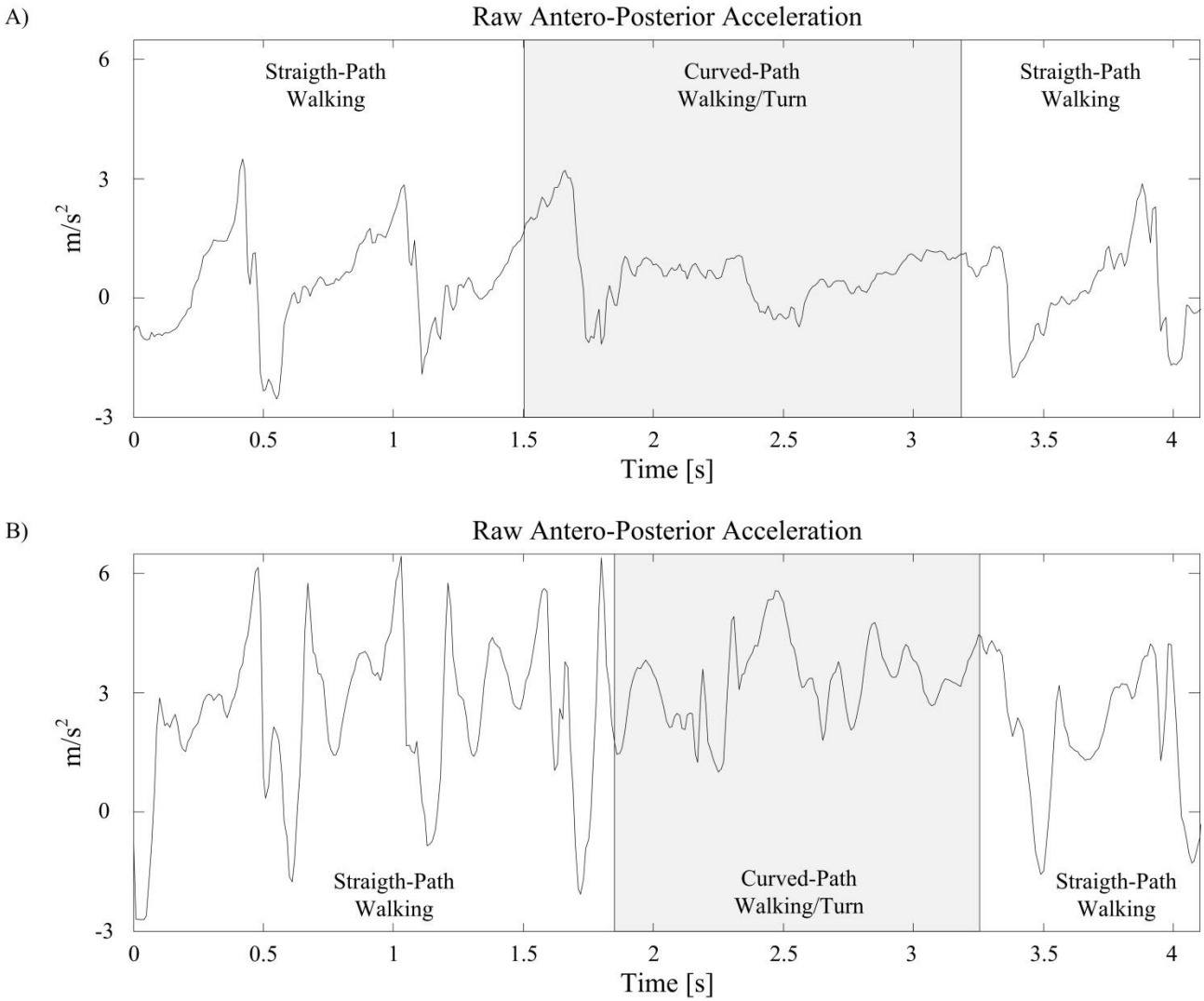

Figure 9 – A) Raw Antero-Posterior component of the acceleration while walking. Example of a pattern, from a healthy subject, which is close to the ideal one. B) Raw Antero-Posterior component of the acceleration while walking. Example of a pattern which is far from the ideal one also recorded from a healthy subject.

2.2.1 HEEL STRIKE DETECTION

In this section the heel strike detection algorithm is described as a flowchart divided in three Figures: Figure 10, Figure 11, and Figure 12: in Figure NEW1 the algorithm takes as input the Antero-Posterior and Vertical components of the trunk acceleration recorded on the lower back. The output of this first part of the algorithm is an array of indices used in the second part of the algorithm called "Anchor Value". The basic idea is exactly to anchor the search for the heel strike to the neighborhood of "trusted" points.

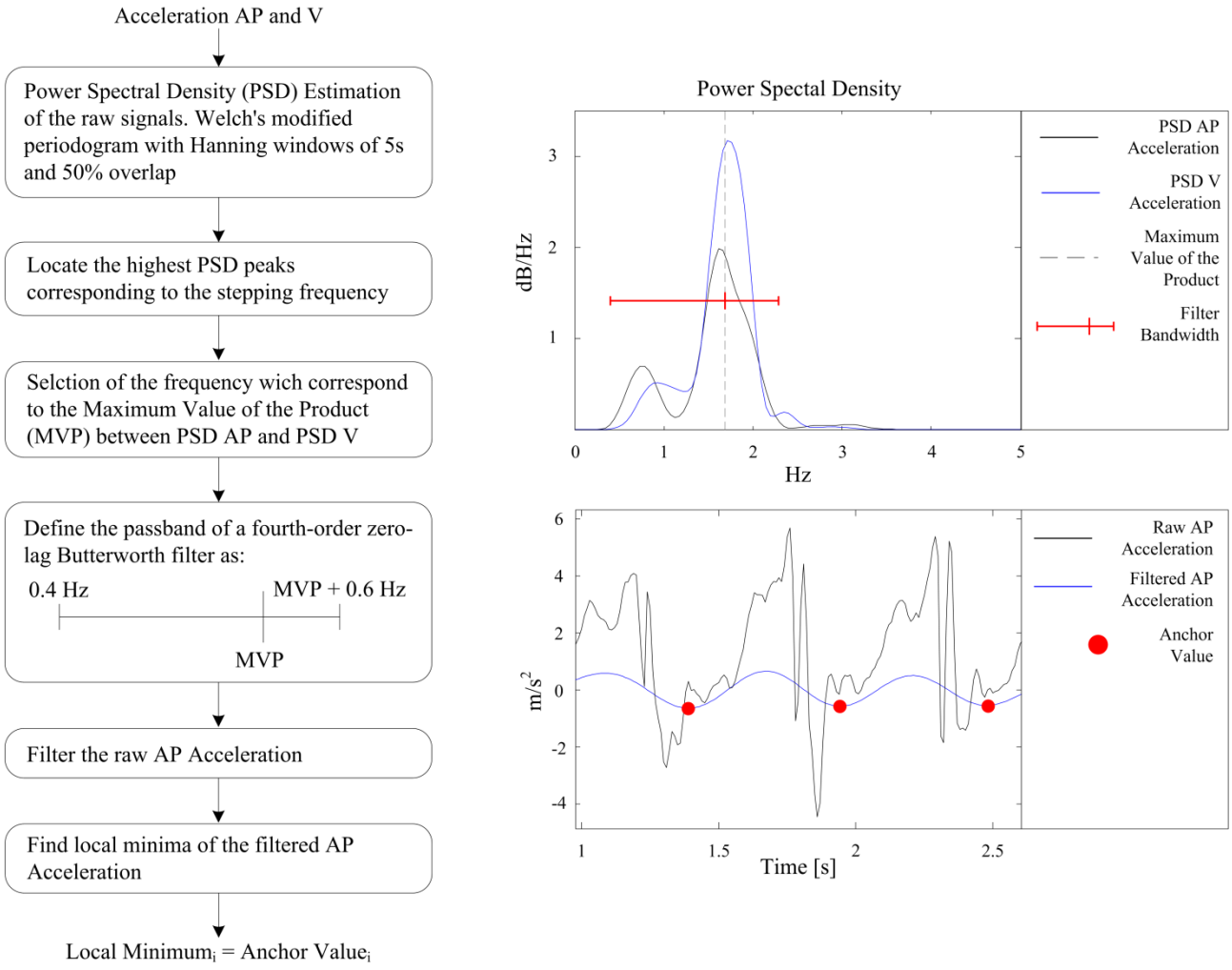

Figure 10 – First part of the heel strike detection algorithm flowchart. Acronyms: AP = Antero-Posterior; V = Vertical; PSD = Power Spectral Density; MVP = Maximum Value of the Product.

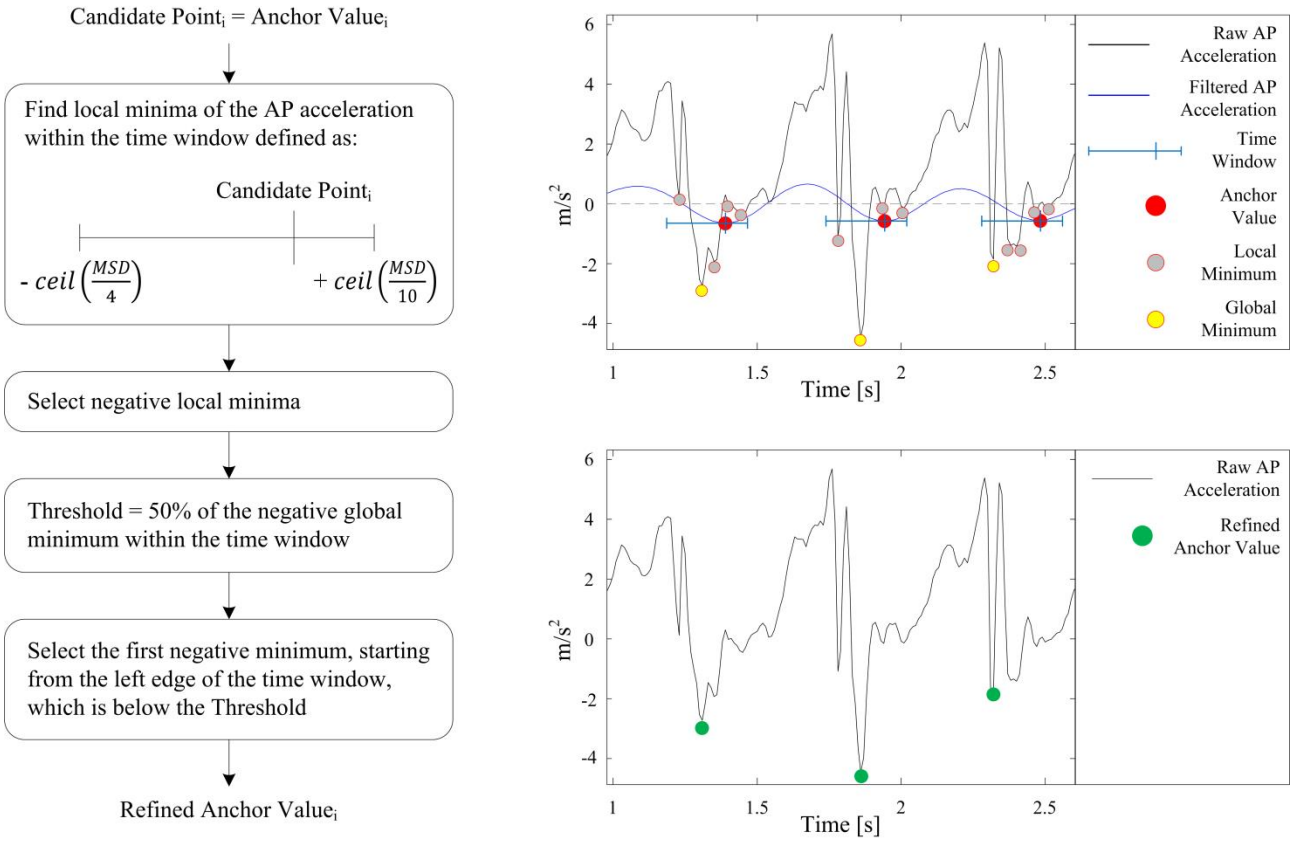

Figure 11 – Second part of the heel strike detection algorithm flowchart. Acronyms: AP = Antero-Posterior; MSD = Mean Step Duration which is the reciprocal of the stepping frequency defined in Figure 10.

In the second part of the algorithm flowchart (Figure 11) the Anchor Values are used to define a time window for refining the selection in order to move closer to the heel strike. The ceil function in Figure 11 rounds the input value to the nearest integer greater or equal to to the input value. The filtered Antero-Posterior acceleration is the one obtained in the first part of the flowchart (Figure NEW1).

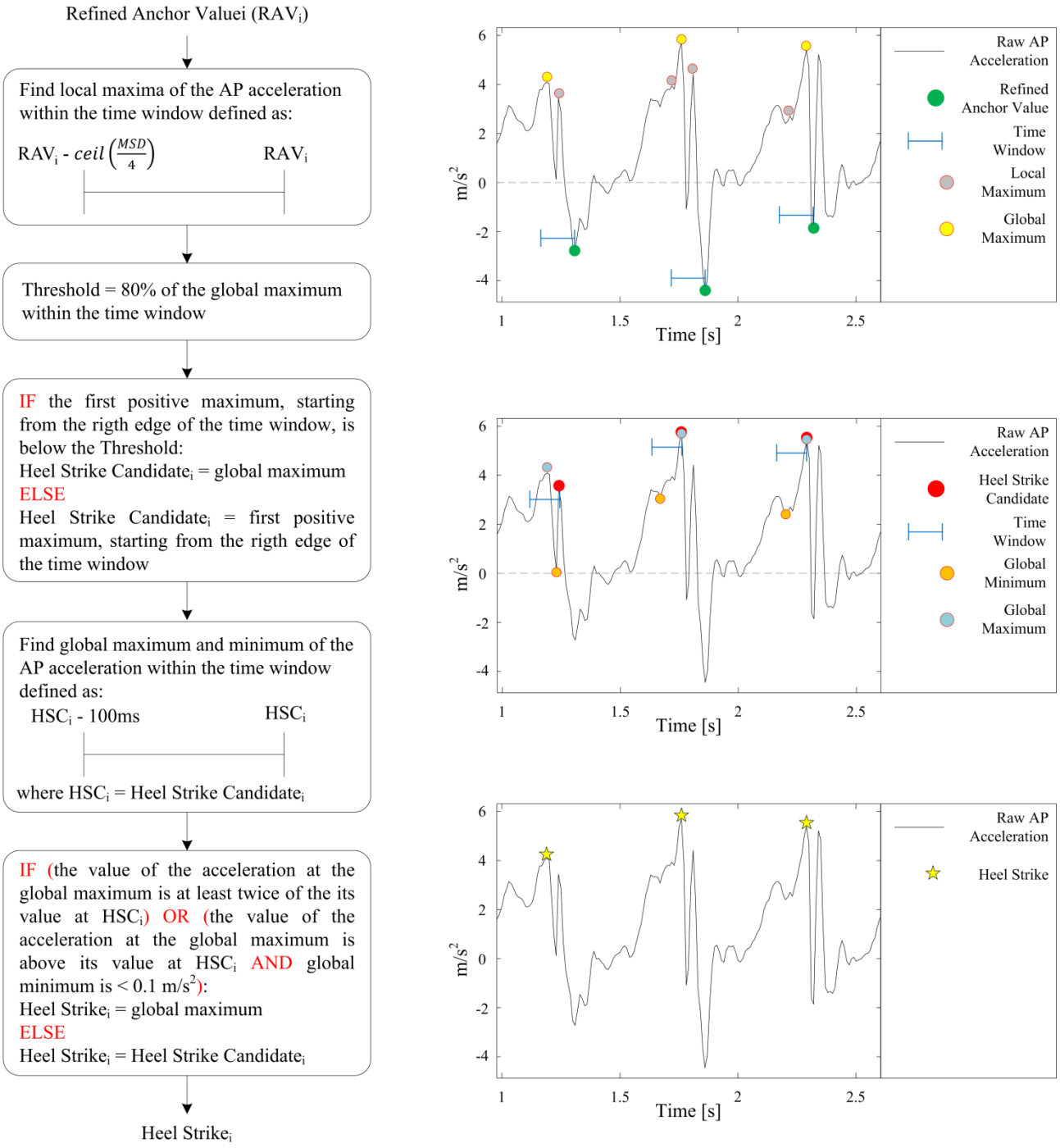

Figure 12 – Third part of the heel strike detection algorithm flowchart: the algorithm takes as input the Refined Anchor Values (Figure 11). In the definition of the time window, the ceil function rounds the input value to the nearest integer ≥ to the input value. The filtered Antero-Posterior acceleration is the one obtained in the first part of the flowchart (Figure 10). Acronyms: AP = Antero-Posterior; RAV = Refined Anchor Value; HSC = Heel Strike Candidate.

In the third part of the flowchart (Figure 12) a set of rules has been implemented for selecting the right peak which corresponds to the initial contact/heel strike.

2.2.2 VALIDATION PROCEDURE AND RESULTS

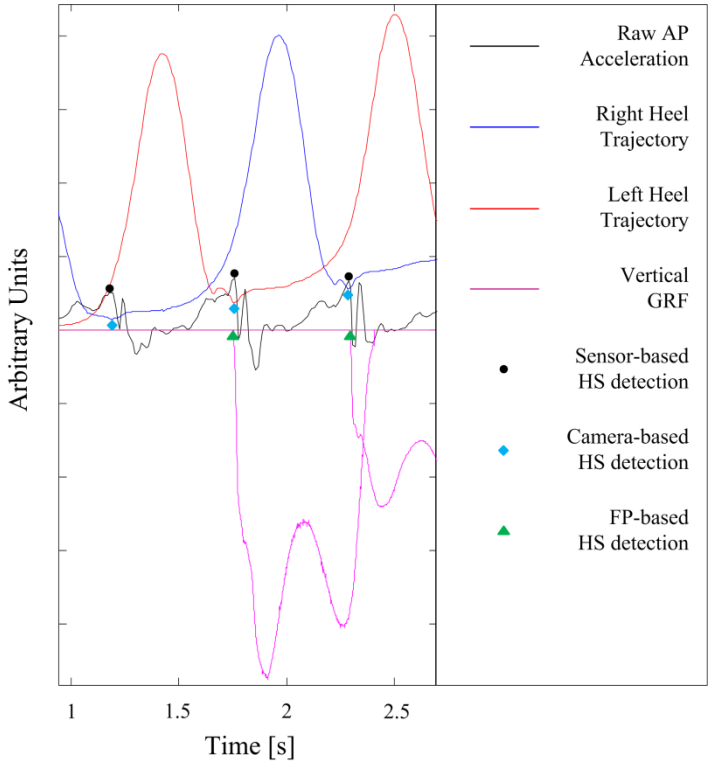

Figure 13 – Heel strike detection: comparison among the method based on the accelerometer worn on the lower back, the stereophotogrammetric system, and force plate.

Methods

30 subjects (40±14 years, range 21-68 years, 17 women) were recruited for this validation study. Subjects were asked to perform a Timed Up and Go (TUG). Each subject performed three repetitions. Trials were recorded by 8 opto-electronical cameras (T10, Vicon, Oxford, UK) with reflective markers in a 3-dimensional coordinate system with a sampling frequency of 200 Hz and by four force plates (BP 400600-2000, AMTI, Watertown, USA, side length 40x60cm) embedded into the ground. The platform measured the 3 orthogonal forces and moment components along the x-, y-, and z-axes, producing a total of 6 outputs, with a sampling frequency of 1.000 Hz. A tri-axial accelerometer worn on the lower back (McRoberts Dynaport Hybrid (MCR): range ±2g, sample rate 100Hz, sensitivity 1mg) has been used to instrument the TUG.

Reflective markers were placed on the trunk (Clavicular notch, Xiphoid, C7 Vertebra, and T10 Vertebra), on the pelvis (Left and Right Anterior Superior Iliac Crests, Left and Right Posterior Superior Iliac Crests, and Sacrum), on left and right heels, on left and right toes, and on the ankles. Heel strikes were detected on heel trajectories as the absolute minimum of the heel height after the swing phase.

From force plates, heel strikes were detected by means of the vertical component of the ground reaction force switching from zero to the value measured after the first contact. Subjects were not instructed to hit the force plates in order to avoid influencing their gait pattern.

Results

291 steps were simultaneously detected by the force plate, the wearable sensor, and the stereophotogrammetric system (Figure 13) while 632 steps were simultaneously detected by the wearable sensor and the stereophotogrammetric system. Results about the heel strikes detection accuracy is reported in Table XYZ. Steps recorded during the 180° turn of the TUG or during the Turn-to-Sit transition were excluded from the analysis.

TABLE XYZ

HEEL STRIKE DETECTION: RESULTS OF THE COMPARISON AMONG FORCE PLATE, STEREOPHOTOGRAMMETRIC SYSTEM, AND WEARABLE SENSOR

Comparison	Dataset	Difference mean(standard deviation)
Force Plate – Wearable Sensor	A	2(23) ms
Stereophotogrammetric System – Wearable Sensor	A	3(23) ms
Force Plate - Stereophotogrammetric System	A	5(20) ms
Stereophotogrammetric System – Wearable Sensor	B	1(24) ms

Dataset A: 291 steps simultaneously detected by the force plate, the wearable sensor, and the stereophotogrammetric system; Dataset B: 632 step simultaneously detected by the wearable sensor and the stereophotogrammetric system

Conclusions

Considering force plates as the gold standard for heel strike detection, the accuracy of the developed algorithm for detecting heel strikes was found to be comparable with the method based on the opto-electronic system. The results obtained on the subset of steps detected by all three systems were confirmed for the steps which were not recorded by force plates.

Heel strikes can be accurately detected during instrumented functional test like the Timed Up and Go where there are continuous speed changes since the test is performed over a distance of three meter including the 180° turn and the Turn-to-Sit transition.

2.2.3 FEATURE EXTRACTION

Gait characteristic can be quantified by means of several parameters computed from the trunk acceleration. Although the method proposed in Section 2.2.1 can only detect heel strikes, hence it is not possible to identify and segment all the phases in the gait cycle, it is still possible to reliably defines and select steps and strides which can be used for estimating feature related with gait variability, coordination[1], and walking smoothness[2]. Parameters are reported and defined in Table XYZ. A novel parameter is also proposed, Gait NJS (Normalized Jerk Score) which is also related to the walking smoothness/control and has been found to be of interest in clinical applications (Section 2.4.2).

TABLE XYZ - LIST OF GAIT PARAMETERS: DEFINITIONS AND MEANING

MEASURE	DESCRIPTION	M.U.	DIRECTIONS
Gait NJS	The NJS during gait is computed for each step (i.e., between two consecutive heel strikes), then normalized to the step duration, and then averaged across all steps: $$Gait\ NJS = \frac{1}{N}\sum_{i=1}^{N}\left(\sqrt{\frac{(hs_{i+1}-hs_i)^5}{2}\int_{hs_i}^{hs_{i+1}}(\ddot{a})^2 dt}\right)$$ where hs_i denotes the time of the i^{th} heel strike and a is the acceleration measured in m/s^2.	[m]	AP, ML, V
Tstep	Mean value of the step duration, computed as the time distance between two consecutive heel strikes.	[s]	NA
Tstep STD	Standard deviation of the step duration, computed as the time distance between two consecutive heel strikes.	[s]	NA
Tstep CV	Coefficient of Variation (CV) of the step duration, computed as the time distance between two consecutive heel strikes. $$Tstep\ CV = 100 \cdot \frac{Tstep\ STD}{Tstep}$$	[%]	NA
Phase	Mean value of the phase denoted in degrees. The i^{th} phase (φ_i), measures the step time with respect to the stride time assigning 360° to each stride (gait cycle): $$\varphi_i = 360^\circ \frac{hs_{Si} - hs_{Li}}{hs_{L(i+1)} - hs_{Li}}$$ Phase is the average of φ_i,where hs_{Li} and hs_{Si} denote the time of the i^{th} heel strike of the legs with the long and short step times, respectively.	[°]	NA
Phase STD	Standard deviation of the phase.	[°]	NA
Phase CV	Coefficient of variation of the phase.	[%]	NA
PCI	Phase Coordination Index (PCI). PCI measures gait coordination (i.e., the accuracy and consistency of the phase generation). $$PCI = Phase\ CV + 100 \cdot \frac{\frac{1}{N}\sum_{i=1}^{N}\lvert \varphi_i - 180^\circ \rvert}{180^\circ}$$	[%]	NA
HR	Stride frequency is used as the fundamental frequency of the periodic acceleration signals during steady state walking; the fundamental period of such signals is a multiple of the stride duration. The coefficients of the first 10 even harmonics and the first 10 odd harmonic are computed by using a finite Fourier series; then HR is calculated by dividing the sum of the amplitudes of the in phase harmonics by the sum of the amplitudes of the out of phase harmonics: $$HR = \frac{\sum_{i=1}^{10} eh_i}{\sum_{i=1}^{10} oh_i}$$ for AP and V direction; $$HR = \frac{\sum_{i=1}^{10} oh_i}{\sum_{i=1}^{10} eh_i}$$ for ML direction where eh_i and oh_i denote the coefficient of the i^{th} even and odd harmonic respectively. The turn is not considered in the computation.	[-]	AP, ML, V

NA = NOT APPLICABLE; AP = ANTERO-POSTERIOR; ML = MEDIO-LATERAL; V = VERTICAL, [-] = UNITLESS; M.U. = MEASUREMENT UNIT

[1] M. Plotnik, N. Giladi, and J. M. Hausdorff, "A new measure for quantifying the bilateral coordination of human gait: effects of aging and Parkinson's disease," Experimental brain research, vol. 181, no. 4, pp. 561–70, Aug. 2007.

[2] Brach JS, McGurl D, Wert D, Vanswearingen JM, Perera S, Cham R, Studenski S. Validation of a measure of smoothness of walking. J Gerontol A Biol Sci Med Sci. 2011 Jan;66(1):136-41.

2.3 THE TIMED UP AND GO TEST

The Timed Up and Go (TUG, Figure 14) is one of the most widely used clinical tests to assess mobility whose outcome is well correlated to established balance assessment tools such as the Berg Balance Scale and the Tinetti Balance[1]. Because of its effortlessness it is often included in screening protocols for fall risk assessment[2]. Instrumented versions of the TUG have already proven to be sensitive to pathologies[3] [4] and useful for fall risk prediction[5].

Figure 14 – Patient performing a modified Timed Up and Go test of 7 meters while wearing an inertial sensing unit on the lower back by means of an elastic belt.

In Section 2.3.1 is presented a method for identifying and segmenting the postural transition: the Sit-to-Walk transition and the Turn-to-Sit transition which are more complex compared to the Sit-to-Stand transition and the Stand-to-Sit transition but also closer to the activities of daily living. Validation procedure and results are reported in Section 2.3.2. An algorithm for detecting turns and/or curved-path walking is described in Section 2.3.3 and validated in Section 2.3.4.

[1] Berg KO, Maki BE, Williams KI. Clinical and laboratory measures of postural balance in an elderly population. Arch Phys Med Rehabil 1992;73:1073–80.

[2] Panel on Prevention of Falls in Older Persons, American Geriatrics Society and British Geriatrics Society. Summary of the Updated American Geriatrics Society/British Geriatrics Society clinical practice guideline for prevention of falls in older persons. J Am Geriatr Soc, 2011, Vol. 59, No. 1, pp. 148-57.

[3] Weiss A, Herman T, Plotnik M, Brozgol M, Maidan I, Giladi N, et al. Can an accelerometer enhance the utility of the Timed Up & Go Test when evaluating patients with Parkinson's disease? Med Eng Phys 2010;32(2):119–25.

[4] Zampieri C, Salarian A, Carlson-Kuhta P, Aminian K, Nutt JG, Horak FB. The instrumented timed up and go test: potential outcome measure for disease modifying therapies in Parkinson's disease. J Neurol Neurosurg Psychiatry 2010;81(2):171–6.

[5] Marschollek M, Nemitz G, Gietzelt M, Wolf KH, Meyer Zu Schwabedissen H, Haux R. Predicting in-patient falls in a geriatric clinic: a clinical study combining assessment data and simple sensory gait measurements. Z Gerontol Geriatr 2009;42(4):317–21.

2.3.1 POSTURAL TRANSFERS

Postural transfers are mobility related activities in daily life which are performed several times a day and are indicators of the overall mobility level and balance control[1]. Studies using a single wearable sensing unit already demonstrated the ability to identify the beginning and end of sit-to-stand transitions[2] but the Sit-to-walk (StW) is a more complex sequential postural locomotor task that consists of two components: sit-to-stand and gait initiation[3] which are merged from the functional point of view and from the point of view of the signals recorded on the trunk. Less investigated is the Turn-to-Sit (TtS) transition which was segmented and assessed during an instrumented Timed Up and Go test but with a multiple sensors setup[4].

StW and TtS selection algorithms start with a common procedure which is described with the flowchart in Figure 15. The algorithm takes as input the angular velocity around the Medio-Lateral (ML) axis (the bending movement is in the Antero-Posterior direction) and the Antero-Posterior component of the acceleration measured with the inertial sensor placed on the lower back. The two signals are processed in parallel and in both cases the result is a Selection Mask (SM) i.e. a binary signal which is "true" (one) in correspondence to the postural transition and "false" (zero) elsewhere. The two SM are then merged into one, this approach has been proven of enhancing the robustness of the selection.

The flowchart of the algorithm for selecting the StW transition is reported in Figure 16. The algorithm takes as input the angular velocity around the ML axis and the SM: starting from the detection of the signal absolute minimum within the SM, the algorithm estimates the beginning and the end of the transition by implementing a set of rules on the signal morphology.

The flowchart of the algorithm for selecting the TtW transition is reported in Figure 17. The algorithm takes again as input the angular velocity around the ML axis and the SM: starting from the detection of the signal absolute maximum within the SM, the algorithm estimates the end of the TtS transition by implementing a set of rules on the signal morphology. The beginning of the TtS is instead estimated by the algorithm for turning detection described in Section 2.3.3.

[1] W Zijlstra, RW Bisseling, S Schlumbohm, H Baldus, A body-fixed-sensor-based analysis of power during sit-to-stand movements, Gait & Posture, Volume 31, Issue 2, February 2010, Pages 272-278.

[2] Najafi B, Aminian K, Loew F, Blanc Y, Robert PA. Measurement of stand-sit and sit-stand transitions using a miniature gyroscope and its application in fall risk evaluation in the elderly. IEEE 2002;49(8):843–51.

[3] R Soangra, T Lockhart, J Lach, E Abdel-Rahman. Effects of Hemodialysis Therapy on Sit-to-Walk Characteristics in End Stage Renal Disease Patients. Annals of Biomedical Engineering, December 2012.

[4] Salarian A, Horak FB, Zampieri C, Carlson-Kuhta P, Nutt JG, Aminian K. iTUG, a sensitive and reliable measure of mobility. IEEE Trans Neural Syst Rehabil Eng. 2010 Jun;18(3):303-10.

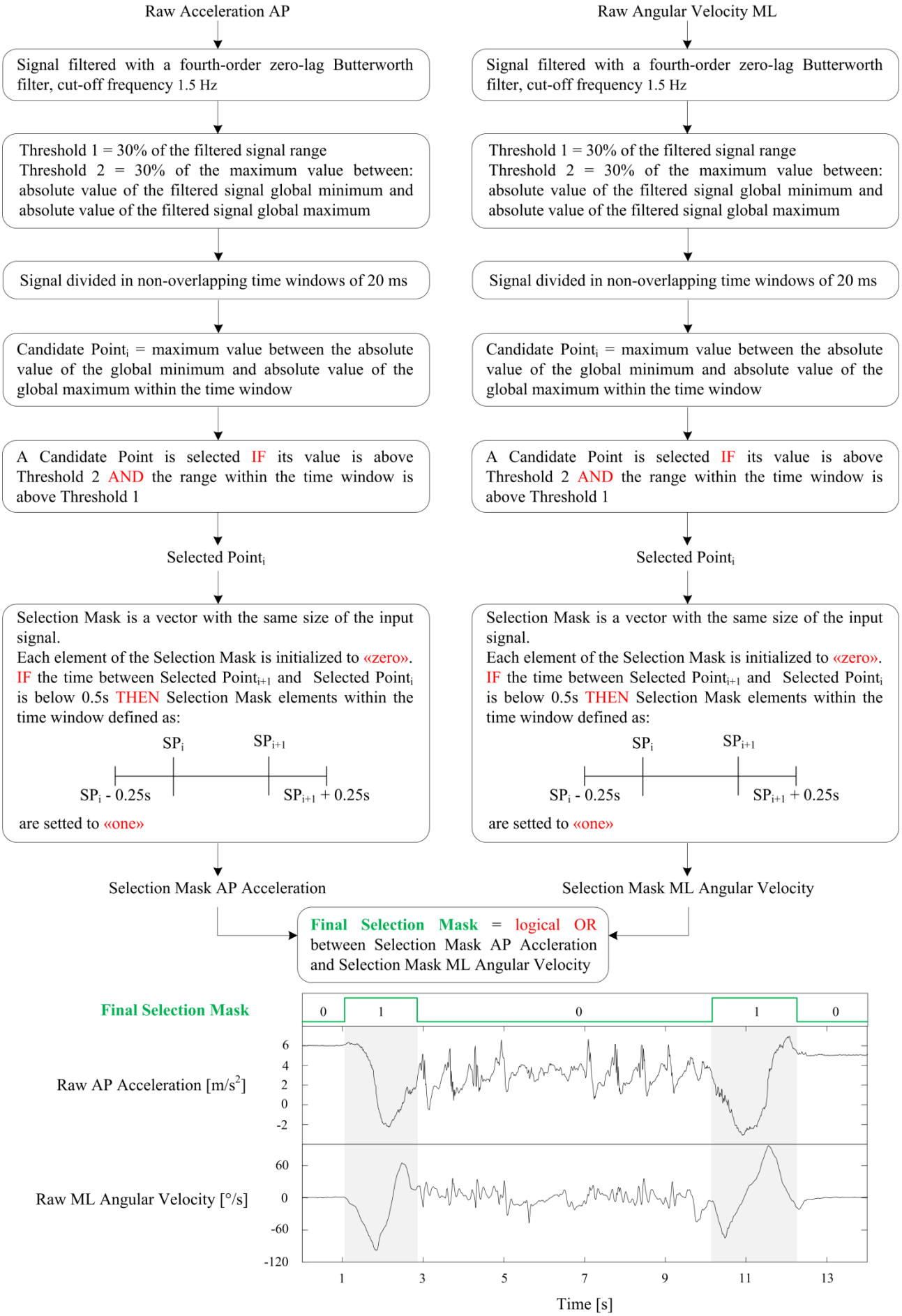

Figure 15 – Postural Transitions selection algorithm flowchart. Acronyms: AP = Antero-Posterior; ML = Medio-Lateral

Sit-to-Walk transition

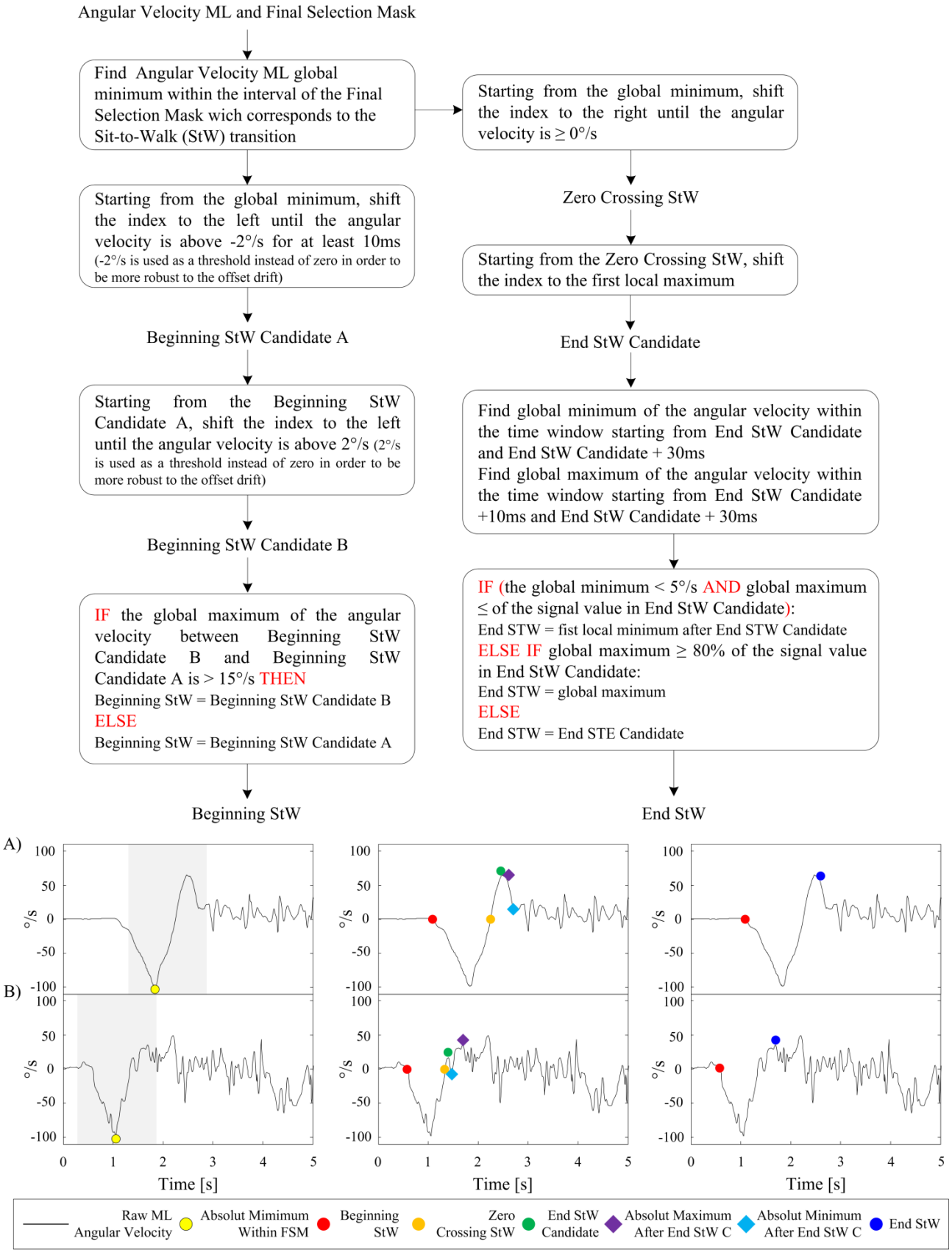

Figure 16 – Sit-to-Walk selection algorithm flowchart. A) and B) are two examples of the algorithm output. Grey area in the graphs on the left is the Final Selection Mask (Figure NEWt1). Acronyms: ML = Medio-Lateral; StW = Sit-to-Walk; End StW C = End Sit-to-Walk Candidate; FSM = Final Selection Mask.

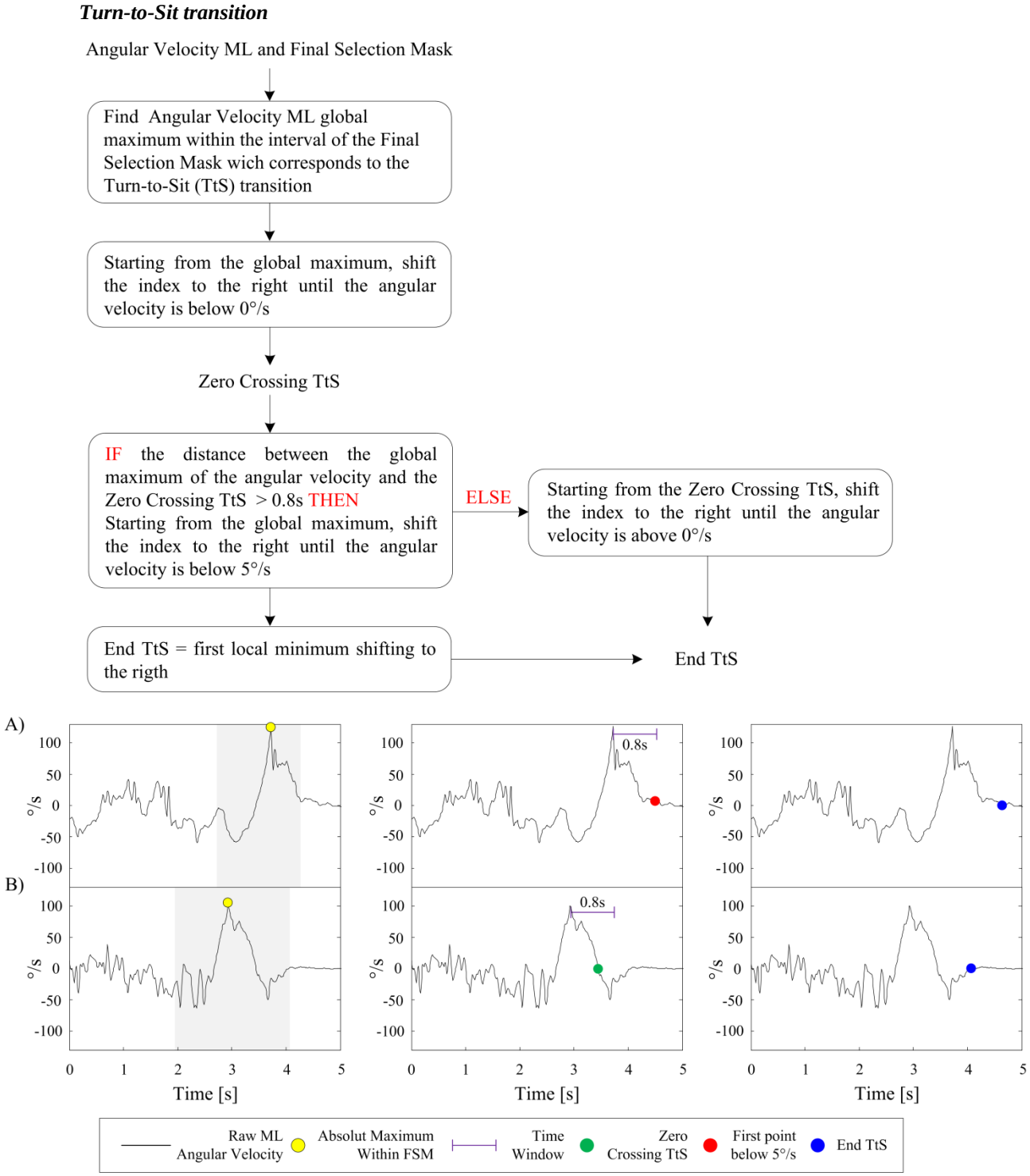

Figure 17 – End of the Turn-to-Sit selection algorithm flowchart. A) and B) are two examples of the algorithm output. Grey area in the graphs on the left is the Final Selection Mask (Figure NEWt1). Acronyms: ML = Medio-Lateral; TtS = Turn-to-Sit; FSM = Final Selection Mask. The beginning of the Turn-to-Sit transition is defined as the beginning of the turn before sitting. The algorith for turning detection is reported in Section 2.3.3.

2.3.2 POSTURAL TRANSFERS: VALIDATION PROCEDURE AND RESULTS

[WORK IN PROGRESS]

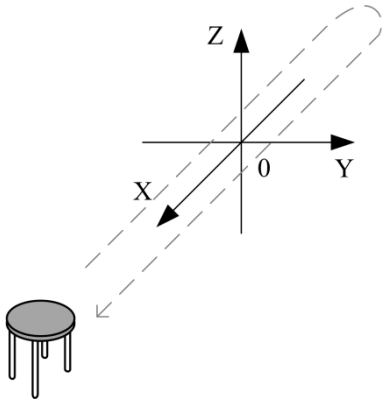

Figure 18 – Laboratory Reference System with respect to the performed Timed Up and Go test. X is the Antero-Posterior direction of the movement, Y is the Medio-Lateral direction of the movement, and Z is the Vertical component of the movement.

Methods

The same group and setup used for validating the heel strike detection algorithm (Section 2.2.2): 30 subjects (40±14 years, range 21-68 years, 17 women) were recruited performing three repetitions of the Timed Up and Go test (TUG). Trials were recorded by 8 opto-electronical cameras (T10, Vicon, Oxford, UK) with reflective markers in a 3-dimensional coordinate system (Figure 18) with a sampling frequency of 200 Hz. A tri-axial accelerometer worn on the lower back (McRoberts Dynaport Hybrid (MCR): range ±2g, sample rate 100Hz, sensitivity 1mg) has been used to instrument the TUG.

Reflective markers were placed on the trunk (Clavicular notch, Xiphoid, C7 Vertebra, and T10 Vertebra), on the pelvis (Left and Right Anterior Superior Iliac Crests, Left and Right Posterior Superior Iliac Crests, and Sacrum), on left and right heels, on left and right toes, and on the ankles.

The end of the Sit-to-Walk transition has been defined as the first local maximum of the Sacrum trajectory vertical component (Figure 19, top panel). The sacrum has been chosen because its range of motion is relatively low compared to the upper part of the trunk and when it reaches the maximum height the postural transition merges with the walking phase.

In order to have a very general definition for the beginning of the Sit-to-Walk transition, all the possible directions of the movement have been considered, Vertical (V), Medio-Lateral (ML), and Antero-Posterior (AP). Starting from the rising edge of the C7 vertebra trajectory vertical component (Figure 19, top panel), a time window of 0.25s has been shifted to the left until the standard deviations, within the time window, of the V, ML, or AP components of the Sacrum trajectory and the C7 Vertebra trajectory were below 1mm and 2mm respectively. In this way both the upper and the lower part of the trunk have been considered. The thresholds were different for taking into account the different range of motion of the two parts of the trunk. The beginning of the Sit-to-Walk transition was defined as the earliest time detected among the V, ML, and AP direction of the movement.

In analogy with the definition of the beginning of the Sit-to-Walk transition, also the definition of the end of the Turn-to-Sit transition takes in to account all the possible directions of the movement. Starting from the falling edge of the C7 vertebra trajectory vertical component (Figure 19, top panel), a time window of 0.25s has been shifted to the right until the standard deviations, within the time window, of the V, ML, or AP components of the Sacrum trajectory and the C7 Vertebra trajectory were below 1mm and 2mm respectively. The end of the Turn-to-Sit transition was defined as the latest time detected among the V, ML, and AP direction of the movement.

The method for detecting turns based on the stereophotogrammetric system is instead reported in Section 2.3.4 as the gold standard for validating the algorithm described in Section 2.3.3.

Results

Results of segmenting the TUG making use of the proposed algorithms are reported in Table XYZ2. A graphical example of the algorithm outputs is shown in Figure 18.

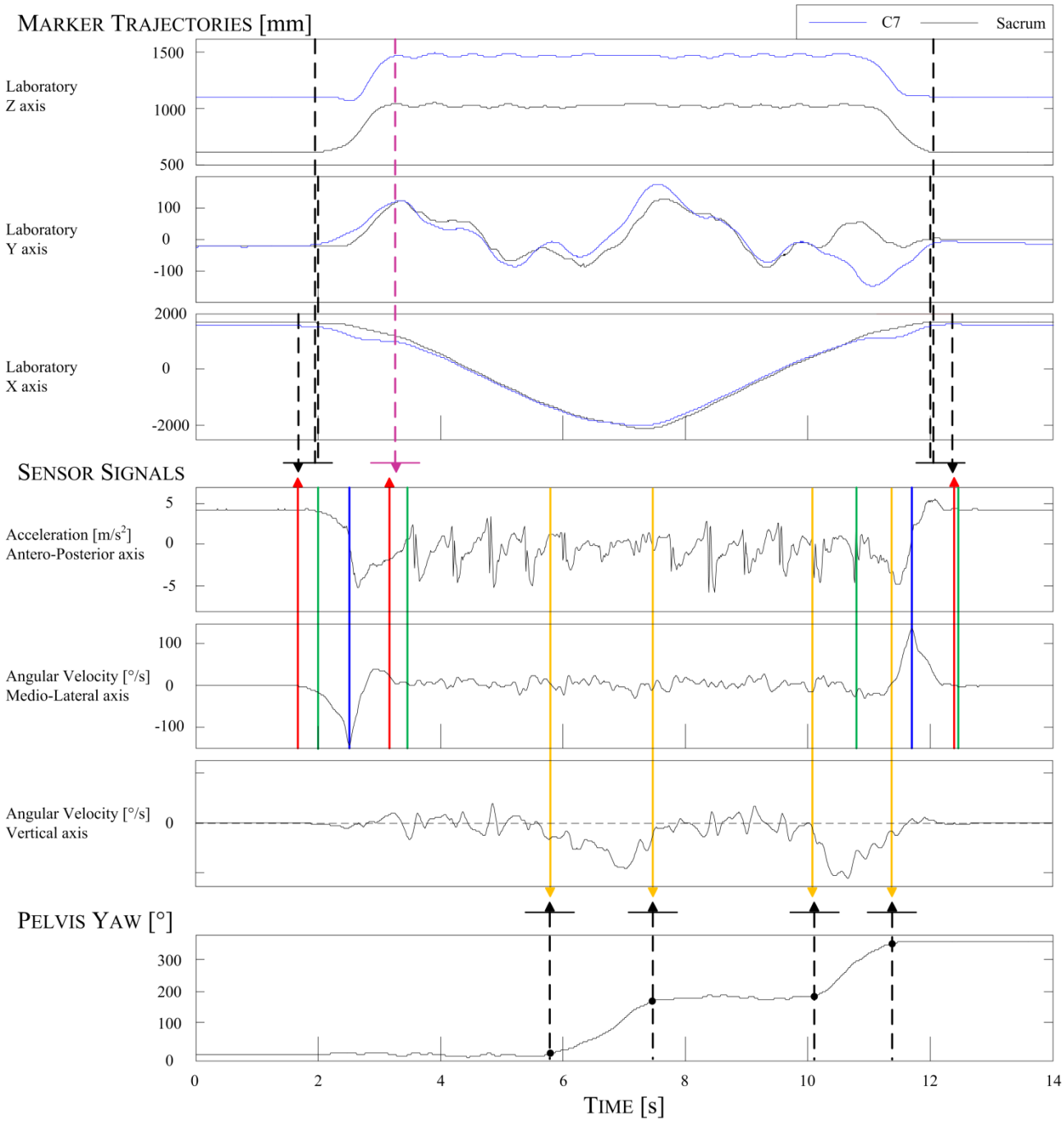

Figure 19 – Example of the algorithm outputs. Top Panel: Marker Trajectories. The trajectories of the Sacrum and the C7 Vertebra are shown in every direction of the movement. The laboratory reference system is shown in Figure 18. The black vertical dashed lines are beginning/end of movement, for each of the movement directions, detected by means of the stereophotogrammetric system. The beginning of the Sit-to-Walk transition is the earliest time detected while the end of the Turn-to-Sit transition is the latest time detected. Central Panel: Sensor Signals. Antero-Posterior Component of the acceleration, angular velocity around Medio-Lateral and Vertical axis are reported. The green vertical lines defines the Selection Mask (Figure 15) Blue vertical lines corresponds to the absolute maximum/minimum of the angular velocity around Medio-Lateral axis within the Selection Mask. Red vertical lines are the output of the selection algorithms reported in Figure 16 and Figure 17. The angular velocity around the Vertical axis is used in the Turn detection algorithm described in Section 2.3.3. Bottom Panel: Pelvis Yaw. The pelvis yaw is measured from the markers placed on the pelvis as reported in Section 2.3.3. Orange vertical lines are the beginning/end of the turns detected by means of the wearable sensor (Section 2.3.3) while the black vertical dashed lines are the beginning/end of the turns detected by means of the stereophotogrammetric system (Section 2.3.4).

Conclusions

As shown in Table XYZ2 the beginning all the TUG phases, with the exception of the end of the Turn-to-Sit transition, are estimated with a good accuracy: the mean difference is few tens of millisecond in the worst case (the end of the Sit-to-Walk Transition with a mean difference of 57ms) and the standard deviation is about a tenth of a second. The end of the Turn-to-Sit transition shows a good mean difference (11ms) but with a relatively high standard deviation which can be ascribed to the small postural adjustments sometimes performed right after seated. The overall accuracy of the proposed methods makes them suitable for clinical applications such as screening protocols. A validation study also involving very frail and/or pathological subjects should be performed before suggesting their use in those populations.

TABLE XYZ2

ALGORITHMS FOR SEGMENTING THE TIMED UP AND GO : COMPARISON BETWEEN STEREOPHOTOGRAMMETRIC SYSTEM AND WEARABLE SENSOR

COMPARISON	DIFFERENCE mean(standard deviation)
Beginning of the Sit-to-Walk Transition	9(117) ms
End of the Sit-to-Walk Transition	57(124) ms
Beginning of the 180° Turn	1(117) ms
End of the 180° Turn	25(112) ms
Beginning of the Turn-to-Sit Transition	14(78) ms
End of the Turn-to-Sit Transition	11(241) ms
Sit-to-Walk Duration	47(162) ms
180° Turn Duration	26(170) ms
Turn-to-Sit Duration	25(250) ms
Timed Up and Go Total Duration	20(284) ms

2.3.3 TURNING

The ability to turn is essential for daily living activities. Laboratory-based based studies investigated control strategies[1], the contribution of vision[2], the Center of Mass trajectory[3], and the body kinematics and kinetics[4] [5]. Nearly every task performed during the day requires some amount of turning nevertheless clinical gait research has focused mainly on straight-path walking and little is known about turning during daily living activities[6].

The Timed Up and Go (TUG) is a complex test that allows evaluating several mobility skills at the same time including the ability to turn. In fact TUG includes two 180° turns, the first one performed while walking and the second one performed before sitting. As already discussed in the present work, the possibility to investigate different aspects of mobility is one of the key factors of its widespread use in clinical practice.

A method for identifying the onset and the offset of a turn during TUG has already been presented in literature which makes use of a single waist mounted inertial sensor but its validity is limited to 180°[7]. In this section a turning detection method is proposed which is developed and validated (Section 2.3.4) for different turning angles and different walking/turning speeds.

The algorithm flowchart is reported in Figure 20. The method makes use of the angular velocity of the trunk around the vertical axis measured with an inertial sensing unit worn on the lower back. The procedure starts with a relatively simple threshold based criterion for segmenting the signal and identifying potential turns, then a set of descriptive features are computed for each of the potential turns. The selected intervals are discarded or merged on the basis of rules and relationships among the features. As for other proposed algorithm, the output is a Selection Mask. An example of the procedure output is reported in Figure 21 where in the bottom panel is shown the pelvis rotation (yaw) measured by means of a stereophotogrammetric system[8].

[11] Hase K, Stein RB. Turning strategies during human walking. J Neurophysiol 1999;81:2914–22.

[2] Courtine G, Schieppati M. Human walking along a curved path. I. Body trajectory, segment orientation and the effect of vision. Eur J Neurosci 2003;18:177–90.

[3] Patla AE, Adkin A, Ballard T. Online steering: coordination and control of body center of mass, head and body reorientation. Exp Brain Res 1999;129:629–34.

[4] Taylor MJD, Dabnichki P, Strike SC. A three-dimensional biomechanical comparison between turning strategies during the stance phase of walking. Human Mov Sci 2005;24:558–73.

[5] Orendurff MS, Segal AD, Berge JS, Flick KC, Spanier D, Klute GK. The kinematics and kinetics of turning: limb asymmetries associated with walking a circular path. Gait Posture 2006

[6] BC Glaister, GC Bernatz, GK. Klute, MS Orendurff, Video task analysis of turning during activities of daily living, Gait & Posture, Vol. 25, no. 2, February 2007, pp. 289-294

[7] Salarian A, Horak FB, Zampieri C, Carlson-Kuhta P, Nutt JG, Aminian K. iTUG, a sensitive and reliable measure of mobility. IEEE Trans Neural Syst Rehabil Eng. 2010 Jun;18(3):303-10.

[8] Cappozzo A, Cappello A, Della Croce U, Pensalfini F. Surface-marker cluster design criteria for 3-D bone movement reconstruction. IEEE Trans Biomed Eng. 1997 Dec;44(12):1165-74.

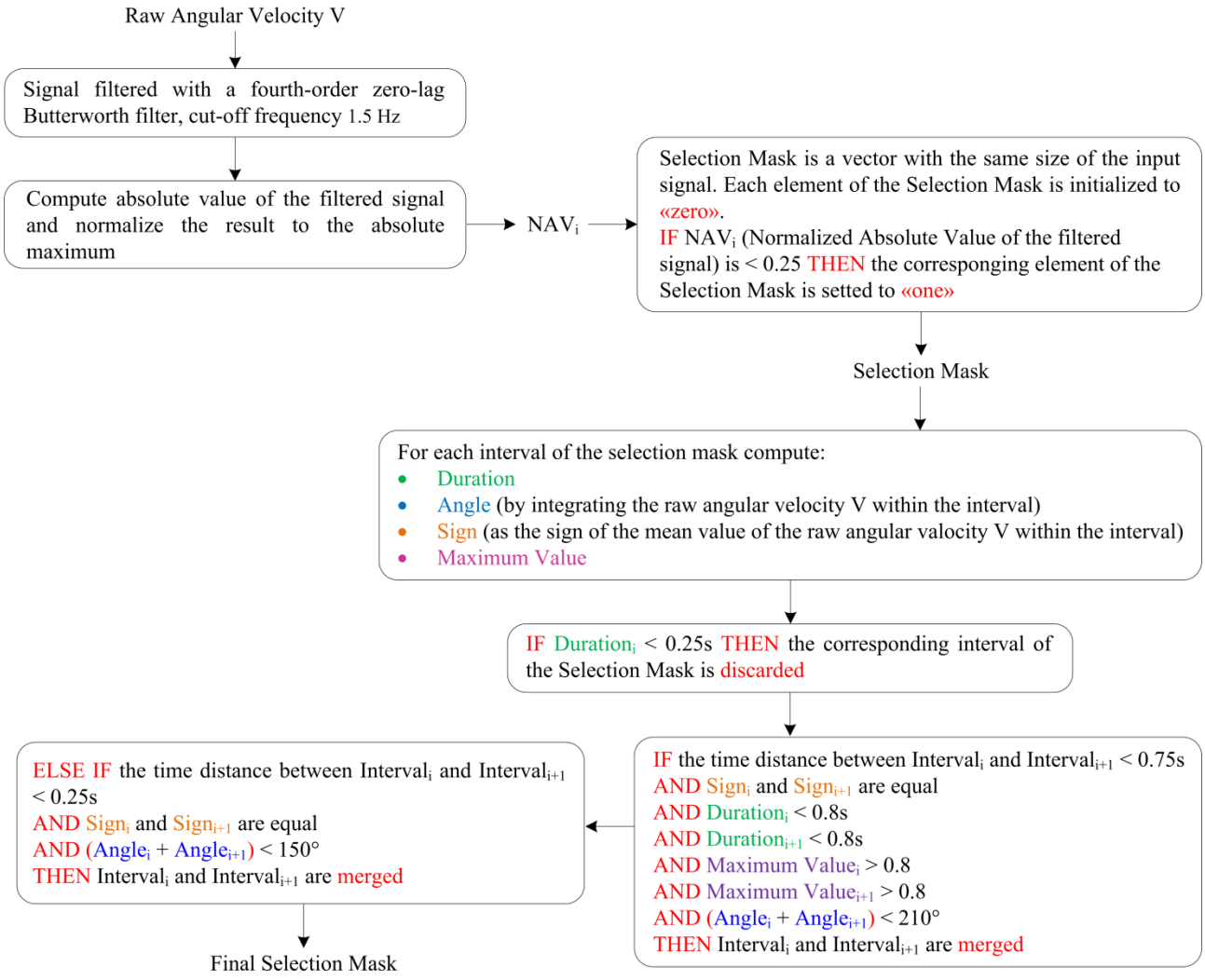

Figure 20 – Turning selection algorithm flowchart. An example of the output is reported in Figure 21. Acronyms: V = Vertical; NAV = Normalized Absolute Value of the filtered signal.

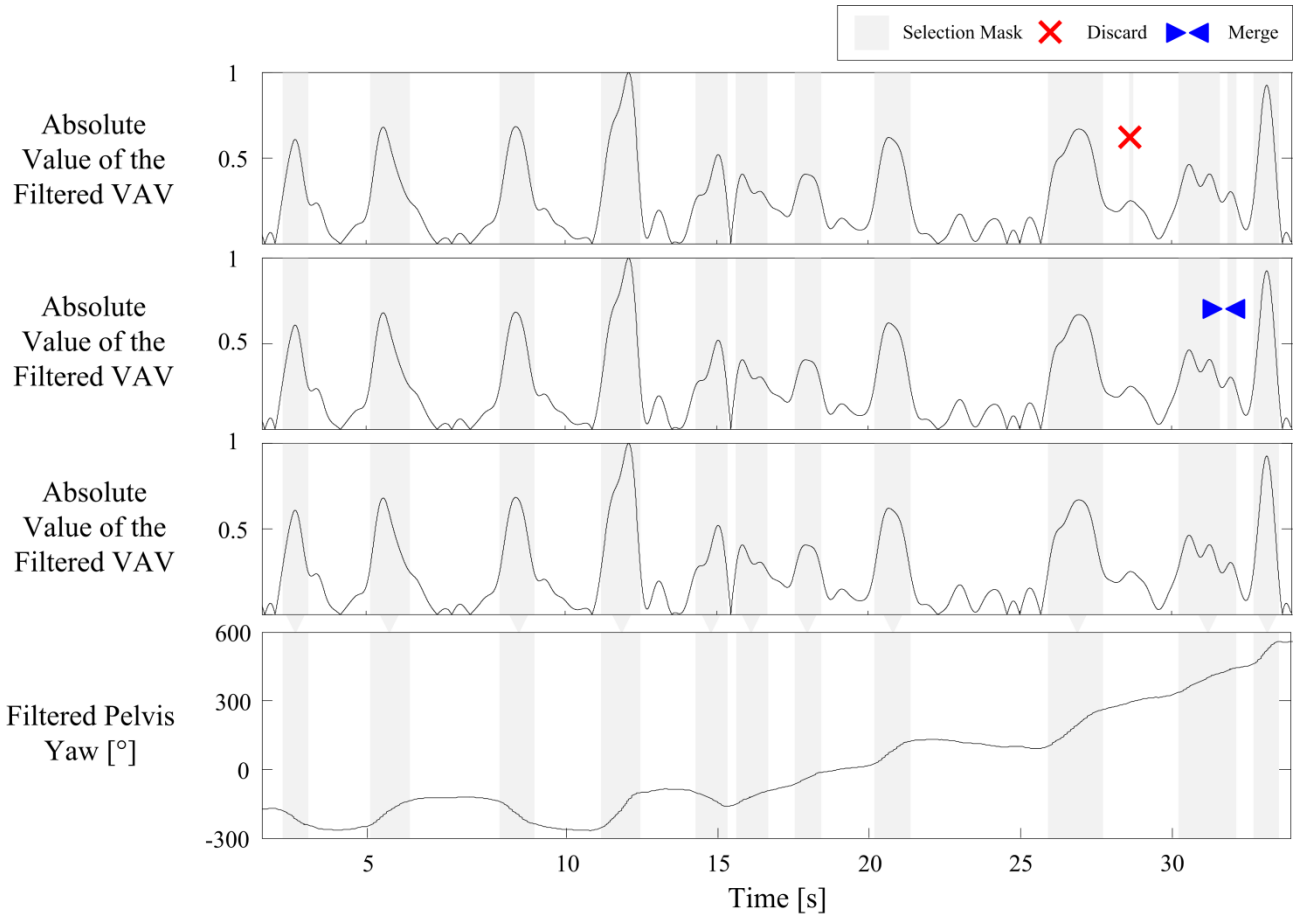

Figure 21 – Example of the output of the algorithm described in Figure 20. The Absolute value of the filtered angular velocity is normalized to highest peak. In the bottom panel is shown the corresponding filtered yaw of the pelvis estimated by means of the stereophotogrammetric system. The superimposed gray area is the Selection Mask, the output of the algorithm described in Figure 20. Acronyms: VAV = Vertical Angular Velocity.

2.3.4 TURNING: VALIDATION PROCEDURE AND RESULTS

Methods

16 patients with Parkinson's Disease (PD) (65±6 years, UPDRS III 24.5±7.5, 5 females) and 9 control subjects (CTRL) (68±8 years, 3 females) where recruited for this validation study. A 9-axis inertial sensor embedding an accelerometer, a gyroscope, and a magnetometer was worn on the lower back (Opal, APDM Inc., sample rate 128Hz).
Reflective markers were placed on the trunk (Left/Right Acromion and Scapula), on the pelvis (Left and Right Anterior Superior Iliac Crests, Left and Right Posterior Superior Iliac Crests), on the head (Left/Right Temporal Bones and Glabella), on left and right heels, on left and metatarsal, and on the ankles. Marker trajectories were recorded by means of a 8-camera stereophotogrammetric system (Motion Analysis system, Santa Rosa, sample rate 60 Hz).
Subjects were instructed to walk on a path composed of a mixed route with short straight paths interspersed with turns ranging from 30° to 180°. (path is reported in Figure 22 A). Each subject performed 12 repetitions: 4 at preferred, 4 at faster, and 4 at slower speed.
The performance of the method for turning detection based on the wearable unit has been compared with a method based on the stereophotogrammetric system which is described as a flowchart and divided into figures: Figure 23 and Figure 24. The method is based on the measure of the pelvis rotation[1] which is segmented on the basis of the yaw slope. Selected intervals are then discarded, merged, and separated depending on the implemented set of rules. The output is a refined selection mask which has been compared with the selection mask of the sensor based algorithm.

Results

Results of comparison are reported in Table XYZ3. A graphical example of the algorithm outputs is shown in Figure 22 where is also shown the shape of the path along with the intervals selected as turns by both methods.

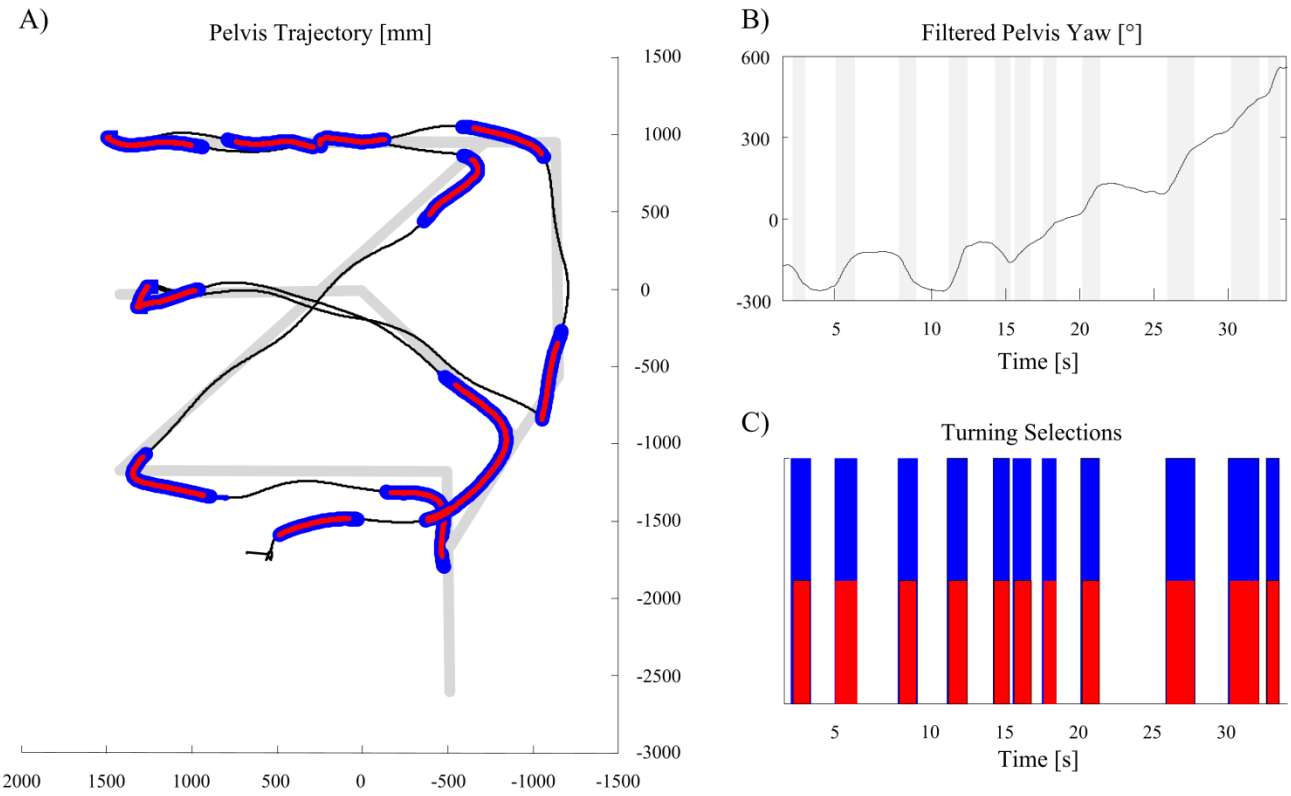

Figure 22 – A) Pelvis trajectory on the horizontal plane (black line), reference on the ground (gray line), turns identified by the stereophotogrammetric system (blue lines), and turns identified by the wearable sensor (red lines). B) Filtered yaw of the Pelvis as also reported in the example in Figure 21 where the Selection Mask was also represented in gray. Area highlighted by the Selection Mask corresponds to the red bars in C) while the blue bars correspond to the turns identified with the stereophotogrammetric system.

[1] Cappozzo A, Cappello A, Della Croce U, Pensalfini F. Surface-marker cluster design criteria for 3-D bone movement reconstruction. IEEE Trans Biomed Eng. 1997 Dec;44(12):1165-74.

Reference based on the Stereophotogrammetric System

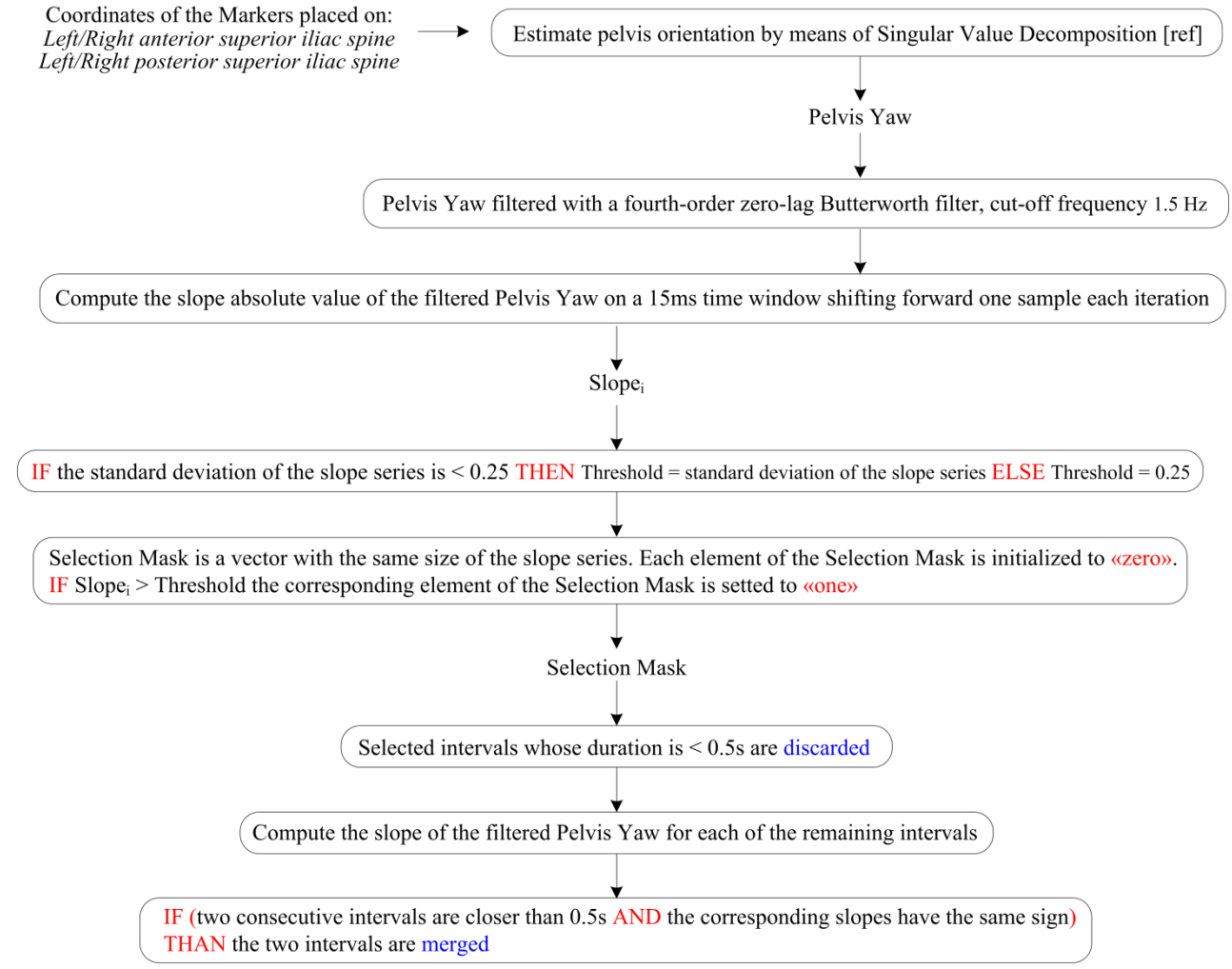

Figure 23 – First part of the turn selection algorithm flowchart. Bottom panels show an example of the algorithm output. [REF] Cappozzo A, Cappello A, Della Croce U, Pensalfini F. Surface-marker cluster design criteria for 3-D bone movement reconstruction. IEEE Trans Biomed Eng. 1997 Dec;44(12):1165-74.

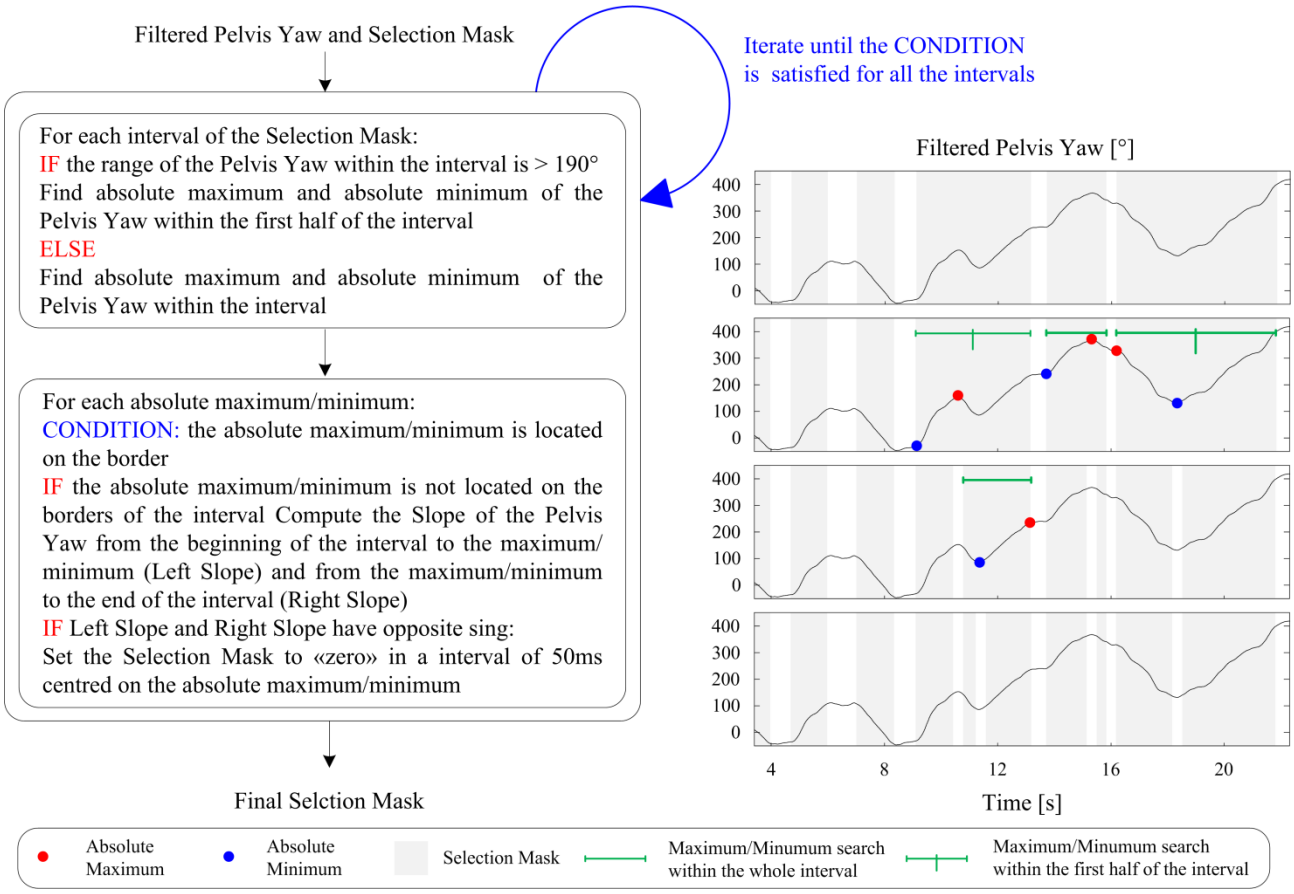

Figure 24 – Second part of the turn selection algorithm flowchart. Right panels show an example of the algorithm output.

Conclusions

The ability to turn while walking is essential for daily living activities. Turning difficulties are a common symptom in Parkinson's disease which is also associated with freezing of gait[1]. In comparison with healthy subjects, turning is usually slower in PD and takes more steps; timing and coordination of the different body segments can also be altered[2]. The validation study was also performed for better understand turning dynamics in PD patients compared with healthy subjects. Considering the complexity and the number of turns performed in a very small volume, the speed changes, and the impairments of the PD subjects, the results shown in Table XYZ3 makes the proposed algorithm an ideal candidate for studying the turning ability in the activities of daily living. When applied to standardized tests like the Timed Up and Go its performances are also improved as can be seen in Table XYZ2 for the detection of the 180° turn and the beginning of the Turn-to-Sit transition.

[1] Bhatt H, Pieruccini-Faria F, Almeida QJ. Dynamics of turning sharpness influences freezing of gait in Parkinson's disease. Parkinsonism Relat Disord. 2013 Feb;19(2):181-5. Epub 2012 Oct.

[2] Hong M, Perlmutter JS, Earhart GM. A kinematic and electromyographic analysis of turning in people with Parkinson disease. Neurorehabil Neural Repair. 2009 Feb;23(2):166-76.

TABLE XYZ3

ALGORITHM FOR TURNING DETECTION: COMPARISON BETWEEN THE STEREOPHOTOGRAMMETRIC SYSTEM AND WEARABLE SENSOR INCLUDING SOME DESCRIPTIVE FEATURES (SECTION 2.3.5)

COMPARISON	CTRL		PD	
	MEAN	STD. DEV.	MEAN	STD. DEV.
Beginning of the Turn Fast Speed [ms]	-58	185	21	336
Beginning of the Turn Preferred Speed [ms]	-41	140	3	300
Beginning of the Turn Slow Speed [ms]	-24	120	41	265
End of the Turn Fast Speed [ms]	8	187	-22	383
End of the Turn Preferred Speed [ms]	-15	218	-70	308
End of the Turn Slow Speed [ms]	-40	182	-102	227
Turning Duration Fast Speed [ms]	42	176	-40	306
Turning Duration Preferred Speed [ms]	30	250	-57	298
Turning Duration Slow Speed [ms]	-18	226	-136	359
Turning Angle Fast Speed [°]	5,6	8,5	1,3	13,3
Turning Angle Preferred Speed [°]	4,1	10,7	-0,5	11,3
Turning Angle Slow Speed [°]	1,1	9,2	-3,6	12,5
Mean Turning Velocity Fast Speed [°/s]	1	8,4	1,35	8,8
Mean Turning Velocity Preferred Speed [°/s]	1,1	7,4	1,5	8,4
Mean Turning Velocity Slow Speed [°/s]	1,5	5,7	2,1	6

ACRONYMS: STD. DEV. = STANDARD DEVIATION; CTRL = CONTROL SUBJECTS; PD = PARKINSON'S DISEASE PATIENTS

2.3.5 Feature Extraction

Characteristic of the different subcomponents of the Timed Up and Go test, automatically identified by the algorithms proposed in Section 2.3.1 and Section 2.3.3, can be quantified by means of several parameters computed from the trunk acceleration and angular velocity. The list of parameters along with their definition is reported in Table XYZ4.

TABLE XYZ4

SET OF DESCRIPTIVE FEATURES OF THE TIMED UP AND GO TEST SUBCOMPONENTS

MEASURE	COMPONENTS	DESCRIPTION	SIGNAL TYPE	M.U.	DIRECTIONS
Duration	Total, Sit-to-Walk, Gait, Turning, Turn-to-Sit	Duration of each Timed Up and Go component.	NA	[s]	NA
Range	Total, Sit-to-Walk, Gait, Turning, Turn-to-Sit	Range of the signal during the considered component	Acceleration; Angular Velocity	[m/s^2]; [°/s]	AP, ML, V
RMS	Sit-to-Walk, Gait, Turning, Turn-to-Sit	Root mean square of the signal, *s*, during the considered component: $RMS = \sqrt{\frac{1}{N}\sum_{i=1}^{N}(s(i) - mean(s))^2}$	Acceleration; Angular Velocity	[m/s^2]; [°/s]	AP, ML, V
TA	Turning	Turning Angle (TA) obtained integrating the angular velocity along the vertical axis: $TA = \int_{Tstart}^{Tend} \omega dt$ where ω is the angular velocity in °/s and *Tend*/*Tstart* are the end and the beginning of the turn respectively.	Angular Velocity	°	V
MTV	Turning	Mean Turning Velocity (MTV) as the mean value of the angular velocity along the vertical axis during the turn: $MTV = \frac{1}{NE - NS}\sum_{i=NS}^{NE}\omega(i)$ where ω is the angular velocity in °/s and *NE*/*NS* are the index of the end and the index of the beginning of the turn respectively.	Angular Velocity	°/s	V
PTV	Turning	Peak Turning Velocity (PTV) as the maximum value of the angular velocity absolute value along the vertical axis during the turn: $PTV = \max(\omega)_{NS}^{NE}$ where ω is the angular velocity in °/s and *NE*/*NS* are the index of the end and the index of the beginning of the turn respectively.	Angular Velocity	°/s	V
NJS	Sit-to-Walk, Turning, Turn-to-Sit	(Time-)Normalized jerk score of the acceleration: $NJS = \sqrt{\frac{T^5}{2}\int_{Tstart}^{Tend}(\dot{a})^2 dt}$ where *T* is the duration (*Tend*-*Tstart*) of the considered component and *a* is the acceleration measured in m/s^2.	Acceleration	[m]	AP, ML, V
NAJS	Turning	Normalized Angular jerk score: $NJS = \sqrt{\frac{T^5}{2TA^2}\int_{Tstart}^{Tend}(\ddot{\omega})^2 dt}$ where *T* is the turn duration (*Tend*-*Tstart*) of the considered component, ω is the angular velocity °/s, and TA is the Turning Angle in °	Angular Velocity	[-]	AP, ML, V

NA = NOT APPLICABLE; AP = ANTERO-POSTERIOR; ML = MEDIO-LATERAL; V = VERTICAL, [-] = UNITLESS; M.U. = MEASUREMENT UNIT

2.4 CLINICAL APPLICATIONS

In this section clinical applications are reported which make use of instrumented functional tests for balance, gait, and motor control assessment. All the reported studies investigated the clinical validity of instrumented tests in differentiating people with Parkinson's Disease (PD) at an early-mild stage (or even just at high risk of developing PD) from healthy age-matched subjects.

2.4.1 INSTRUMENTED ANALYSIS OF POSTURAL SWAY

A) Correlates with clinical expression of Parkinson's Disease[1]

There is evidence that the variability in clinical expression of PD can be explained by the existence of different phenotypes with distinct clinical patterns. Two phenotypes have been identified which divide the course of the disease into benign and malign forms: the Tremor-dominant subgroup, considered the benign form, is characterized by minor motor impairment, slower progression and severe postural, action and rest tremor. The malign form is instead characterized by a more aggressive course with a faster progression, little or no tremor, bradykinesia, rigidity, and gait and posture disabilities[2].

Considering the validation study reported in Section 2.1.3, the classification of PD into subgroups, PD-T and PD-NT, is based solely on the presence of tremor in the quiet standing trials; the elements in each group are the trials and not the subjects. It is true that in most cases, particularly in DT, subjects' behavior is quite homogeneous (only two subjects show both tremorous and non tremorous trials in DT) but it is not enough to identify the PD-NT and the PD-T groups with the malign and benign form, respectively. Being aware of this limitation, it is found interesting that the results obtained using HHT closely match the above described clinical patterns.

As shown by the HHT values in Table II, the PD-NT group in ST condition usually shows values slightly lower for RMS, RANGE, MV and JI than the other two groups, but there are no statistically significant differences and the three groups show a similar behavior. In contrast, parameters in the frequency domain (F95 and CF) show values slightly higher than the other two groups, but again there are no statistically significant differences, with the exception of F95 in DT condition. The most important finding comes from DT condition where, although PD-T and CTRL significantly increase their postural sway in every aspect, the PD-NT group has values that are near to those obtained in ST condition, as if the subjects in this group were not able to vary their postural strategies. In contrast, the PD-T group's behavior is almost like the CTRL group's in every condition; the presence of tremor itself is the only discriminating factor. The LPF values of the PD-T group, on the other hand, are systematically higher than the other two groups and this often leads to statistically significant differences with the other two groups.

B) disclosing preclinical signs of developing Parkinson's Disease[3]

Enlarged Substantia Nigra hyperechogenicity (ESNH) assessed by transcranial sonography (TCS) is present in about 90% of subjects with Parkinson's Disease (PD) independent of age and disease stage[4], and may be the best risk marker for PD known to date. It is hypothesized that instrumented analysis of postural function may identify "high risk" subjects for PD (HR) characterized by ESNH. In order to preliminary test this hypothesis, combinations of postural measures, extracted from acceleration signals during quiet standing (QS), has been searched which in order to discriminate between HR and control subjects (CTRL). Combinations of parameters were defined through feature selection based on classification algorithms[5].

A study involving 21 HR subjects (62±5 yrs) and 15 CTRL subject (64±7 yrs) has been performed. Accelerometer (DynaPort Hybrid, McRoberts) was worn on the lower back during QS trials performed with eyes open (EO) and with eyes open on a foam rubber support (EOF). The foot placement was semi-tandem. Acceleration signals were filtered making use of the HHT-based method defined in Section 2.1.1 and postural sway measures were computed as described in Section 2.1.2.

As result, the quadratic discriminant classifier built on two measures had 83.4% accuracy: the 83.4% of the subjects were assigned to their correct class (CTRL or HR). The two measures were frequency dispersion (FD) in the medio-lateral (ML) direction and median frequency (F50) in the antero-posterior (AP) direction, both taken in the EOF

---

[1] S. Mellone, L. Palmerini, A. Cappello, L. Chiari, Hilbert-Huang Based Tremor Removal to Assess Postural Properties from Accelerometers, IEEE Transactions on Biomedical Engineering, Vol.58, No.6, pp. 1752-61, June 2011

[2] J. Jankovic, M. McDermott, J. Carter, S. Gauthier, C. Goetz, L. Golbe, S. Huber, W. Koller, C. Olanow, I. Shoulson, M. Stern, C. Tanner, W. Weiner and the Parkinson Study Group, "Variable expression of Parkinson's disease: a base-line analysis of the DATATOP cohort. The Parkinson Study Group", Neurology, vol. 40, no. 10, pp. 1529-1534, Oct.1990.

[3] L Chiari, I Liepelt, L Palmerini, J Streffer, D Berg, W Maetzler. Can accelerometer-based evaluation of postural function identify individuals with Enlarged Substantia Nigra Hyperechogenicity? Proceedings of the 1st Joint World Conference of ISPGR and Gait & Mental Function, Trondheim, Norway, June 2012

[4] A Gaenslen, B Unmuth, J Godau, I Liepelt, A Di Santo, KJ Schweitzer, T Gasser, HJ Machulla, M Reimold, K Marek, D Berg. The specificity and sensitivity of transcranial ultrasound in the differential diagnosis of Parkinson's disease: a prospective blinded study. The Lancet Neurology, May 2008, Vol. 7, no. 5, pp. 417-424.

[5] R Kohavi, G John. Wrappers for Feature Subset Selection. Artificial Intelligence. Vol. 97, Nos 1-2, pp. 273-324

condition. The specificity was 86.7% and the sensitivity was 81%. FD ML values in HR were significantly lower than in CTRL.
In conclusion, two frequency domain postural measures were able to discriminate with a good accuracy between HR and CTRL. This result suggests for the first time that instrumented posture analysis may be able to disclose preclinical signs of a high risk of developing PD.

C) characterizing the postural behavior in Parkinson's Disease at an early mild stage[1]

Analysis of posture and balance in quiet standing is one of the components of the clinical evaluation of Parkinson's disease (PD). Postural instability is an important and disabling symptom of PD, often leading to falls[2] and injuries; therefore, assessing the standing balance of a PD patient is a promising method for identifying individuals with a high risk of falling due to balance impairments[2]. Several studies, mostly using force plates, have investigated posture in PD subjects both in static and dynamic conditions[2 3 4 5 6 7 8]. Results from these studies suggest that quantitative posturography may be useful, in addition to clinical measures, for the objective assessment of postural impairments and a better understanding of the pathological deficits in postural control of PD subjects. Even though accelerometers are not yet routinely used for measuring quiet standing in PD, they have already been used to assess several motor complications in PD[9 10 11 12].
Since subjects in early stages of PD do not show severe clinical signs of postural instability[13 14], quantitative evaluation of the postural performance could provide early markers for later developing problems[7]. It has been hypothesized that differences in postural behavior between controls and early mild PD subjects could be detected and described by quantitative features derived from accelerometer signals recorded during quiet stance (QS).
In order to test this hypothesis, 20 early-mild PD OFF medication (Hoehn & Yahr ≤ 2.5, 62 ± 7 years old, 12 males) and 20 healthy age-matched control subjects (CTRL, 64 ± 6 years old, 7 males) have been recruited. Subjects worn an accelerometer (McRoberts Dynaport Micromod, sample rate 100 Hz) on the lower back by means of an elastic waist belt, at the level of the fifth lumbar vertebra. The OFF condition was obtained by a levodopa washout of at least 18 h and a dopamine agonist washout of at least 36 h. The unified PD rating scale (UPDRS) was assessed for each subject by an expert neurologist the same day of the experimental sessions. In this study, Sections II and III of the UPDRS were considered. The average value of motor UPDRS (Section III) in PD subjects was $26.6 \pm 7.1/108$. Subjects were asked to stand upright, barefoot, with arms crossed on the chest, looking at a visual marker (a black circle, 5 cm in diameter) placed on a wall 2.5 m in front of them. Foot placement was kept consistent over trials using an averaged preferred position traced on the floor[15]. The subjects were tested in five different QS conditions. Descriptions of conditions, acronyms, and perturbed subsystems are reported in Table I. The dual task administered in the eyes open dual task (EODT) condition consisted of a concurrent cognitive task: counting audibly backward from 100 by 3's. Each trial lasted 30 s. Acceleration signals were filtered making use of the HHT-based method defined in Section 2.1.1 and postural sway measures were computed as described in Section 2.1.2.
Regarding postural measures computed from acceleration, five of them quantify the properties of the acceleration in the frequency domain (F50, F95, CF, FD, and Entropy), and two in the time domain (JI, NJI). Measures derived from displacement are computed in the time domain and describe the amount and direction of sway. Among these, mean

---

[1]] L. Palmerini, L. Rocchi, S. Mellone, F. Valzania, L. Chiari: Feature Selection for Accelerometer-Based Posture Analysis in Parkinson's Disease, IEEE Transactions on Information Technology in Biomedicine, Vol. 15, No. 3, pp. 481-90, May 2011

[2] J.W. Blaszczyk, R. Orawiec, D. Duda-Klodowska, and G. Opala, "Assessment of postural instability in patients with Parkinson's disease," Exp. Brain Res., vol. 183, no. 1, pp. 107–114, Oct. 2007.

[3] A. Nardone and M. Schieppati, "Balance in Parkinson's disease under static and dynamic conditions," Mov. Disord., vol. 21, no. 9, pp. 1515–1520, Sep. 2006.

[4] L. Rocchi, L. Chiari, and F. B. Horak, "Effects of deep brain stimulation and levodopa on postural sway in Parkinson's disease," J. Neurol. Neurosurg. Psychiatry, vol. 73, no. 3, pp. 267–274, Sep. 2002.

[5] R. Marchese,M. Bove, and G. Abbruzzese, "Effect of cognitive andmotor tasks on postural stability in Parkinson's disease:Aposturographic study," Mov. Disord., vol. 18, no. 6, pp. 652–658, Jun. 2003.

[6] L. Rocchi, L. Chiari, A. Cappello, and F. B. Horak, "Identification of distinct characteristics of postural sway in Parkinson's disease: A feature selection procedure based on principal component analysis," Neurosci. Lett., vol. 394, no. 2, pp. 140–145, Feb. 2006.

[7] M. A. McVey, A. P. Stylianou, C. W. Luchies, K. E. Lyons, R. Pahwa, S. Jernigan, and J. D. Mahnken, "Early biomechanical markers of postural instability in Parkinson's disease," Gait Posture, vol. 30, no. 4, pp. 538–542, Nov. 2009.

[8] F. B. Horak, D. Dimitrova, and J. G. Nutt, "Direction-specific postural instability in subjects with Parkinson's disease," Exp. Neurol., vol. 193, no. 2, pp. 504–521, Jun. 2005.

[9] M. Mancini, C. Zampieri, P. Carlson-Kuhta, L. Chiari, and F. B. Horak, "Anticipatory postural adjustments prior to step initiation are hypometric in untreated Parkinson's disease: An accelerometer-based approach," Eur. J. Neurol., vol. 16, no. 9, pp. 1028–1034, Sep. 2009.

[10] A. Weiss, T. Herman, M. Plotnik, M. Brozgol, I. Maidan, N. Giladi, T. Gurevich, and J. M. Hausdorff, "Can an accelerometer enhance the utility of the Timed Up & Go Test when evaluating patients with Parkinson's disease?," Med. Eng. Phys., vol. 32, no. 2, pp. 119–25, Nov. 2009.

[11] R. J. Dunnewold, C. E. Jacobi, and J. J. V. Hilten, "Quantitative assessment of bradykinesia in patients with Parkinson's disease," J. Neurosci. Methods, vol. 74, no. 1, pp. 107–112, Jun. 1997.

[12] P. Bonato, "Clinical applications of wearable technology," Conf. Proc. IEEE Eng. Med. Biol. Soc., vol. 1, pp. 6580–6583, Sep. 2009.

[13] D. J. Gelb, E. Oliver, and S. Gilman, "Diagnostic criteria for Parkinson disease," Arch. Neurol., vol. 56, no. 1, pp. 33–39, Jan. 1999.

[14] G. Becker, A. Muller, S. Braune, T. Buttner, R. Benecke, W. Greulich, W. Klein, G. Mark, J. Rieke, and R. Thumler, "Early diagnosis of Parkinson's disease," J. Neurol., vol. 249, no. 3, pp. III/40–III/48, Oct. 2002.

[15] W. E. McIlroy and B. E. Maki, "Preferred placement of the feet during quiet stance: Development of a standardized foot placement for balance testing," Clin. Biomech. (Bristol, Avon), vol. 12, no. 1, pp. 66–70, Jan. 1997.

velocity is obtained through the derivative of the displacement. Both tremor and postural measures were computed for the AP and ML directions, with the exception of five postural measures that describe planar (bidimensional) characteristics of the displacement (SA, CEA, mSCEA, MSCEA, and 90-Mdir (deviation of the sway form the Antero-Posterior direction supposed at 90°), see Section 2.1.2). A wrapper feature selection approach[1] has been implemented whose objective function is the predictive accuracy of a given classifier.
Classifiers performed at the same Misclassification Rate of 5%, even on different subsets, making use of subsets of three features. On the contrary the number of selection times (ST) varies among subsets and between different classifiers. The highest ST value (36 out of 40) is found for a subset chosen by the feature selection procedure based on Mahalanobis Classifier[2] [3], consisting of (Figure 25):

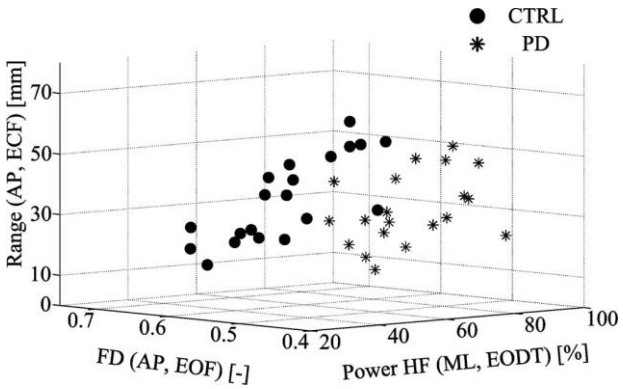

Figure 25 – 3-D view of the values of the three measures selected for the Mahalanobis Classifier. Acronyms: EODT = Eyes-Open Dual-Task; EOF = Eyes-Open Foam; ECF = Eyes-Closed Foam; Power HF = percentage of the total power in the tremor band; FD = Frequency Dispersion; CTRL = Control subjects; PD = patients with Parkinson's Disease.

1) power of the signal for high frequencies (power HF) in ML direction during eyes-open dual-task condition;
2) frequency dispersion (FD) in AP direction during eyes-open foam condition;
3) range in AP direction during eyes-closed foam condition.
Results of the feature selection procedure revealed that quantitative measures computed from accelerometers seem to be able to identify postural and tremor characteristics of PD subjects even when in an early-mild stage of the disease, these may not be evident from a clinical evaluation. Identification of testing conditions that are specific to PD with respect to CTRL subjects may be considered important from a clinical point of view. In fact, this result may lead one to think that the method plausibly characterizes PD and, hence, may be used for evaluation, follow-up, and possibly remote monitoring of PD subjects after therapy. In particular, the dual task condition is shown to be particularly discriminating.

[1] R Kohavi, G John. Wrappers for Feature Subset Selection. Artificial Intelligence. Vol. 97, Nos 1-2, pp. 273-324
[2] G. A. F. Seber, Multivariate Observations, 1st ed. New York: Wiley, 1984.
[3] W. J. Krzanowski, Principles of Multivariate Analysis a User's Perspective. Oxford: Clarendon, 1988.

2.4.2 INSTRUMENTED TIMED UP AND GO TEST

A) characterizing motor impairment in Parkinson's Disease at an early mild stage[1]

As reported in Section 1, the traditional clinical outcome of the Timed Up and Go test (TUG) is its total duration measured by means of a stop-watch[2] This single measure evaluates the locomotor performance as a whole, providing no information regarding the performance in specific components of the test. This is why instrumented versions of the test (instrumented Timed Up and Go, iTUG) have been proposed [3] [4] [5] [6] [7] [8], in which inertial sensors were used as the measurement system. These studies showed the potential of using inertial sensors to boost the quantitative information about the TUG performance for fall risk estimation in the elderly[6] [7] assessment of cognitive decline[3], and motor function evaluation of PD subjects[3] [4] [5]. In this latter group, in particular, the total test duration measured by a stop-watch was not able to differentiate either between moderate PD and age-matched healthy subjects[4] or between early-mild PD and age-matched healthy subjects[3]. It is clear, then, that the traditional clinical outcome is not appropriate for assessing the distinctive locomotor signs of PD, especially in an early stage.

It was hypothesized that the locomotor evaluation using iTUG, followed by a feature selection process, would be able to discriminate between early-mild PD subjects, whose locomotor function is only slightly impaired, and healthy age-matched control subjects. To test the accuracy of the classification rule, we planned an iTUG evaluation on a group of early-mild PD subjects and age-matched healthy controls.

The subjects and the set-up were the same described in Section 2.4.1-C. Eighteen PD subjects were in Hoehn & Yahr stage 2.5, one in stage 2, and one in stage 1.5; the motor-UPDRS score (section III of UPDRS) was 26.6 ± 7.1 (range: 13-41); the mean disease duration was 5.2 ± 4.1 years (range: 9 months – 14.2 years). Subjects were instructed to perform the iTUG at their preferred speed with a distance of 7m instead of the 3m of the traditional TUG. Each subject performed three consecutive trials. The following clinical data were collected from the PD subjects: age, disease duration, UPDRS scores. The following UPDRS subscores were computed by summing the scores of selected items of the UPDRS: 1) postural instability and gait difficulties (PIGD) subscore[9]; 2) gait and posture subscore[3]; 3) rigidity subscore[3]; 4) bradykinesia subscore[3]; 5) motor-UPDRS subscore. Only age was collected from the CTRL subjects.

The iTUG was segmented applying a previous version of the algorithms presented in Section 2.2 and 3.3 which relied only upon a tri-axial accelerometer. The TUG was divided into four components: Sit-to-Walk (STW), Gait, Turning, and Walk-to-Sit (WTS). Walk-to-Sit was selected instead of the Turn-to-Sit transition because gyroscope was not available for identifying turns. The AP acceleration signal was used to identify postural transitions[4] and heel strikes[10]; Turning was marked manually during the trial by means of a remote control. Table XYZ shows mean value and standard deviation of the iTUG measures along with statistical significances of the repeated-measures ANOVA for the within (consecutive trials) and the between (group) factors, and Test-Retest reliability. Description of the measures can be found in Section 2.2.3 and 3.3.5.

---

[1] L Palmerini, S Mellone, G Avanzolini, F Valzania, L Chiari, Quantification of Motor Impairment in Parkinson's Disease Using an Instrumented Timed Up and Go Test, IEEE Transactions on Neural Systems and Rehabilitation Engineering, Jan 2013. [epub ahead of print]

[2] D. Podsiadlo and S. Richardson, "The timed 'Up & Go': a test of basic functional mobility for frail elderly persons," Journal of the American Geriatrics Society, vol. 39, no. 2, pp. 142–8, Feb. 1991.

[3] C. Zampieri, A. Salarian, P. Carlson-Kuhta, K. Aminian, J. G. Nutt, and F. B. Horak, "The instrumented timed up and go test: potential outcome measure for disease modifying therapies in Parkinson's disease," Journal of Neurology, Neurosurgery, and Psychiatry, vol. 81, no. 2, pp. 171–6, Feb. 2010.

[4] A. Weiss, T. Herman, M. Plotnik, M. Brozgol, I. Maidan, N. Giladi, T. Gurevich, and J. M. Hausdorff, "Can an accelerometer enhance the utility of the Timed Up & Go Test when evaluating patients with Parkinson's disease?," Medical Engineering & Physics, vol. 32, no. 2, pp. 119–25, Mar. 2010.

[5] A. Salarian, F. B. Horak, C. Zampieri, P. Carlson-Kuhta, J. G. Nutt, and K. Aminian, "iTUG, a sensitive and reliable measure of mobility," IEEE Transactions on Neural Systems and Rehabilitation Engineering, vol. 18, no. 3, pp. 303–10, Jun. 2010.

[6] B. R. Greene, A. O'Donovan, R. Romero-Ortuno, L. Cogan, C. N. Scanaill, and R. A. Kenny, "Quantitative falls risk assessment using the timed up and go test," IEEE Transactions on Biomedical Engineering, vol. 57, no. 12, pp. 2918–26, Dec. 2010.

[7] A. Weiss, T. Herman, M. Plotnik, M. Brozgol, N. Giladi, and J. M. Hausdorff, "An instrumented Timed Up and Go: the added value of an accelerometer for identifying fall risk in idiopathic fallers," Physiological Measurement, vol. 32, no. 12, pp. 2003–18, Dec. 2011.

[8] B. R. Greene and R. A. Kenny, "Assessment of cognitive decline through quantitative analysis of the timed up and go test," IEEE Transactions on Biomedical Engineering, vol. 59, no. 4, pp. 988–95, Apr. 2012.

[9] J. Jankovic, M. McDermott, J. Carter, S. Gauthier, C. Goetz, L. Golbe, S. Huber, W. Koller, C. Olanow, and I. Shoulson, "Variable expression of Parkinson's disease: a base-line analysis of the DATATOP cohort. The Parkinson Study Group," Neurology, vol. 40, no. 10, pp. 1529–34, Oct. 1990.

[10] W. Zijlstra, "Assessment of spatio-temporal parameters during unconstrained walking," European Journal of Applied Physiology, vol. 92, no. 1–2, pp. 39–44, Jun. 2004.

TABLE XYZ

VALUES OF ITUG MEASURES FOR CTRL AND PD GROUPS, RESULTS OF REPEATED MEASURES ANOVA, AND RESULTS OF TEST-RETEST RELIABILITY ANALYSIS

MEASURE	CONTROL SUBJECTS		PARKINSONIAN SUBJECTS		SIGNIFICANT FACTORS
	MEAN (STD)	ICC(3,1) [LB-UB]	MEAN (STD)	ICC(3,1) [LB-UB]	
Tot Duration	16,08(2,42)	0.89 [0.74-0.95]	17.54 (2.95)	0.81[0.65-0.91]	
STW Duration	1,24(0,23)	0.47 [0.2-0.71]	1.3 (0.46)	0.75[0.55-0.88]	
STW RMS AP	2,67(0,53)	0.74[0.53-0.87]	2.43(0.53)	0.63[0.4-0.82]	
STW RMS ML	0,68(0,3)	0.38[0.11-0.65]	0.59(0.22)	0.55[0.29-0.77]	
STW RMS V	1,77(0,46)	0.61[0.36-0.8]	1.51(0.4)	0.78[0.6-0.9]	
STW NJS AP	11,52(6,71)	0.39[0.11-0.66]	10.74(10.42)	0.66[0.44-0.83]	
STW NJS ML	5,9(7,18)	0.39[0.12-0.66]	5.02(6.09)	0.46[0.2-0.71]	
STW NJS V	11,23(7,32)	0.43[0.15-0.69]	9.88(9.78)	0.54[0.29-0.76]	
Gait Duration	7,79(1,59)	0.84[0.59-0.94]	8.72(2.18)	0.63[0.37-0.81]	
Gait Tstep	0,52(0,05)	0.94[0.83-0.98]	0.52(0.04)	0.86[0.74-0.94]	
Tstep STD	0,02(0,01)	0.37[0.11-0.64]	0.03(0.02)	0.1[0-0.42]	
Tstep CV	4,6(2,09)	0.4[0.13-0.66]	6.51(4.3)	0.12[0-0.44]	
Phase	179,93(4,46)	0[0-0]	178.72(6.29)	0.15[0-0.46]	
Phase STD	5,57(2,79)	0.25[0.01-0.54]	7.17(5.79)	0.33[0.05-0.61]	
Phase CV	3,1(1,56)	0.24[0-0.53]	4.06(3.41)	0.31[0.03-0.6]	
PCI	5,98(2,96)	0.37[0.11-0.64]	7.97(5.24)	0.33[0.06-0.62]	
Gait NJS AP	1,15(0,14)	0.81[0.65-0.91]	0.92(0.2)	0.96[0.92-0.98]	Group (p = 0.01)
Gait NJS ML	1,11(0,26)	0.93[0.86-0.97]	0.75(0.33)	0.95[0.9-0.98]	Group (p = 0.01)
Gait NJS V	1,1(0,24)	0.9[0.8-0.95]	1.08(0.25)	0.9[0.79-0.95]	
HR AP	1,81(0,28)	0.72[0.51-0.86]	1.48(0.32)	0.92[0.85-0.97]	Group (p = 0.03)
HR ML	2,02(0,47)	0.71[0.5-0.86]	1.59(0.55)	0.83[0.67-0.92]	
HR V	2,33(0,43)	0.69[0.47-0.85]	1.82(0.41)	0.79[0.63-0.9]	Group (p = 0.01)
Turning Duration	3.26 (0.6)	0.72 [0.52-0.87]	3.68 (0.61)	0.57[0.31-0.78]]	
Turning Tstep	0.56 (0.05)	0.86 [0.73-0.94]	0.56 (0.07)	0.87 [0.75-0.94]	
Turning RMS AP	1.58 (0.34)	0.73 [0.52-0.87]	1.43 (0.42)	0.92 [0.84-0.96]	
Turning RMS ML	1.61 (0.44)	0.86 [0.74-0.94]	1.44 (0.37)	0.91 [0.82-0.96]	
Turning RMS V	1.96 (0.45)	0.79 [0.61-0.9]	1.87 (0.51)	0.93 [0.85-0.97]	
Turning NJS AP	1.11 (0.2)	0.8 [0.63-0.91]	0.87 (0.21)	0.61 [0.36-0.81]	Group (p = 0.01)
Turning NJS ML	1.13 (0.28)	0.81 [0.64-0.91]	0.78 (0.27)	0.84 [0.71-0.93]	Group (p = 0.01)
Turning NJS V	1.08 (0.26)	0.84 [0.7-0.93]	1.12 (0.35)	0.78 [0.61-0.9]	
WTS Time	3.46 (0.53)	0.52 [0.25-0.75]	3.6 (0.59)	0.52 [0.26-0.75]	
WTS RMS AP	2.53 (0.43)	0.68 [0.46-0.85]	2.32 (0.42)	0.55 [0.28-0.77]	
WTS RMS ML	1.41 (0.44)	0.85 [0.71-0.93]	1.15 (0.27)	0.46 [0.19-0.71]	
WTS RMS V	1.78 (0.47)	0.74[0.54-0.88]	1.48 (0.35)	0.63 [0.39-0.82]	
WTS NJS AP	224 (87.8)	0.08 [0-0.39]	193,8 (102,5)	0.45 [0.18-0.7]	
WTS NJS ML	230.5 (90.2)	0.28 [0.01-0.57]	180.2 (93.4)	0.37 [0.1-0.65]	
WTS NJS V	267.2 (92.2)	0.21 [0-0.51]	249.5 (101.6)	0.27 [0.02-0.56]	

THE MEASURES WHICH WERE CONSIDERED TO BE RELIABLE (WITH AN ICC LOWER BOUND GREATER THAN OR EQUAL TO 0.4 FOR BOTH THE CTRL AND PD GROUPS), ARE HIGHLIGHTED IN GRAY. STD = STANDARD DEVIATION; ICC = INTRACLASS CORRELATION COEFFICIENT; LB = LOWER BOUND OF 95% CONFIDENCE INTERVAL; UB = UPPER BOUND OF 95% CONFIDENCE INTERVAL

Results of the classification procedure showed as the best classifier (the one with the lowest MR, 22.5%) is the Linear Discriminant Analysis (LDA) classifier and the corresponding best subset is made of one measure from STW and two measures from Turning: STW RMS AP, Turning NJS ML, and Turning NJS V.

As expected [5], the total duration of the iTUG is characterized by excellent test-retest reliability (ICC > 0.8) but it is not sensitive to group differences for early stages of the disease. However, it positively correlates with the severity of clinical subscores of gait and posture impairment and rigidity in PD subjects. As shown in Table XYZ, the average total

trial duration of a CTRL subject does not significantly differ from that of a PD subject. It could be argued that the lack of sensitivity observed in the current study is due to the differences in walking distances, 7 meter instead of the traditional 3-meter TUG; however a study in a comparable population[1] the traditional 3-meter TUG did not show any significant group differences.

In this study the locomotor function of early-mild PD subjects was quantitatively evaluated using a minimal setup (a single wearable sensing unit) to measure the performance of a simple clinical test (Timed Up and Go). Using the reliable measures that were extracted from the acceleration signals in different components of the test the following observations were made: the performance of early-mild PD subjects OFF-medication is characterized by normal temporal measures (duration of the test, average step duration), a reduced smoothness and dynamics in trunk movement during gait, and reduced lateral dynamics in trunk movement during turning. In addition an easily interpretable classification algorithm was found to be able to discriminate between the locomotor pattern of CTRL and PD subjects with a combination of three measures. This discrimination is achieved with a misclassification rate of 22.5% in the early-mild stage of the disease, when the temporal outcome of the traditional TUG test would not be able to discriminate between the healthy and the pathological performance.

[1] C. Zampieri, A. Salarian, P. Carlson-Kuhta, K. Aminian, J. G. Nutt, and F. B. Horak, "The instrumented timed up and go test: potential outcome measure for disease modifying therapies in Parkinson's disease," Journal of Neurology, Neurosurgery, and Psychiatry, vol. 81, no. 2, pp. 171–6, Feb. 2010.

3 FROM BENCH TO BEDSIDE

The choice of a single sensor approach, the need of a quick and easy setup, the idea of instrumenting already existing and widely used functional tests, and the need to develop novel and reliable algorithms for movement analysis, everything presented and discussed so far had one final ambitious objective of…

…taking healthcare out of the hospital.

What is pursued is to embed healthcare into people's lives.

3.1 PERSONAL HEALTH SYSTEMS

Personal Health Systems (PHS) are ICT-enabled tools and services, in the form of wearable and/or portable systems, allowing the patient (or the user) to become an active member of the healthcare process[1]. A PHS puts literally healthcare in the hands of the user. PHS are intelligent digital companions which integrate biomedical sensors, communication modules, user-friendly interfaces, and signal/data processing capabilities. A PHS do not replace health professionals, on the contrary a PHS supports clinical decision by providing monitoring and diagnostic data.
Transparent PHS can support and promote healthy lifestyles, can be used for disease management and prevention, for and even for detecting early signs and symptoms of movement disorders. Hence, PHS have the potential to make a major contribution to the sustainability of healthcare systems for an ageing society.
Wearable sensing units offer pervasive but unobtrusive solutions which can be suitable for developing population-based approaches and new primary preventive strategies for community dwelling older persons. Smartphone technology, presented in Section 3.3, has been used for gaining information on indoor and outdoor activities of daily living which will enable the definition of physical activity profiles. Methods developed in Chapter 3 not only provide instrumented version but can be also used for the long-term monitoring specific physical activities like gait as reported in the next session.

3.2 LONG-TERM MONITORING

The ICT approach offers unique advantages for long-term health monitoring. Wearable sensor systems are an emerging trend and may enable proactive personal health management. One of the primary aims of a PHS is to support individuals in their efforts to stay healthy by encouraging preventive lifestyle and enabling early diagnosis of diseases, cognitive decline, and functional decline. The remote supervision of the health state and functional state can help frail elderly persons and people with disabilities to stay as long as possible in their own environment allowing increased independence. This approach may also considerably decrease indirect and societal costs.
PHSs are able to provide early detection and adaptive support to changing individual needs related to ageing like the increased risk of falls. Long-term trend analysis of basic daily behavioral data, physiological data, and physical activity can provide new insights into the detection of fall risk factors. Because of the aging society, falls are considered a major public health problem. Approximately one in three older persons falls unintentionally each year. This causes massive stress and constitutes a burden on the individual, such as loss of independence as well as enormous direct and indirect costs on the society[2]. Even if extensive research has been conducted in this area, some of the fall mechanisms remain unclear. Falls in older persons have multiple causes[3] [4] [5]. Risk factors can be intrinsic and extrinsic. Intrinsic factors include a history of falls, high age, impaired mobility and gait, medical diseases, medication, sedentary behavior, fear of falling, visual impairments, foot problems, nutritional deficiencies and impaired cognition. Extrinsic factors include environmental hazards (like poor lighting, slippery floors, uneven surface), footwear and clothing and inappropriate walking aids or assistive devices. Meta-regression analysis of the predisposing risk factors has shown that gait difficulties, muscular weakness and an impaired standing balance are the most prevalent risk factors for fall[6].
Monitoring of daily physical activity not only enables the detection, the prevention, and the prediction of fall risk factors but it also enables the real time detection of fall events. Different methods for automatic fall detection are

[1] Conference on "Personal Health Systems: Deployment opportunities and ICT research challenges", February 12-13, 2007, Brussels
[2] Heinrich S, Rapp K, Rissmann U, Becker C, König HH. Cost of falls in old age: a systematic review. Osteoporos Int, 2010, Vol. 21, No. 6, pp. 891-902.
[3] Tinetti ME, Kumar C. The patient who falls: ''It's always a trade-off.'' JAMA 2010; 303:258–266.
[4] Cesari M, Landi F, Torre S, Onder G, Lattanzio F, Bernabei R. Prevalence and Risk Factors for Falls in an Older Community-Dwelling Population. Journal of Gerontology, 2002, Vol. 57A, No. 11, M722–M726
[5] Delbaere K, Close JCT, Heim J, Sachdev PS, Brodaty H, Slavin MJ, Kochan NA, Lord SR. A Multifactorial Approach to Understanding Fall Risk in Older People. JAGS, 2010, VOL. 58, NO. 9, pp. 1679–85.
[6] Panel on Prevention of Falls in Older Persons, American Geriatrics Society and British Geriatrics Society. Summary of the Updated American Geriatrics Society/British Geriatrics Society clinical practice guideline for prevention of falls in older persons. J Am Geriatr Soc, 2011, Vol. 59, No. 1, pp. 148-57.

proposed in the literature: monitoring the floor or the sound vibrations[1] [2]; image-based recognition using cameras[3]; monitoring body motion by means of body worn devices, usually including inertial sensors like tri-axial accelerometers and/or gyroscopes[4] [5]. As recent Cochrane reviews on falls and fall prevention[6] [7] have shown that it is possible to significantly reduce the fall risk and the fall rate in older adults, a PHS may also become an ideal tool for supporting prevention and intervention strategies.

3.2.1 IT IS ALL ABOUT RELIABILITY

Wearable systems for long-term monitoring need to satisfy a great variety of criteria and constraints, these include small weight and size, privacy of medical data, unobtrusiveness, ease of use, low cost, reliability and low power consumption. Designing such a system is a challenging task since a lot of highly constraining and often conflicting requirements have to be considered from the designers. Small body worn inertial sensors are a cost effective and unobtrusive solution for ambulatory movement analysis. Nowadays there are several wearable systems able to recognize activities such as laying, sitting, standing, and walking; the outcome is usually limited to the duration and intensity of each activity and to the number of steps for each walking period. A robust monitoring method of everyday activities would fulfill the need to have a tool for supporting evidence-based practices. Impaired gait is associated to frailty[8] and fall risk[9] hence it would be important to monitor even subtle gait changes during the day but gait measures are sensitive to many factors such as path, speed, and dual tasking so obtaining reliable measures in unsupervised settings is a challenge.
Gait analysis is usually performed in supervised settings making use of standardized functional tests like the 10 meter walking test[10] which are very simple and controlled. It has been hypothesized that walk characteristics would be very different if measured in unsupervised settings during activities of daily living.
In order to verify this hypothesis 20 healthy young subjects (24±4 years old, 11 women) have been recruited. Each subject was wearing an inertial sensor (McRoberts Dynaport Hybrid, sample rate 100Hz), embedding a tri-axial accelerometer and gyroscope, on the lower back. In a first phase, subjects were instructed to perform a 10 meter walking test (10MW, Figure 26) three times at their preferred speed. Signals recorded with the inertial sensing unit have been processed as described in Section 2.2 and gait characteristics have been assessed by computing a subset of the features reported in Section 2.2.3. The mean values of the parameters calculated for the three 10MW repetitions have been used as reference values. The subjects were than instructed to walk on two different paths: the first path (PATH 1) was composed of ST alternated with turns of 90 and 180 degrees. In the second path (PATH 2, Figure 27) we asked the subject to move freely in a room, like he was looking for something, to walk in a corridor to reach another room, to move freely again, and to come back.

[1] Majd Alwan, Prabhu Jude Rajendran, Steve Kell, David Mack, Siddharth Dalal, Matt Wolfe, and Robin Felder. A smart and passive floor-vibration based fall detector for elderly.

[2] Mihail Popescu, Yun Li, Marjorie Skubic, and Marilyn Rantz. An acoustic fall detector system that uses sound height information to reduce the false alarm rate. 30th Annual International IEEE EMBS Conference, August 2008.

[3] Tracy Lee and Alex Mihailidis. An intelligent emergency response system: preliminary development and testing of automated fall detection. Journal of Telemedicine and Telecare, 11(4):194–198, 2005.

[4] Bourke AK, Van de Ven P, Gamble M, O'Connor R, Murphy K, et al. (2010) Evaluation of waist-mounted tri-axial accelerometer based fall-detection algorithms during scripted and continuous unscripted activities. J Biomech 43: 3051–3057.

[5] A.K. Bourke, G.M. Lyons, A threshold-based fall-detection algorithm using a bi-axial gyroscope sensor, Medical Engineering & Physics, Volume 30, Issue 1, January 2008, Pages 84-90

[6] Gillespie LD, Gillespie WJ, Robertson MC, Lamb SE, Cumming RG, Rowe BH (2009). Interventions for preventing falls in elderly people. Cochrane Database Syst Rev.:CD007146.

[7] Cameron ID, Murray GR, Gillespie LD, Robertson MC, Hill KD, Cumming RG, Kerse N (2010). Interventions for preventing falls in older people in nursing care facilities and hospitals. Cochrane Database Syst Rev.:CD005465.

[8] M Montero-Odasso, SW Muir, M Hall, TJ Doherty, M Kloseck, O Beauchet, M Speechley. Gait Variability Is Associated With Frailty in Community-dwelling Older Adults J Gerontol A Biol Sci Med Sci (2011) 66A(5): 568-576.

[9] ML Callisaya, L Blizzard, MD Schmidt, KL Martin, JL McGinley, LM Sanders, VK Srikanth. Gait, gait variability and the risk of multiple incident falls in older people: a population-based study Age Ageing (2011) 40(4): 481-487.

[10] Bohannon, R. W. Comfortable and maximum walking speed of adults aged 20-79 years: reference values and determinants." Age Ageing. 1997;26(1): 15-9.

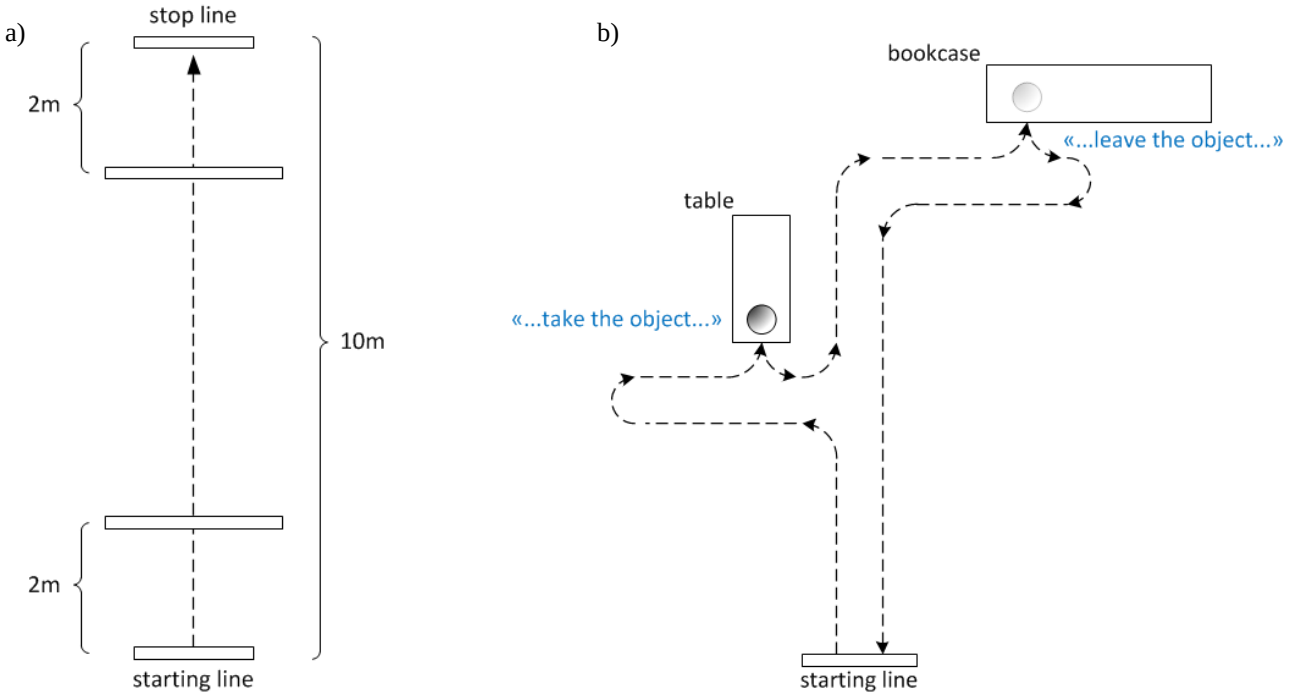

Figure 26 – a) 10 meters walking test; b) PATH1: path composed of straight-path walking intervals alternated with turns of 90 and 180 degrees.

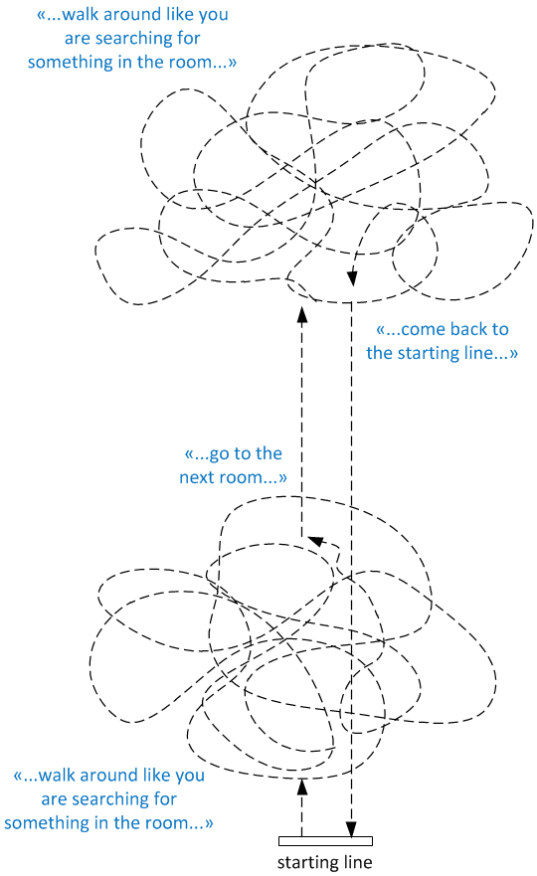

Figure 27 –PATH2: in this second path the subjects were asked to move freely in a room, walk in a corridor to reach another room, move freely again, and come back to the starting point.

An algorithm has been implemented in order to automatically detect and segment walking periods (Figure 28). The algorithm makes use of the trunk angular velocity around the vertical axis and is able to detect turns and curved-path walking intervals as described in Section 2.3.3. Turns, walking on curvilinear trajectories, short gait intervals (< 5s) were identified and excluded from the feature extraction procedure. Results obtained with and without the gait intervals selection method have been compared and reported in Table XXY.

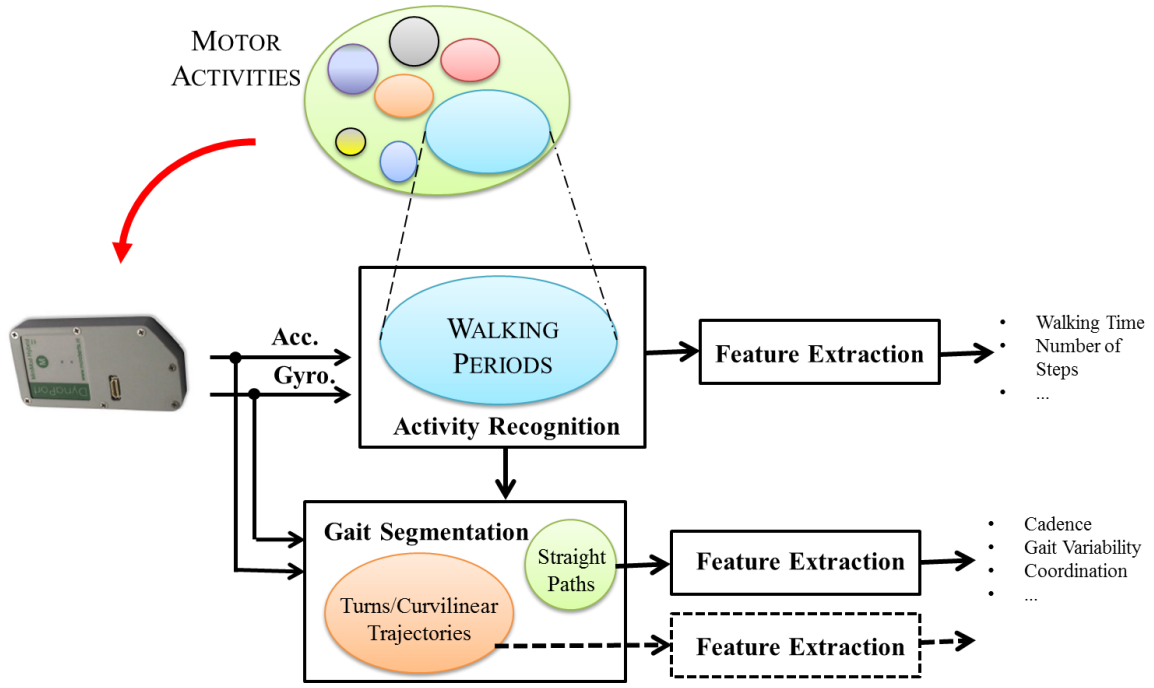

Figure 28 – Procedure for the automatically segment walking intervals. It is possible to extract feature at different levels, from summary statistics like the number of steps and the cumulative walking time, which do not require any segmentation algorithm, to the feature reported in Section 2.2.3 for straight-path walking intervals. Turns and curved-path walking intervals can be used for computing features like the ones reported in Section 2.3.5.

The algorithm selected about 28% of the total walking time on the average, range 14-60%. Table 1 shows the values of the gait parameters obtained during the 10MW, PATH 1 and PATH 2. Table 1 also reports the results of ANOVA between the gait reference values estimated in the 10MW and the two paths.

TABLE 1
GAIT PARAMETER VALUES: MEAN VALUE(STANDARD DEVIATION)

		PATH 1		PATH 2	
PARAMETER	10MW	WITHOUT A	WITH A	WITHOUT A	WITH A
Mean Step Time [s]	0,54(0,05)	0,57(0,04)	0,54(0,04)	0,60(0,05)**	0,56(0,05)
Step Time STD [s]	0,03(0,01)	0,06(0,02)**	0,03(0,01)	0,08(0,02)**	0,04(0,01)
Step Time CV [%]	5,81(1,65)	11,34(3,13)**	6,13(2,67)	13,32(2,62)**	6,84(2,45)
Mean Phase [°]	181,7(3,0)	180,1(5,2)	180,6(5,6)	178,9(5,0)†	179,5(5,2)
Phase STD [°]	6,41(1,92)	11,91(4,43)**	7,71(3,94)	13,26(3,09)**	7,14(3,36)
Phase CV [%]	3,55(1,07)	6,64(2,54)**	4,25(2,13)	7,43(1,79)**	3,97(1,84)
PCI [%]	7,14(2,37)	11,96(4,43)**	8,08(4,09)	13,08(2,99)**	7,58(3,69)

10MW: 10 meters walking; STD: standard deviation; CV: coefficient of variation; PCI: phase coordination index; With A: using the gait interval selection algorithm; Without A: without using the gait interval selection algorithm. ANOVA, 10MW versus Path1 or Path2: †p<0.05; *p<0.01; **p<0.001

A representative example of the algorithm output is reported in Figure 29. As hypothesized, the estimated gait characteristics are statistically different from the reference values in both PATH 1 and PATH 2 without using the gait intervals selection algorithm; gait variability and coordination apparently worsen not for a change in the subject health status but just as an effect of the subject activity. Using the proposed selection algorithm such statistical differences disappear. In conclusion monitoring gait characteristics without strengthening the reliability of the feature extraction

procedure may results in misleading results or interpretation. The proposed selection criterion is able to remove one of the sources of gait variability. This allows monitoring the subject's gait characteristic in a condition which is more similar to standardized functional test performed in clinical settings enhancing robustness and reliability of the follow up.

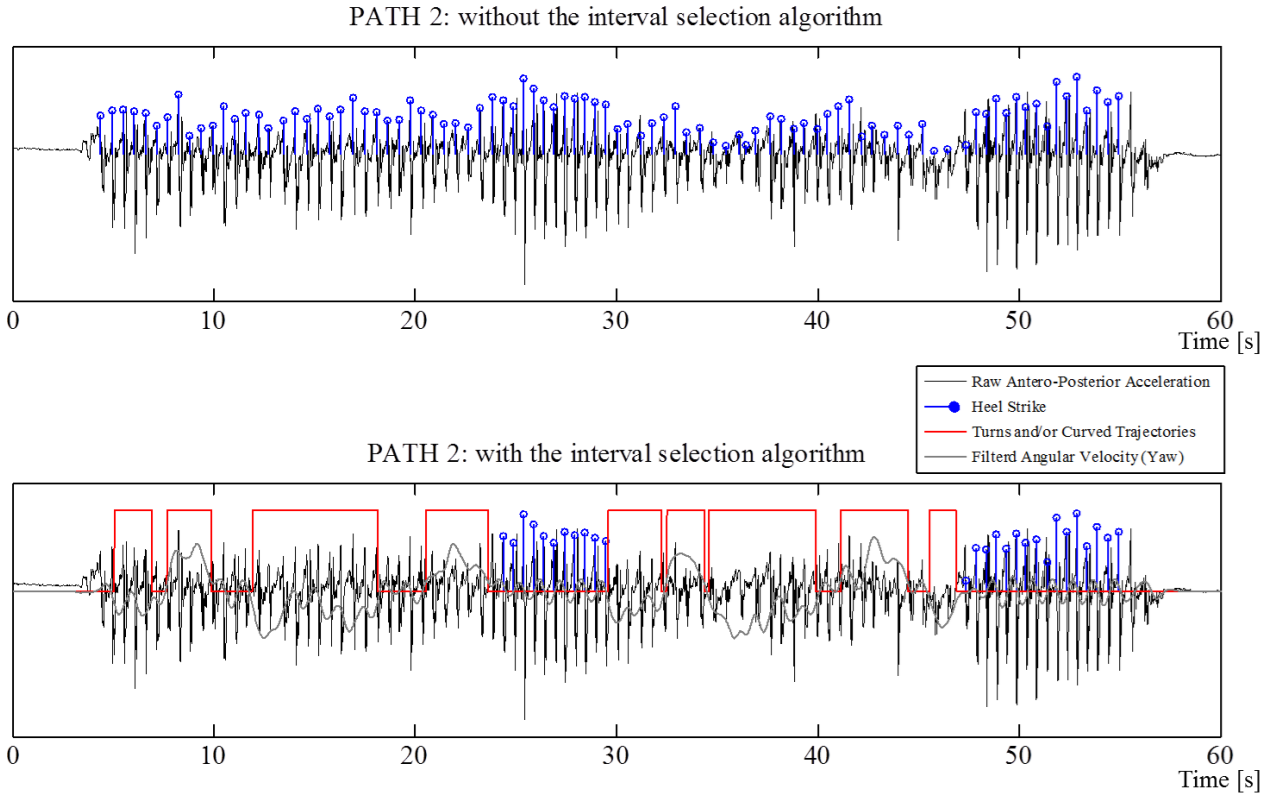

Figure 29 – Example, output of the gait segmentation algorithm. The identified gait interval (Top Panel) is segmented into straight-path walking intervals and curved-path walking intervals (Bottom Panel). Short gait intervals (<5s) are also excluded for the analysis.

3.3 SMARTPHONES

To date, mobile phones are the most ubiquitous consumer electronics devices in the world. The last Eurostat investigation about the use of mobile phones in the Euro-area, referring to 2008, reported that 88% of the total population used a mobile phone (90% Italy, 86% Germany). Looking at the population between 65 and 74 years of age, the percentage becomes 64% (70% Italy, 67% Germany) while for the population aged 75 years and older the percentage is 37% in Italy and 39% in Germany. From 2008 until today these percentages have most likely risen further. A modern smartphone (SP) is a mobile phone built on a mobile computing platform. Recent SP computational capability is at least comparable to the one of a netbook. SPs come with a rich set of embedded sensors which include accelerometer, magnetometer, gyroscope, GPS, microphone, and camera. By its nature a SP has a variety of connectivity options enabling to send and receive data to and from other electronic devices regardless of the distance between the two devices. User interfaces include high-resolution touchscreens with different form factors, physical or virtual keyboards, and speakers. Collectively, these features are enabling new applications across a wide variety of domains including healthcare[1] and environmental monitoring, and give rise to a new area of research called mobile phone sensing[2].

Mobile Phone Sensing is a relatively new concept with the potential to revolutionise many aspects of our lives but is still in an early phase in the practice. Acting as a personal health system a SP has the potential to reduce health-care costs and hospitalisation, to support chronic disease management, to function as a tool for early detection of motor and non-motor markers for certain diseases (e.g. Parkinson's Disease), to function as an assistive device (e.g. providing real-time feedbacks helping the user to perform a certain activity or exercise) and to provide indoor/outdoor monitoring. The possibility of continuous sensing is a key factor in a number of sectors especially in healthcare. Since by its nature a SP is not optimised for continuous sensing, its operating system must be very flexible. The most important requirement is

[1] Consolvo S et al. (2008). Activity sensing in the wild: A field trial of Ubifit garden, Proc. 26th Annual ACM SIGCHI Conf. Human Factors Comp. Sys., pp.1797–806

[2] Lane ND et al. (2010). A Survey of Mobile Phone Sensing. In IEEE Communications Magazine.

that the SP operating system must support true multitasking and background processing. Android OS support multitasking, on the contrary Apple iOS is still inadequate for continuous sensing[1].

A) The Smartphone potential

With respect to long-term monitoring solutions, issue of users' acceptance becomes even more relevant in relation to effectiveness and social significance. Successful application of technologies is strongly influenced by factors that relate to fit between demands of the technology and specific capabilities of the user[2] [3] [4], obtrusiveness of monitoring method[5] [6], and fit with users' expectations[7] [8]. In overview there is a paucity of evidence about older people's and other stakeholders views, beliefs and attitudes towards the use of technologies in the detection and prevention of falls, and more generally in the promotion of active and independent living. Elderly people and their caregivers report that they feel that assistive technology is meant for the frail and dependent elderly people and not for healthy and independent people. They state therefore that wearing or using a device is a symbol for frailty and dependence and is therefore stigmatising. A modern SP is a piece of design. Although capable of running very advanced applications, a SP is still a mobile phone. Mobile phones are everywhere, owned by people of all ages; a SP is not a device which is associated to a frail and/or dependant people. Continuous monitoring is a background process which is transparent to the user and to the people around him/her and it does not affect SP functionality.

The high precision and high resolution touchscreens of modern SP are suitable for measuring stimulus duration and behavioral responses becoming a powerful and portable tool for cognitive training and assessment [ref]; it is possible implementing tools for investigating memory, language, arousal and attention, manual dexterity, and reaction times. A modern SP has the potential of becoming a pervasive tool for both motor and cognitive assessment.

A SP can be programmed to act as an electronic diary, it is able to provide reminders, and it can be used to administer at home questionnaires; the big and sensitive touchscreens enable developing clear and intuitive interfaces and it is possible to draw the attention of the user by means of audio, video, and vibrotactile stimuli/feedbacks. There is evidence about the efficacy of handheld computers in comparison with the traditional paper method for data collection; a handheld computer like a SP can be programmed to provide determinate responses, it can register the data entry date and time, it can prevent retroactive data entry and limit the 'look back' to previous data. Handheld computers are well accepted and usually preferred by the users[9].

A SP is capable of becoming a mobile front-end for telemedical services like fall detection and/or fall prevention programs. Aside the alarm management when detecting a fall, information about fall risk through long-term monitoring of movement, activity pattern, and cognitive function can be collected and processed by a telemedical service; reports about the user profiling can be sent to the physician or physiotherapist, who can use this information for supporting clinical decision making.

User's fall/health risk factors as an output of monitoring, signal analysis, and reasoning, would allow tailoring a personalized intervention or motivational strategy (e.g. rehab programs focused on physical, physiological or social aspects) also taking advantage of the SP capability to act as a guidance and to provide a variety of feedbacks both in real time and offline.

B) Limits of Smartphone Technology

Privacy and anonymity remain a significant problem when it comes to users monitoring by means of wearable devices including the SP. Wearable computing devices must not:

- allow individuals to be located on a permanent and/or occasional basis without the individual's prior knowledge and consent;
- allow information to be changed remotely without the individual's prior knowledge and consent;
- be used to support any kind of discrimination;
- be used to manipulate mental functions or change personal identity, memory, self-perception, perception of others;

---

[1] Consolvo S et al. (2008). Activity sensing in the wild: A field trial of Ubifit garden, Proc. 26th Annual ACM SIGCHI Conf. Human Factors Comp. Sys., pp.1797–806

[2] Salvendy G (1997). Handbook of human factors and ergonomics. Wiley, New York.

[3] Rogers WA & Fisk AD (2003). Technology Design, Usability, and Aging: Human Factors Techniques and considerations. In: Impact of technology on successful aging, eds N Charness & KW Schaie, Springer, New York p.14

[4] Czaja SJ, Sharit J, Charness N, Fisk AD & Rogers WA (2001). The Center for Research and Educationon Aging and Technology Enhancement (CREATE): A program to enhance technology for older adults. Gerontechnology 1: pp.50-9

[5] Hensel BK, Demiris G & Courtney KL (2006). Defining obtrusiveness in home telehealth technologies: a conceptual framework. J Am Med.Inform.Assoc. 13: pp.428-31

[6] Courtney KL, Demiris G, Hensel BK (2007). Obtrusiveness of information-based assistive technologies as perceived by older adults in residential care facilities: a secondary analysis. Med Inform Internet Med.; 32(3): pp.241-9

[7] Oliver R (1980). A cognitive model of the antecedents and consequences of satisfaction decisions. Journal of Marketing Research; 17: pp.460-9

[8] Spreng RA, Mackenzie SB, Olshavsky RW (1996). A reexamination of the determinants of consumer satisfaction. Journal of Marketing; 60: pp.15-32

[9] Lane SJ, Heddle NM, Arnold E, Walker I. A review of randomized controlled trials comparing the effectiveness of hand held computers with paper methods for data collection. Med Inform Decis Mak. 2006 May 31;6:23.

- be used to enhance capabilities in order to dominate others, or enable remote control over the will of other people.

Although nowadays mobile phones are commonly used by people of all ages, many aging people have never used a SP; some hold the false notion that they will not be able to use advanced devices. SP usage must be made intuitive and simple in every sense; user interfaces are a critical point and elderly-friendly interfaces and interfaces developed ad hoc for people with disabilities are needed. A user-centered design approach must be adopted for developing the user interfaces and the telemedical service models. Despite the SP capability to run in parallel multiple processes its battery life is still limited. Battery life is a common problem even in the normal SP usage, substantial improvements will only be achieved with a technological advancement.

3.3.1 A SMARTPHONE FOR INSTRUMENTING THE TIMED UP AND GO TEST: UTUG

Methods and advantages of instrumenting functional tests by means of inertial sensors have been discussed in chapter 3. On the other hand the potentiality of using a Smartphone as a clinical tool has been discussed in the previous section along advantages and disadvantages of this approach. As reported in the previous section, modern smartphones also embed tri-axial inertial sensors. These considerations naturally raise the question if a smartphone can also become a valid tool for obtaining valuable clinical information by instrumenting motor tests. Since it is one of the most widely used clinical tests, the Timed Up and Go test has been chosen in order to answer this question: 49 subjects (59±16 years old, 24 women) performing a TUG of 7m[1] [2] have been involved in this study. The subjects were recruited in the consulting room of a general practitioner without any inclusion criteria regarding their health condition.

A tri-axial accelerometer (McRoberts Dynaport Hybrid (MCR): range ±2g, sample rate 100Hz, sensitivity 1mg) has been used to instrument the TUG. A smartphone has been selected in addition to the dedicated inertial sensing unit: HTC Desire, Operating System (OS) Android 2.1, embedding an accelerometer Bosch BMA150 with a measurement range of ±2g. The embedded accelerometer has a resolution of 4mg and it is sampled at 50Hz. The two devices were firmly fixed together and attached to an elastic belt worn on the lower back.

Android Software Development Kit (SDK) has been used for developing a custom application to manage the embedded accelerometer. MCR signals were down-sampled at 50Hz for the comparison. Data recorded with both devices were processed using the same algorithms, implemented in Matlab.

We evaluated the SP-based instrumentation on a subset of parameters already used in the literature to characterize the Sit to Stand (StS) transition[3] and gait[4]. In order to value the meaning of the comparison, only parameters which showed a clear clinical value have been included: Total duration, jerk, and range of StS, which can discriminate between Parkinsonian patients and healthy subjects[3]; cadence, here computed as the mean value of the Step Time (ST), medio-lateral (ML) and antero-posterior (AP) interstride autocorrelation coefficient (ACORR), which can discriminate between fit and frail older adults[5]; step variability (here computed as the ST standard deviation), which is associated to an increased risk of falling[6].

A high correlation does not imply that there is good agreement between two methods and/or two measurement tools, for this reason it has been applied a test specifically designed for investigating the statistical agreement between measures obtained from two devices: The Bland-Altman test[7]. Upper and lower Limit of Agreement (LoA) have been computed. 25 out of 49 subjects (49±14 years old, 9 women) also performed an additional trial to assess inter-rater reliability by means of Intraclass Correlation Coefficient (ICC, type 1,1); the devices were put back between the first and the second trial. ICC (type 2,1) was used to asses intra-rater reliability.

[1] Zampieri C, Salarian A, Carlson-Kuhta P, Aminian K, Nutt JG, Horak FB. The instrumented timed up and go test: potential outcome measure for disease modifying therapies in Parkinson's disease. J Neurol Neurosurg Psychiatry 2010;81(2):171–6.

[2] Salarian A, Horak FB, Zampieri C, Carlson-Kuhta P, Nutt JG, Aminian K. iTUG, a sensitive and reliable measure of mobility. IEEE Trans Neural Syst Rehabil Eng 2010;18(3):303–10.

[3] Weiss A, Herman T, Plotnik M, Brozgol M, Maidan I, Giladi N, et al. Can an accelerometer enhance the utility of the Timed Up & Go Test when evaluating patients with Parkinson's disease? Med Eng Phys 2010;32(2):119–25

[4] Moe-Nilssen R, Helbostad JL. Estimation of gait cycle characteristics by trunk accelerometry. J Biomech 2004;37(1):121–6.

[5] Moe-Nilssen R, Helbostad JL. Interstride trunk variability but not step width variability can differentiate between fit and frail older adults. Gait Posture 2005;21(2):164–70.

[6] Hausdorff JM, Rios DA, Edelberg HK. Gait variability and fall risk in community-living older adults: a 1-year prospective study. Arch Phys Med Rehabil 2001;82(8):1050–6.

[7] Bland JM, Altman DG. Statistical methods for assessing agreement between two methods of clinical measurement. Lancet 1986;i:307–10.

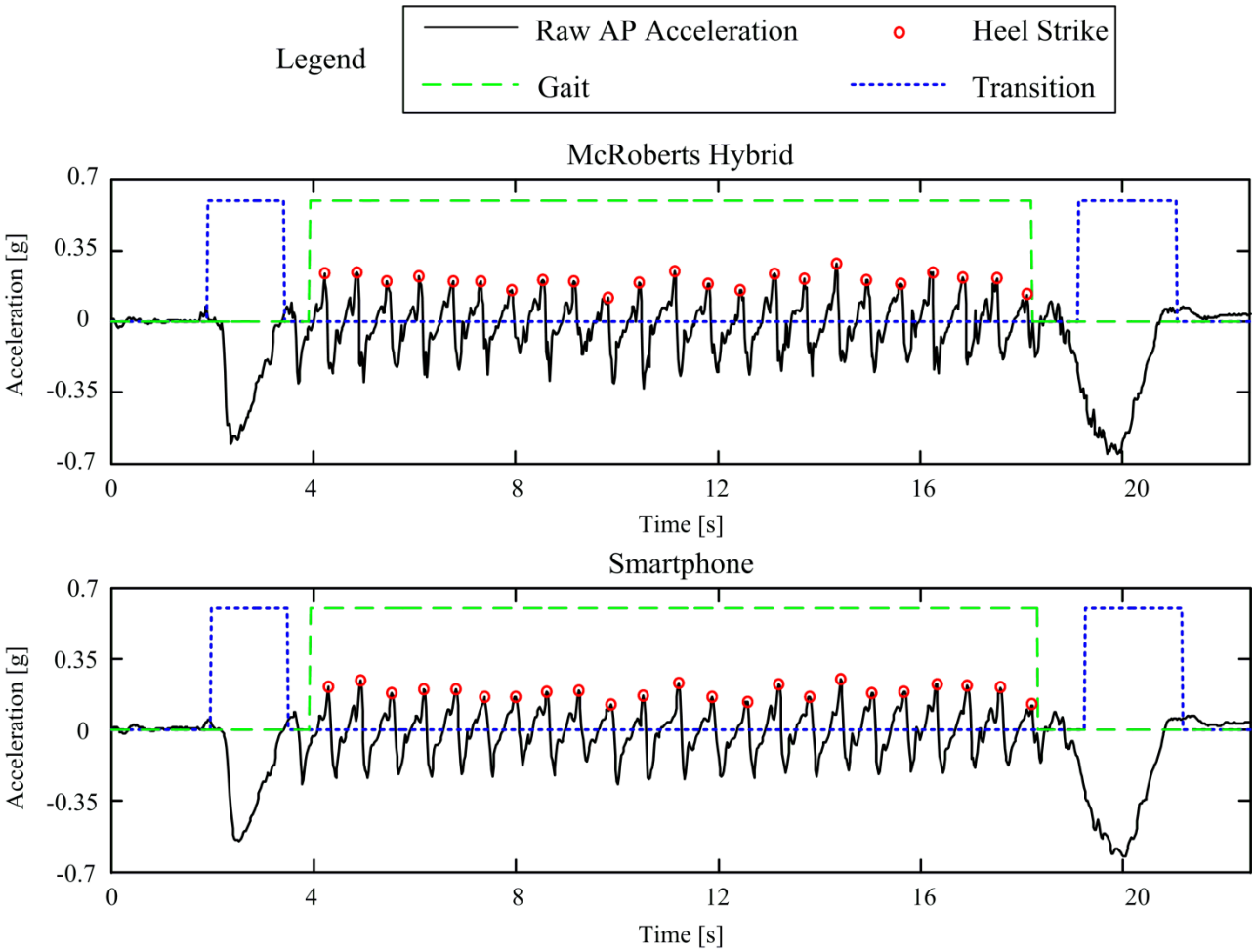

Figure 30 - Antero-Posterior (AP) acceleration measured by both the McRoberts Hybrid (top panel) and the smartphone (bottom panel) during a Timed Up and Go test: the continuous black line is the raw AP acceleration, the dashed green line identifies the time interval classified as the walking phase, the blue dotted line identifies the time intervals classified as transition, and the red circles identify the points classified as heel strikes.

Figure 30 shows a representative example of the acceleration measured by both devices and the outcome of the algorithm which classifies TUG phases and identifies heel strikes. Mean value and standard deviation of each parameter are reported in Table xyz; the table also shows the results of the Bland-Altman test and ICC values along with 95% confidence intervals. Despite selecting a sample rate of 50Hz, we found that the SP OS dynamically manage its sampling (Figure 31). Most of the sampling intervals are indeed distributed in the neighborhood of the nominal sample rate (0.02s, Figure 31-a); however, there is a significant fraction of values near twice the nominal value. Occasionally the sampling interval undergoes large changes probably due to concurrent processes with higher priority. Sampling variability also reflects the signal magnitude so that during the TUG the sample rate is almost nominal (Figure 31-b). For this reason we used the absolute time reference associated with each sample for a linear interpolation and only afterwards we re-sampled each signal at 50Hz. It is important to note that it was crucial to define an appropriate pre-processing of the SP signals in order to avoid incorrect results.

Mean values and standard deviation of the parameters are in agreement with those reported by Weiss et al.[1] and Moe-Nilssen et al.[2] for both MCR and SP. The mean value and the standard deviation of ST show LoA which are lower than the time resolution of the devices making them acceptable. Total duration and StS duration show LoA of about 0.04s, a difference that is negligible; jerk and range of StS are almost identical to those reported by Weiss et al.[1] for healthy subjects with MCR while SP underestimates them; AP and ML ACORR show LoA comparable to or lower than the standard deviations reported by Moe-Nilssen et al.[3]; considering that the distribution of ACORR values obtained with MCR and SP are really close, particularly in ML direction, the statistical agreement can be acceptable. Intra-rater reliability confirms the above considerations; all the parameters display a fair to excellent reliability with the exception of jerk and range of StS whose lower bounds make them unreliable. Inter-rater reliability is the same for both devices.

[1] Weiss A, Herman T, Plotnik M, Brozgol M, Maidan I, Giladi N, et al. Can an accelerometer enhance the utility of the Timed Up & Go Test when evaluating patients with Parkinson's disease? Med Eng Phys 2010;32(2):119–25

[2] Moe-Nilssen R, Helbostad JL. Estimation of gait cycle characteristics by trunk accelerometry. J Biomech 2004;37(1):121–6.

[3] Moe-Nilssen R, Helbostad JL. Interstride trunk variability but not step width variability can differentiate between fit and frail older adults. Gait Posture 2005;21(2):164–70.

In conclusion, a mass-market accelerometer embedded in a modern SP has been compared with a commercial unit, specifically designed for posture and motion detection in clinical settings, for instrumenting the TUG. In our opinion, an SP fulfills the need for a user-friendly device able to perform ubiquitous sensing with a variety of connectivity options. After this study we see evidence that an SP may soon become a pervasive and low-cost means for providing suitable testing solutions for quantitative movement analysis with a clear clinical value, ultimately providing enhanced balance and mobility support to an aging population.

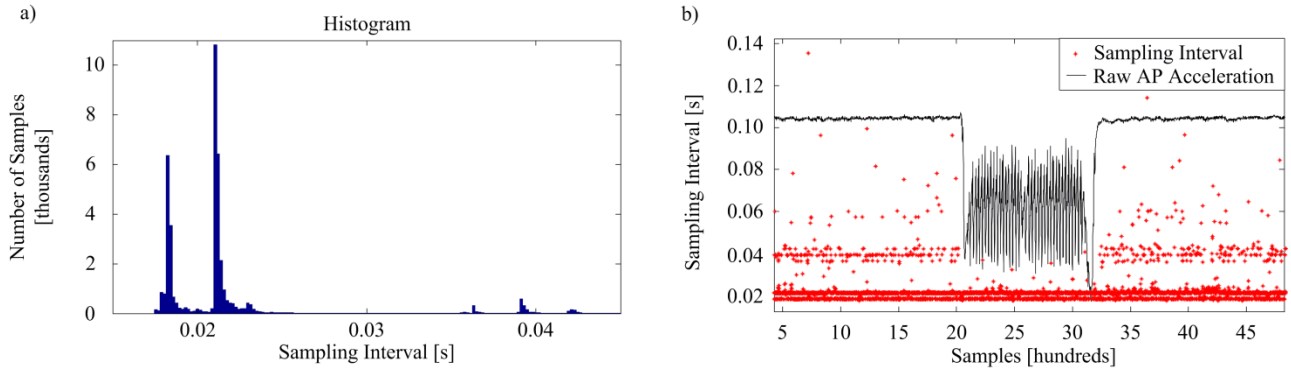

Figure 31 - a) Histogram of the sampling interval values measured while wearing the Smartphone; observation time is about 15 minutes. b) Sampling interval variability while performing a Timed Up and Go; the raw Antero-Posterior (AP) acceleration is reported as a reference in arbitrary units.

TABLE XYZ

Instrumented timed up and go: parameter values obtained with MCR and SP; results of the Bland-Altman test, interrater reliability and intrarater reliability.

PARAMETER	Measured Value		Bland-Altman		Interrater Reliability ICC(1,1)		Intrarater Reliability ICC(2,1)
	MCR Mean(STD)	SP Mean(STD)	LLoA	ULoA	MCR r[Lb-Ub]	SP r[Lb-Ub]	r[Lb-Ub]
Sit to Stand Duration [s]	1.320(0.332)	1.331(0.331)	-0.038	0.016	0.73[0.48-0.87]	0.72[0.46-0.86]	0.99[0.99-1.00]
Jerk Sit to Stand [g/s]	1.694(0.537)	1.537(0.468)	-0.042	0.355	0.59[0.27-0.79]	0.61[0.29-0.80]	0.93[0.18-0.98]
Range Sit to Stand [g]	0.966(0.310)	0.816(0.206)	-0.105	0.404	0.55[0.21-0.77]	0.57[0.24-0.78]	0.76[0.08-0.92]
Total Duration [s]	18.46(3.751)	18.46(3.746)	-0.045	0.040	0.92[0.84-0.96]	0.92[0.83-0.96]	1.00[1.00-1.00]
Mean Step Time [s]	0.568(0.066)	0.568(0.065)	-0.005	0.006	0.95[0.89-0.98]	0.96[0.91-0.98]	0.99[0.99-1.00]
Step Time STD [s]	0.043(0.025)	0.042(0.024)	-0.018	0.019	0.42[0.04-0.69]	0.46[0.10-0.72]	0.92[0.86-0.96]
AP-ACORR	0.764(0.096)	0.783(0.094)	-0.047	0.009	0.57[0.24-0.78]	0.58[0.25-0.79]	0.97[0.56-0.99]
ML-ACORR	0.599(0.125)	0.598(0.127)	-0.056	0.057	0.85[0.70-0.93]	0.88[0.74-0.94]	0.98[0.96-0.99]

MCR = McRoberts; SP = SmartPhone; STD = Standard Deviation; CV = Coefficient of Variation; ACORR = Interstride Trunk Autocorrelation; AP = Antero-Posterior; ML = Medio-Lateral; LLoA = Lower Limit of Agreement; ULoA = Upper Limit of Agreement; r = Intraclass Correlation Coefficient; Lb = Lower bound of 95% confidence interval; Ub = Upper bound of 95% confidence interval.

uTUG

Having demonstrated the validity of a SP-based instrumented TUG[1] an Android application has been developed to this end. The application was named uTUG and it makes use of the SP embedded accelerometer and gyroscope to instrument the Timed Up and Go test (TUG). The SP is placed on the lower back by means of a custom waist belt. Methods implemented for signal processing are the ones described in Section 2.3. Feature extraction includes a subset of the parameters reported in Section 2.3.5. The application performs the signal recording, signal processing, features extraction, and it is able to send a report to a remote server everything without anything else but the smartphone**.**

The uTUG user interface is made of three panels: in the first panel the user can enter an ID for the subject or reload an existing one, then start or stop the test by pressing the "Start/Stop" button, or press the "Report" button to visualize the parameters after the processing. The second panel can be used to visualize and process previously recorded trials. The last panel is for the settings where the user can select the sensors to be included in the recording, set the sample frequency, and enable or disable the data processing, the audio trigger, and the data transfer to a remote server. The data processing is available only if the accelerometer and the gyroscope are both selected with a sample frequency of 100Hz or 50Hz. In this case, the signal processing and the feature extraction will start automatically as soon as the recording is completed. The audio trigger indicates the beginning and the end of the recording. The SP generates a sound when the user is seated quietly, indicating that the test can be started. When the user is seated quietly after completing the test, the SP generates another sound. To transfer the data, it is possible to define the IP address of a remote server and send the test report by means of an Internet connection. All signals recorded during a trial are stored on the local memory. Log files are in TXT format.

Once configured, the uTUG application, whose user interface is shown in Figure 32 and Figure 33, can be started by simply pressing the 'Start' button after entering an ID for the subject. Then the SP is placed inside the belt. The clinician obtains the results right after the TUG. Enabling the audio cueing, the test performance will be facilitated for the user. About 200 TUG were performed, mostly by laboratory staff, in order to test the application features. The audio cue was always generated correctly when the subject was seated quietly. An error is generated when the subject performed a completely different task (e.g. standing up and sitting down immediately without walking).

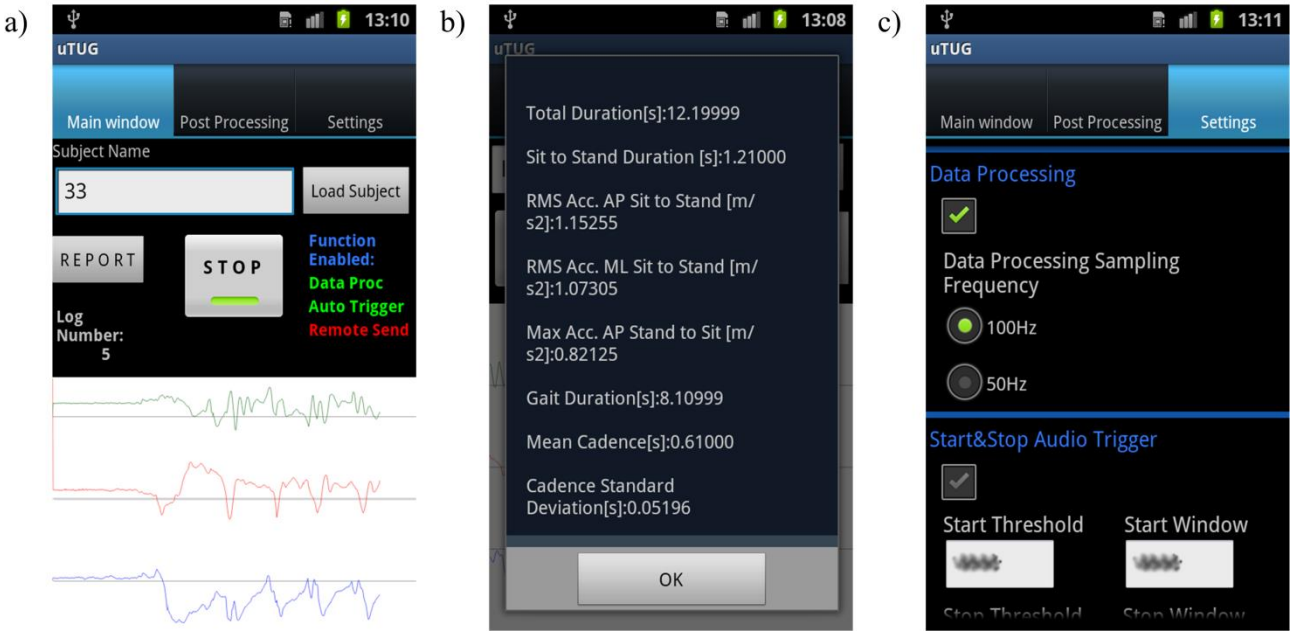

Figure 32 – Screenshots of the uTUG application user interface. a) The main panel. The user can enter an ID for the subject or reload an existing one. On the right it is possible to verify which function is enabled; on the left there is the button to visualize the parameter list after the processing. The central button is used to start/stop the test. The white bottom panel is used to visualize the signals during the recording: the Anterior-Posterior acceleration is displayed in blue, the Medio-Lateral acceleration is displayed in green, and the Vertical acceleration is displayed in red. The Post Processing panel can be used to load, visualize, and process previous trials stored on the local memory. b) Portion of the parameter list; this panel can slide up and down to visualize all the parameters. c) Portion of the settings panel; this panel can slide up and down. In this portion of the panel the user can enable/disable the automatic data processing when the test ends and he can also enable/disable the audio triggers for user guidance.

[1] S. Mellone, C. Tacconi, L. Chiari, Validity of a Smartphone-based Instrumented Timed Up and Go, Gait & Posture, Vol. 36, No. 1, pp 163-165, May 2012

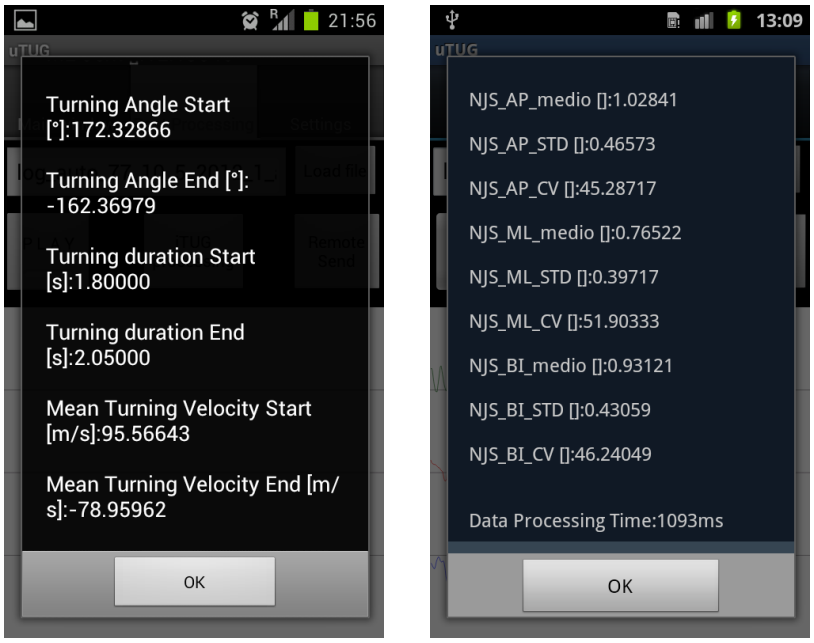

Figure 33 – Two additional portions of the parameter list.

The Matlab (The MathWorks Inc., Natick, MA).implementation of the algorithms has been compared with their Android implementation obtaining almost identical results[1] as reported in Table xyz14. This implies that SP signal processing capabilities enable the implementation of the same numerical methods which would be used in popular software like Matlab. The average time taken to process a TUG trial and to present the result is about 1-2s depending on the memory and CPU loading at that moment. uTUG is a tool designed for fast screening protocols in order to assess the patient's mobility and balance and hence identifying possible risk factors. The application allows to follow up the patient even at home and to perform pre-post intervention assessments targeting specific risk factors (e.g. enhance muscle strength in order to improve the motor performance during the sit to stand transition).

TABLE XYZ14
COMPARISON BETWEEN THE MATLAB IMPLEMENTATION OF THE ALGORITHMS AND THE ANDROID IMPLEMENTATION

PARAMETER	**MA Values** **Mean Value (Standard-Deviation)**	**(MA – uTUG) Values** **Mean Value (Standard-Deviation)**
Total Duration [s]	18,68 (3,66)	0 (0)
Sit to Stand Duration [s]	1,36 (0,32)	0 (0)
RMS Acc. AP Sit to Stand [m/s^2]	1,87 (0,56)	7,9074e-10 (4,8401e-09)
RMS Acc. ML Sit to Stand [m/s^2]	0,58 (0,18)	2,4180e-08 (1,3924e-08)
Max Acc. AP Stand to Sit [m/s^2]	1,23 (1,32)	3,4044e-08 (7,5138e-08)
Gait Duration [s]	13,50 (3,03)	0 (0)
Mean Cadence [s]	0,57 (0,06)	0 (0)
Cadence Standard Deviation [s]	0,05 (0,03)	0 (0)
Cadence Coefficient of Variation [%]	8,59 (5,33)	0 (0)
Overall computation time of the smartphone ~ 1 second; ***it depends on the Smartphone CPU and memory loading at that moment.***		
MA: MATLAB algorithms implementation; **uTUG**: uTUG algorithms implementation; **Acc.** = Acceleration; **AP** = Antero-Posterior; **ML** = Medio-Lateral; **RMS** = Root Mean Square;		

[1] Tacconi C, Mellone S, Chiari L. uTUG: A smartphone application for home-based TUG testing. Proceedings of the 1st Joint World Conference of ISPGR and Gait & Mental Function, Trondheim, Norway, pp. 329-330, June 2012

3.3.2 A SMARTPHONE AS A WEARABLE SENSING UNIT AND FALL DETECTOR: UFALL

Having verified the validity of the smartphone' embedded inertial sensors for instrumenting functional tests and having also realized how ubiquitous are this kind of devices, its validity for long-term monitoring of physical activity has also been assessed. Approaches have been made in using mobile-phone-based solutions for physical activity monitoring and real-time fall detection: the iFall[1] application makes use of the embedded accelerometer in order to detect falls. The application asks for the user to respond when a fall is suspected. If the user does not respond (by pressing a button), the system sends an alert message via SMS. The Mover[2] application has been developed to monitor human motor activities, categorising the user's activity level as "Sleeper, Sitter, Lagger, Walker, Mover, and Hyper". It also includes an experimental fall detection algorithm, able to send an alert to the user's emergency contacts. The PerFallD[3] is a fall detection system based on a SP, which takes advantage of an optional magnetic accessory (consisting in a magnet fixed on the leg). The sensitivity and specificity of a fall detector based on accelerometers embedded into SP's have also been compared to the ones of a dedicated hardware[4].
Several Android smartphones have been tested in order to assess their embedded sensors in terms of signal quality and ergonomics. The Android OS has been chosen since it is an open platform capable of managing all the relevant processes running on a SP. Samsung Galaxy S II (GT-I9100) has been selected because of its good signal quality, high data processing capabilities and its size, being lightweight (116gr) and thin (0.84cm) enough to be comfortably worn. The embedded accelerometer has a range of ±2g and a measured resolution of about 1.5mg while the embedded gyroscope has a range of ±600°/s and a measured resolution of about 0.02°/s. The maxim sample frequency is 100Hz. Accelerometer and gyroscope are manufactured by STMicroelectronics, their codes are K3DH and K3G respectively but they do not correspond to any datasheets in the STMicroelectronics website (www.st.com). The reported characteristics have been directly measured. The device is attached to a custom elastic belt, worn at the waist (Figure XYZ34 and Figure XYZ35). The soft belt material ensures a close but comfortable fit while minimizing relative movements between the trunk and the device, even if placed above clothes. The belt is worn in a way that firmly keeps the SP on the lower back. This placement is not optimal for the original SP usage but the user is not asked to interact with the device and the applications; the smartphone is only used as inertial sensing unit.

Figure XYZ34 – Smartphone worn on the lower back. The screen is off during the monitoring.

[1] Sposaro F, Tyson G., iFall: an Android application for fall monitoring and response. Conf Proc IEEE Eng Med Biol Soc. 2009;2009:6119-22
[2] http://mover.projects.fraunhofer.pt/index.html
[3] Jiangpeng Dai, Xiaole Bai, Zhimin Yang, Zhaohui Shen, and Dong Xuan. 2010. Mobile phone-based pervasive fall detection. Personal Ubiquitous Comput. 14, 7 (October 2010), 633-643.
[4] Lee RY, Carlisle AJ., Detection of falls using accelerometers and mobile phone technology. Age Ageing. 2011 Nov;40(6):690-6.

Figure 35 – A) Smartphone protective case; B) and C) custom Neoprene waist belt.

An Android application, named uFall, has been developed to continuously acquire inertial sensor data for monitoring at home. It is able to record the signals from the embedded accelerometer, gyroscope, and magnetometer. The sampling frequency can be selected in the range 4-100 Hz. Battery life depends on the sampling frequency and the number of selected sensors. Equipped with a standard battery and sampling at 100Hz, the battery life ranges from 16h up to 30h, using all three sensors or just one sensor, respectively. The data is stored on the SP internal memory and can be exported using a USB cable. Log files are in TXT format in order to be easily read and imported into any other software. The application starts automatically every time the device starts up and it continuously runs in the background. The recording of data also stops automatically when the SP is being charged and starts again as soon as the charger is removed.

The application's provisional name is "uFall" because it supports real-time fall detection algorithms. The algorithm implemented for testing purpose makes use of the acceleration Sum Vector (SV) (i.e. the acceleration vector norm[1]). If the SV is greater than a threshold (2.3g, empirically defined) an impact is detected. An impact is considered a fall when the vertical axis orientation before the impact is "vertical" (acceleration of the vertical axis between -0.7g and -1g or between 0.7g and 1g) and the orientation after the impact is "horizontal" (acceleration of the vertical axis between 0g and 0.7g or -0.7g to 0g) or both the orientations, before and after the impact, are "horizontal" (e.g. falling out of bed). The aim is not to validate the fall detection algorithm but to verify the possibility to: (i) continuously acquire the signals from the embedded accelerometer, gyroscope, and magnetometer; (ii) run another process that simultaneously acts as a fall/event detector. The implemented algorithm is similar to the ones already proposed in literature in order to test the system using an algorithm with an adequate complexity. When a fall is detected, an audio alarm is generated for 30 seconds waiting for the user to press a "Stop Alarm" button. If the user does not press the button he is assumed unconscious and an alarm is automatically sent to the caregivers (by e-mail or SMS). The inertial signals recorded in the event of a fall are sent to a remote server by means of a secure (Secure Sockets Layer, SSL) connection. Data can then be analyzed in order to get additional information about the (potential) fall.

[1] Maarit Kangas, Antti Konttila, Per Lindegren, Ilkka Winblad, Timo Jamsa. Comparison of low-complexity fall detection algorithms for body attached accelerometers. Gait Posture. 2008 Aug;28(2):285-91.

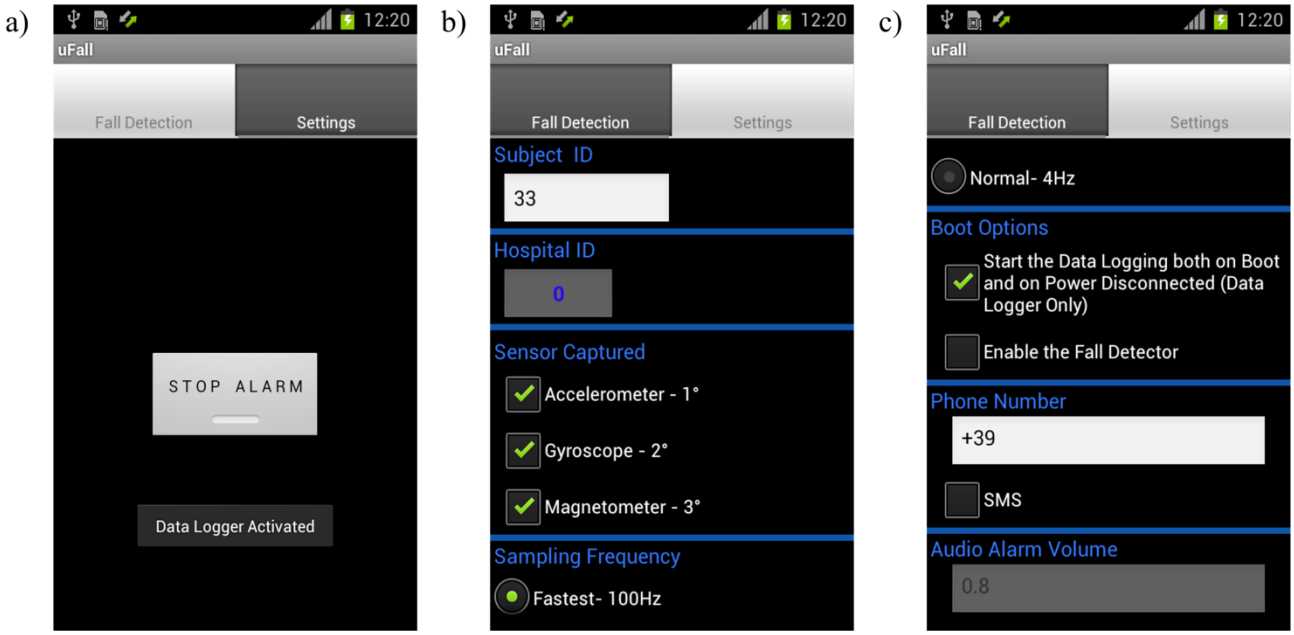

Figure 36 – Screenshots of the uFall application user interface. a) The main panel; it only contains the 'Stop Alarm' button, allowing the user to stop the alarm process if a fall is detected. b) Portion of the settings panel where the user can enter a subject ID, select the sensors to be included in the recording and the sampling frequency; this panel can slide up and down. The hospital ID is fixed (0), there is a unique ID associated to each clinical site. c) Portion of the settings panel. In this portion of the panel the user can enable the fall detector and the automatic data logging.

The application user interface is composed of two panels: the first panel contains the "Stop Alarm" button; the second one is the settings panel where the user can enable or disable all the features like the start on boot, the fall detector, and the sensors to be included. Furthermore, it can set all the parameters like the sampling frequency, the caregiver's telephone number or e-mail, and the remote server IP address (Figure 36). The uFall application can be configured before the SP is given to the patient/participant. The user is not required to interact with the application. He only has to charge the battery. The device/application has been stressed with hundreds of recording hours (approx. 500 hours cumulatively) in order to precisely estimate the battery life. Recording tests were performed both in static and in dynamic conditions for example carrying the SP outside the laboratory or wearing it during daily activities. During the test we periodically applied a forcible shaking in order to trigger the fall detector. The alarm was always audible and an SMS was received each time to the chosen mobile number indicating / confirming that the background process was always running properly. No errors or system crashes were generated during the tests. No user's action can influence the recording or the fall detection process; on the other hand, the application does not interfere with the typical phone usage except contributing to discharging the battery.
During the application development it has been chosen to stress the prevention aspect rather than the detection aspect. The uFall application is capable of recording the user's motor activities on a daily basis and it is completely transparent to the user (i.e. no direct interaction with the user is required). In addition the possibility to run parallel real-time fall detection algorithms has been verified. The fall detector is able to trigger local and remote alarm procedures. A good acceleration resolution is preferable instead of a wide measurement range in order to assess the activities of daily living particularly those immediately before and after the fall. The aim is to identify fall risk factors in the user motor profile. At this stage the uFall application does not include any algorithm for activity recognition; it enables the recording of high quality signals from the SP embedded sensors. The SP acts as an Inertial Measurement Unit and it is possible to apply any activity recognition method in literature which makes use of wearable inertial sensors (placed on the lower back in this case). Although tested, prove the validity of the fall detection algorithm is not one of the aims but it has been verified the capability of the system to run this kind of real-time process. The implemented method is similar to the ones already presented in the literature, which all share a very weak spot: they are all designed and tested relying upon simulated falls. Instrumental data about real-world falls is in general, extremely rare. From the few data available, it is clear that simulated falls and real-world falls can be quite different in terms of acceleration magnitude and dynamics[1]. As a consequence, the performance of the published algorithms is unsatisfactory when applied to falls recorded in real world conditions[2].

[1] J. Klenk, C. Becker, F. Lieken, S. Nicolai, W. Maetzler, W. Alt, W. Zijlstra, J.M. Hausdorff, R.C. van Lummel, L. Chiari, U. Lindemann, Comparison of acceleration signals of simulated and real-world backward falls. Medical engineering & physics 1 April 2011 volume 33 issue 3 Pages 368-373

[2] Bagalà F, Becker C, Cappello A, Chiari L, Aminian K, et al. (2012) Evaluation of Accelerometer-Based Fall Detection Algorithms on Real-World Falls. PLoS ONE 7(5): e37062.

3.4 CLINICAL APPLICATIONS

THE FARSEEING PROJECT

The FARSEEING project, started on January 2012, is co-funded by the European Commission, Seventh Framework Programme (Cooperation-ICT). FARSEEING project aims to provide solutions for health promotion, fall prevention and technical development. Smartphones will be one approach of intervention in a population-based scenario. Newly developed Apps will:

- locally collect and (pre)process sensor data coming from the embedded sensing units (the data collection will be available for both indoor and outdoor activities)
- run real-time fall-detection algorithms
- instrument clinical tests for functional assessment providing instrumental measures of the motor performance in addition to the traditional clinical outcomes
- interact with home automation systems to provide exercise guidance or stimuli to the user.

The use of a smartphone as a clinical tool is assessed within the InCHIANTI study. InCHIANTI ("Invecchiare in Chianti", aging in the Chianti area) is a cohort study of factors contributing to loss of mobility in late life carried out in two Italian towns located in the Chianti region 89. In 1998, 1270 persons aged 65 years and above were randomly selected from the population registries of the two sites (Greve in Chianti and Bagno a Ripoli). Among eligible persons (N=1260), 91.6% participated in 1998, including 842 persons aged 70 and older. The initial cohort was reassessed every three years for a total of 9 years using the same extensive assessment protocol developed for the baseline examination that included a home interview, a standardized medical and functional evaluation by a geriatrician and an experienced physical therapist. This examination included the most extensive collection of measures of strength, balance, mobility, flexibility and manual dexterity ever implemented in the context of an epidemiological study. In addition, the physiologic domains that are important for mobility were assessed using state of the art tests, including anthropometric measures, computerized tomography and more than 50 circulating biomarkers. From this point of view, InChianti is widely considered the state of the art project for the study of mobility disability in the older population with more than 150 publications in high ranked peer review scientific journals over the last 10 years. Some of these publication focus on the relationship between poor mobility and/or mobility disability and aging process itself 90 91 and the trajectories of the functional decline observed in the oldest persons enrolled in the cohort over the 9 years period 92. Because of these characteristics, the InChianti study is the ideal ground for the germination of the FARSEEING project since having access to such a representative epidemiological cohort has the major advantage that information is already available from its longitudinal database. The InChianti study is the starting point for the development of the population-based scenario; the instrumental assessment is validated by comparing the information on mobility collected and interpreted by Smartphone technology with performance-based and self-reported measures of mobility obtained by objective examination or by previously validated standard questionnaires.

An Android application has been developed to enable data collection also during functional tests performed at the hospital. The patient wears the same SP used for the at-home monitoring running the uFALL application described in Section 3.3.2 while the clinician uses another SP running the master application. Samsung Galaxy Note (GT-N7000) has been selected for the clinician because of its screen form factor (5.3") which is optimal in order to implement a wide and clear graphical user interface but its weight is limited to 178gr enabling to hold and carry the device for long time periods with ease. The system is named "uChianti" and it is then composite of: a SP acting as Sensing Unit (SU) for data logging and a second SP acting as a Remote Controller (RC). Once the applications are started the communication between the two devices is automatically established via Bluetooth. The slave application is named "uChianti Subject" while the application installed on the RC is named "uChianti Clinician". The SU is worn on the lower back by means of the same elastic case belt used for the monitoring at home.

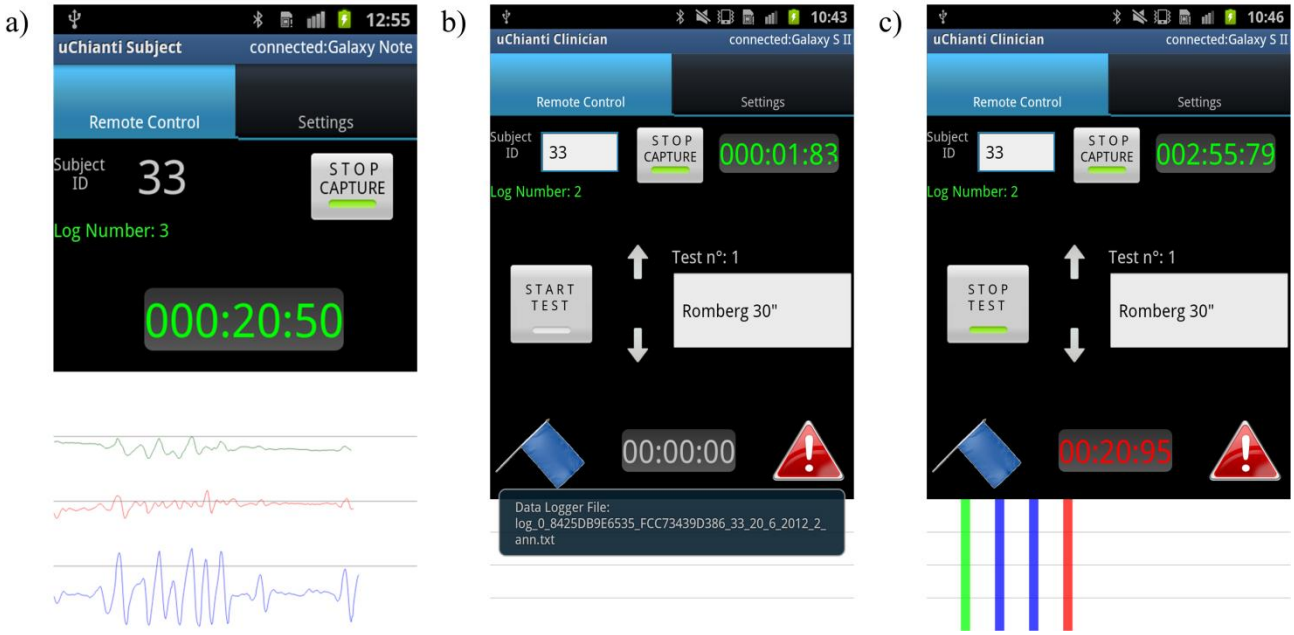

Figure 37 – Screenshots of the uChianti applications user interfaces. a) Main panel of the uChianti Subject application. In this panel it is possible to visualize the signals in real-time, the time elapsed from the beginning of the data recording, and it is possible to stop the data recording manually. The settings panel enables to change the sensors included in the recording and the sample frequency. b) Main panel of the uChianti Clinician application. The user can insert an ID for the subject, start/stop the data recording, select the functional test from the list, and start/stop the test. When a test starts/stops special time markers are inserted automatically. c) Main panel of the uChianti Clinician application. The "Flag" button can be used to segment the recording, a chronometer starts automatically measuring the time elapsed between two consecutive "Flags". The "Warning" button can be used to insert the so called "bad" markers meaning that the signal portion before the marker should be ignored. In the settings panel the user can define and edit the list of functional tests.

The uChianti Subject application (Figure 37-a) captures and stores the data recorded with the embedded accelerometer, gyroscope, and magnetometer; the default sampling frequency is 100Hz. The user interface only allows stopping the data recording in case the connection with the RC is lost (otherwise the RC stops the data recording). The uChianti Clinician application (Figure 37-b and c) is used to manage the data acquisition process. While the SU is recording it is possible to select the functional test to be performed by choosing among a user-defined list of available tests. During the recording of each test it is possible to insert time markers using the "Segment" button and it is also possible to insert special markers using the "Bad" button in order to invalidate the test portion recorded before the mark. The RC usage is quite similar to the one of a chronometer; the button used for segmenting the recording, also measures the time between consecutive markers. The master application generates a log file which includes all the information needed in order to segment the recording by identifying the performed functional tests; the signals associated to each functional test are then post-processed in a workstation equipped with MATLAB. Aside the main control panel, the uChianti Clinician application also has a setting panel where it is possible to define and edit the functional test list. Data, collected instrumenting the functional tests, allows developing and validating standalone applications like uTUG (Section 3.3.1). In addition, the use of the same sensing unit for both functional tests performed at the hospital and the monitoring at home allows comparing the motor performance measured during activities of daily living with the motor performance measured during a clinical examination.

4 CONCLUSIONS

Reliable and validated signal processing methods have been successfully implemented in Personal Health Systems based on smartphone technology. At the end of this research project there is evidence that such solution can really and easily used in clinical practice in both supervised and unsupervised settings. Smartphone based solution, together or in place of dedicated wearable sensing units, can truly become a pervasive and low-cost means for providing suitable testing solutions for quantitative movement analysis with a clear clinical value, ultimately providing enhanced balance and mobility support to an aging population.

Future Developments

A walking interval selection method has been developed which is suitable for long term monitoring in unsupervised settings. A feature extraction procedure was also applied if the walking interval lasted for at least 5s and no turns were performed. The feature extraction procedure computes a set of parameters like the cadence, the step/stride variability, the coordination, and the smoothness of movement. An example of the method applied to a frail elderly subject, who also fell during the monitoring, is shown in Figure 38.

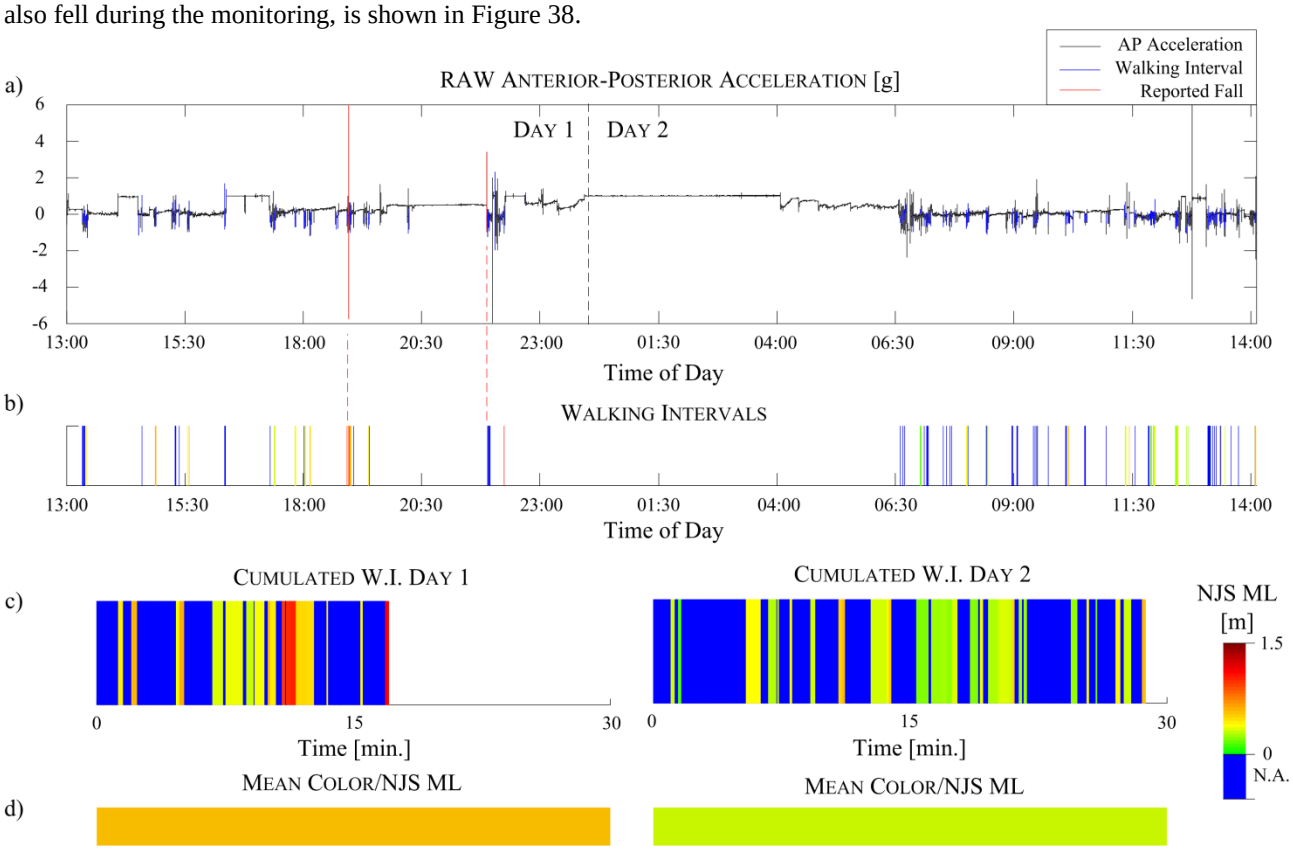

Figure 38 – a) Walking interval selection algorithm applied to a 25 hours monitoring. The waling intervals selected are reported in blue while two falls are reported in red; the first one at about 19:00 o' clock and the second one at about 22:00 o' clock. b) A colored bar is plotted for each of the selected walking intervals; the color depends on the value of the time Normalized Jerk Score in the Medio-Lateral direction (NJS ML) which is a measure of smoothness. If a walking interval lasts less than 7s and/or the walking trajectory is curved the bar is reported in blue c) Cumulated walking time, along with the chosen parameter values, of the first and the second day monitoring. d) Mean value of the NJS ML (reported as a color) during the first and the second day of monitoring.

The results reported in Figure 38 are very preliminary since many more subjects are needed in order to properly validate the methods but the proposed algorithm allows for example to search for potential fall risk factors in the gait parameter values, or in the gait parameter trends, or even in the distribution of the walking intervals and the cumulated walking time.